Synthesis of prenylated pterostilbene and testing of its effect on human colon epithelial cells

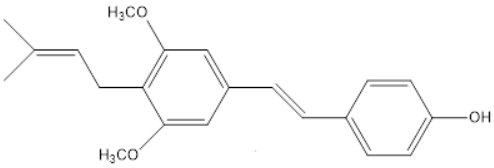

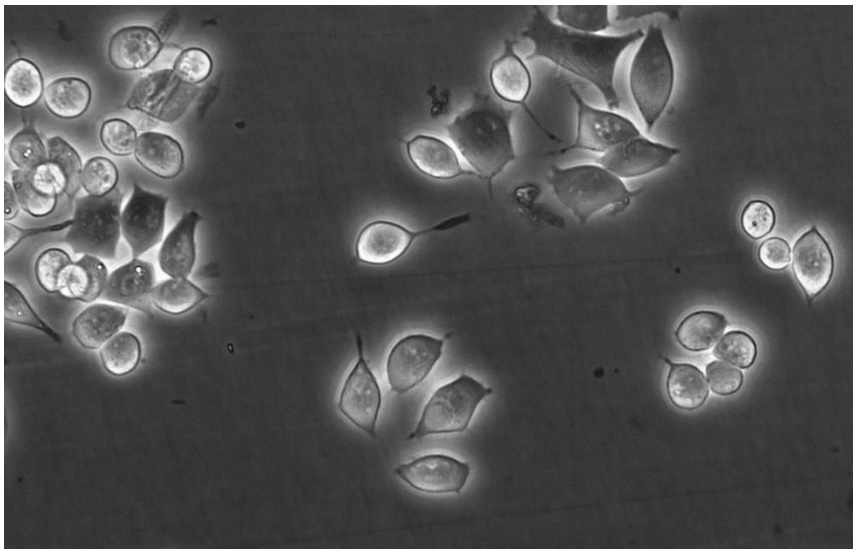

Master thesis in chemistry & medicinal biology

Author: Bob Nikzad
Supervisor: Bill Goldring
Ole Vang

Department of science, system and models

Roskilde University

September 2016

Acknowledgement

This thesis is written in chemistry & medicinal biology at Roskilde University. The present work has been carried out at the department of Science system and models at Roskilde University during the period of September 2015 to September 2016, under the supervision of associated Professor Ole Vang and Bill Goldring.

First, I would like to thank Ole Vang and Bill Goldring for their guidance and support during this project. Further, I would like to thank Professor Poul Erik Hansen for great guidance during the first 6 month of my thesis. I would like to thank laboratory technician Marianne Laudrisen for the introduction to the cell laboratory. I would also like to thank laboratory technician Annette Christensen, Britt Clemmensen and Jacob Krake for running of all NMR and GC-MS samples.

I would also like thank the students from the master group and the MMDC group for relevant discussion and good time during work in laboratory.

Lastly, I would like to thank Ph.D. Bahjat Saeed for his help and his vast knowledge in chemistry.

Abstract

RV and its lesser studied analogue Pter are a naturally occurring phytoalexin found in grapes and blueberries, respectively. There is evidence of the protective effects of resveratrol and some other stilbenoids which include anti-proliferative, anti-inflammatory and anti-oxidant. Different studies have shown that by prenylation of polyphenolic compounds can improve its biological and its pharmacological properties.

In the present study prenylated pterostilbene (Pr. Pter) was synthesized in 6 steps. Characterization of compounds was carried out with ^{1}HNMR and GC-MS. This compound commercially unavailable and it was not synthesized before. The effect of the compound on human colon cancer cell line DLD-1 cells was investigated. The effect of Pr.Pter, Pter and RV on cell growth, cell viability, cell cycle progression and apoptosis was examined by Coulter counter, MTT and FACS assay. Cell morphology was also studied by phase contrast microscopy and the cell diameter was measured by FitterBJ03 program.

It was found that Pr.Pter, Pter and RV reduce the cell number and the effect is both time and dose dependent. The IC_{50} values of Pr. Pter and Pter were determined with MTT assay. The IC_{50} values for Pr.Pter exposure were 39.6µM and 29.70µM after 48 and 72 hours respectively. Further, treatment the cells with Pr.Pter reduced the cell diameter and arrested the cells in G_1 phase after 24 hours and G_2 phase after 72 hours.

It was found the IC_{50} for Pter exposure were 42.7µM and 30.3µM at 48 and 72 hours respectively. Pter and RV treatment increased the cell diameter at 24, 48 and 72 hours. It was observed that Pter and RV arrested the cells in S phase at 24, 48 and 72 hours.

In conclusion, Pr.Pter and Pter reduce the cell number and IC_{50} showed better activity for Pr.Pter. The cell diameter was increased after treatment of the cells with Pter and RV, while the cell diameter was reduced after treatment with Pr.Pter. These finding indicated that Pr.Pter has another targeting molecule, however further investigations are needed.

Abstrakt

RV og nogle andre stilbenoider er naturligt forekommende kemisk stoffer, som findes i druer og bære. Over de seneste par årtier, har RV og analogen, Pter været et meget attraktive forsknings emner grundet dets beskyttende virkningsmekanismer som omfatter anti-proliferativ, anti-cancer, anti-inflammatorisk og antioxidant. Ydermere har undersøgelser vist at en prenylering af polyphenol stoffer kan forbedre dets biologiske og farmakologiske egenskaber.

I denne studie, Pr. Pter blev syntetiseret i 6 trin. Det nye syntetiseret stof er kommercielt utilgængeligt og er ikke blevet syntetiseret før. Efter syntetisering blev produktet karakteriseret med ^{1}HNMR og GC-MS, hvorefter forskellige teknikker såsom Coulter counter, MTT og FACS var brugt til at undersøge effekten af Pr. Pter, Pter og RV, på kolon cancer cellelinje DLD-1 celler. Herunder har vi undersøgt cellevækst, celle antal, cellecyklusprogression og apoptose. Derudover blev cellemorfologi undersøgt med fasekontrast-mikroskopi og celledíameteren blev determineret med FitterBJ03, programmet.

Dette studie har vist, at Pr. Pter, Pter og RV har en hæmmende effekt på celletallet men den observeret effekt er tid- og dosisafhængig. IC_{50} værdierne for celler, der er behandlet med Pr. Pter var 39.6µM og 29.7µM efter henholdsvis 48 og 72 timer. Medmere viste celler behandlet med Pr. Pter en reduceret cellestørrelse og cellerne ophobede sig i G1 fase efter 24 timer samt G2 efter 72 timer.
Desuden viste IC_{50} for celler der var behandlet med Pter viste 42.7µM og 30.3µM efter henholdsvis 48 og 72 timer. Derudover viste celler behandlet med Pter, efter 24, 48 og 72 timer, en stigende cellestørrelse og cellerne ophobede sig i S fase ved 24,48 og 72 timer.

De viste resultater indikerer at Pr. Pter virker på en anden måde og herunder må påvirke forskellige mekanismer sammenlignet med Pter og RV. Dette studie konkludere, at Pr. Pter og Pter reducerede cellevæksten og IC_{50} viser bedre aktivitet for Pr. Pter sammenlignet med Pter.

Introduction

Cancer in different forms is one of the leading causes of death in human population and a major health problem in the world. Colorectal cancer is the third most common cancer in the men and the second most common in the women with higher incidence rate from western countries[1]. Diet, nutrient and lifestyle factors are believed to act as pro and antitumor risk modifiers across the entire multistep process of colorectal tumorigenesis[2]. Difference in rates by country, and elevated risk among second generations of new migrants from a low to high risk country support effect of environmental factor in colorectal cancer risk. Regular consumption of vegetables and fruits is associated with reduced risk of cancer, particular cancer of digestive tract. Because polyphenolic compounds such as resveratrol which are found in fruits and vegetables can switch on or turn off specific signalling molecule pathway and preventing abnormal cell proliferation or cell growth.[3,4,5] RV & Pter with similar structure are natural polyphenolic compounds that are found in red wine and blueberries respectively.[6,7] The bioactivity of resveratrol has been studied extensively and its anti-tumorigenesis effect in different cell line has attracts many attention[8,9]. Other stilbenoids such as Pter share many of RV bioactivities, including anti-cancer activities[10]. Different studies have shown by prenylation of polyphenolic compounds such as flavonoids and stilbenoids can improved its biochemical and pharmacological properties.[11,12,13] It is believed that prenyl portion act as a transporter of the phenolic portion through the cell walls and combination of a prenyl group with a phenolic backbone can provide a series of new interesting biological activities. Therefor the presence of isoprene side chain in different positions plays as an important role in biological activity of polyphenolic compounds[14].

Aim

The aim of this thesis is synthesis of prenylated pterostilbene (Pr.Pter) and testing of its biological activity on human colon cancer cell line DLD-1 to see if the presented of the prenylated side chain has any effect on its biological activity.

Chapter 1

Background

This chapter reviews the theory behind cancer, cell cycle, biology and chemical properties of polyphenolic compounds. The review contains the basic information for the subject in question. Cancer is a multiple process involving abnormal activation of oncogenes, inactivation of tumour suppressor genes, through mutation and genomic instability which increasing capacity for proliferation, survival, invasion and metastasis[15]. These mutations can be either inherited or mutations that are acquired in somatic cells during tumour development. In 2000 Hannah & Weinberg proposed the six hallmarks of cancer which explain difference between a cancer cell and a normal cell (see figure 1). A short description of the six hallmarks of cancer is given.

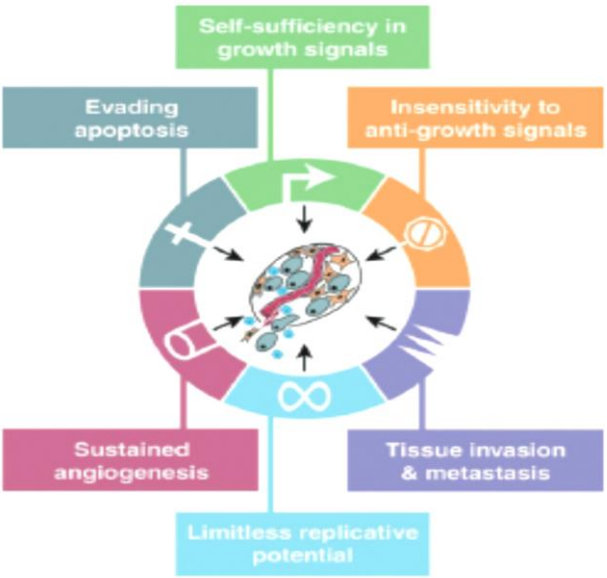

Figure 1

This figure summarizes common feature that find in different neoplastic diseases[15]. Not all of the hallmarks are seen in all types of cancer.

1-6-Self-sufficiency in Growth factor

Normal tissues accurately control production and the release of growth promoting signals. But cancer cells can produce both growth factors and their receptors, resulting in autocrine proliferative stimulation. They can also send signal to normal cell within the stroma, which in turn supplying the cancer cells with various growth factor[15].

2-6-Evading Growth suppressor

Cancer cells can also evade growth suppressors, which are often tumour suppressor genes (TSGs). Growth suppressors prevent cell growth and proliferation when cells become abnormal. Both RB and p53 are TSGs, which function in cell cycle arrest, DNA repair and apoptosis. In cancer cell TSGs are usually mutated. Alternations in TSGs are found in almost all cancer cells including colorectal cancer [15].

3-6-Evading Apoptosis

Programmed cell death by apoptosis serves as a barrier against cancer development. The regulators and the effectors of apoptotic pathway are deregulated in cancer cells, so they can survive in stress conditions.[15,16]

4-6-Sustained angiogenesis

Angiogenesis is a process which new blood vessels form, from pre-existing vessels. This is a normal and vital process in growth and development of tissues. Cancer cells as well as normal cell need to oxygen and nutrient to grow and will undergo apoptosis without oxygen and nutrient. Cancer cell secret pro-angiogenetic factors such as VEGF which recruit endothelial cells and promote grow of new vessels. Vascular Endothelial Growth Factor (VEGF) is up-regulated in many types of cancer.[17,15]

5-6-Invasion & metastasis

Many cancer cells will metastasize when the primary tumour reaches a certain size. They can become invasive and enter into other organs through bloodstream or lymphatic system. Metastatic is the main cause of cancer related death.[18,15]

6-6-Limitless replicative potential

Non cancer cell dies or stop growing and enter senescence after a certain number of cell division but cancer cells like stem cells have a limitless replicative potential and follow uncontrolled proliferation which leading to the production of a tumour. It is believed that immortalization is linked to telomere length. Telomeres are complex structures which protect the ends of the chromosomes, as they shorten in non-immortalized cell, because of the absence of telomerase. Telomerase is an enzyme which adds DNA repeat sequence at the end of telomers. Up-regulation of telomerase is found in many types of cancer.[19,15]

Colorectal cancer

CRC which arises from the colon or rectum is the third most common type of cancer globally[1]. According to GLOBOCAN, about 600.000 are dying each year from colorectal cancer. In Denmark 39.253 cancer cases was registered in 2014 which has an increasing of 5.8 per cent in compare to 2013(37.075). The incident rate was 609 (pr. 100.000 persons) which is 1.5 pct. higher than in 2013 and this is because a significant increase in diagnose of CRC in both men and women[20].

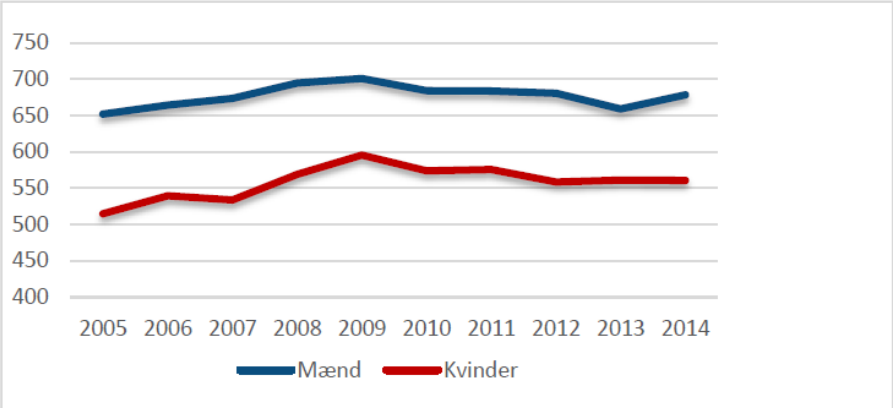

Figure 2

Incidence rate of cancer from 2005 to 2014 based on www.sst.dk [20]

The development of CRC is a slow process. The entire process, from the first cellular change until cancer is developed, takes about 10 years[21]. CRC incidence rate are highest in the western world and counties with a western lifestyle. Inflammatory bowel disease, smoking, obesity increase the risk of CRC. Metastatic, most prominently to the liver is occurring to 40% of CRC patient and 50% will die of it[22]. Only about 5% CRC cases are inherited, where important TSGs or DNA repair genes are inactivated[23].

Anatomy of colon and rectal

The colon and rectum are located in the abdominal cavity starting in the right lower quadrant with the caecum where the small bowel enters the large bowel. Then colon continues upward into ascending colon before it turns via the right flexure to transverse colon. This part is defined as the right colon. The remaining part of the colon consists of the left flexure, descending colon, before it reaches the sigmoid colon is defined as the left colon. The rectum is defined as the section that is 15 cm from the anal verge. One-third of colorectal patients have rectal cancer, while two-thirds have colon cancer[24].

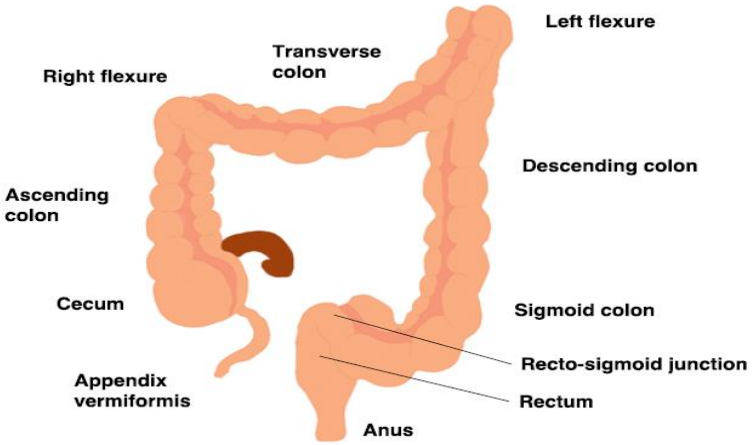

Figure 3

Anatomy of colon and rectum[24]

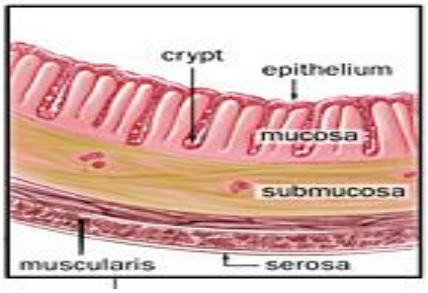

Figure 4[25]

The intestinal wall is composed of four layers: serosa, muscularis, submucosa and mucosa from outside to inside as shown in figure 4.[25] Each layer has different tissues and functions. The serosa layer consists of connective tissue and cover digestive tube. The muscularis layer surrounds submucosa and is responsible for intestinal peristalsis. The submucosa layer is rich in vessels like arteries, lymphatic and nerves supply intestine with blood. The innermost layer is the mucosa which is lined by absorptive and secretor epithelium. The epithelium consists of simple columnar epithelium layer with millions of crypt that are finger like invaginations of the epithelium into the underlying connective tissue. The enterocyte, enteroendocrine, goblet and stem cells are found in the crypt. The enterocyte are absorptive cells, while enteroendocrine and goblet cells are secretory and secrete various gut hormones. All these type of cells originate from the stem cells that are found in the bottom of crypt. 95% of all CRCs are derived from crypt epithelium[1]

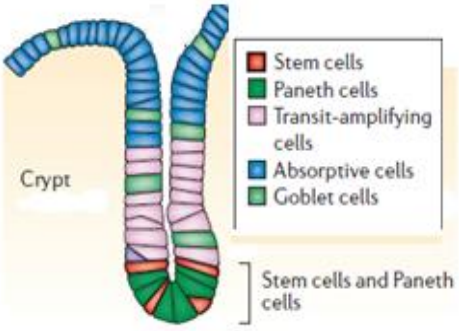

Figure 5[25]

The epithelial renewal occurs in the crypt through a coordinate series of events by stem cell which is compensated by apoptosis. In normal condition cells proliferated at the bottom of crypt, differentiated as they migrated from the base crypt toward the surface. They die and extruded into lumen. In colon cancer there is an expansion of the proliferative zone to the whole crypt[26].

Morphological change in CRC

One of the earliest events in CRC is change of the proliferative pattern of epithelial cells in the colonic crypt; resulting crypts which are appear larger, thicker and darker than normal under light microscope. These crypts are referred as aberrant crypt or aberrant crypt foci (ACF) in the cluster form [27]. A Small number of ACF will progress to a tumour mass or polyp which is protrusion into the lumen. Histologically, polyp can be either hyperplastic (non-neoplastic) or dysplastic (adenomatous) polyp. Hyperplastic is consists of large number of cells with normal morphology and dysplastic is consists of large number of cells with abnormal morphology. A dysplastic polyp can grow in disorganized fashion from premalignant adenoma to lesions called carcinoma through several genetic alternations. Finally, malignant adenoma-carcinomas are characterized by the ability to invade the surrounding tissues and migrate to distal organ for example liver can forms[26,28,28].

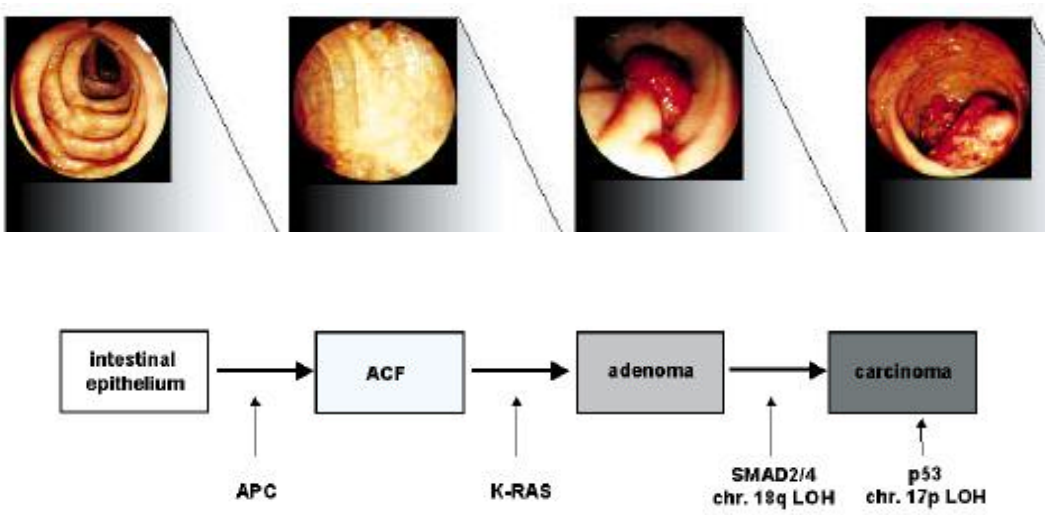

Figure 6

The adenoma carcinoma sequence: stepwise progression from normal epithelium to carcinoma due to a series of genetic change

Genetic changes in CRC

CRC occurs as a result of a sequence of genetic mutation and genomic instability in a step wise manner that lead to uncontrolled cell division and tumour formation. Identification of genetic abnormalities that accumulate in a step wise manner has led to a well-known model, called the adenoma carcinoma sequence introduced by Fearon and Vogelstein[29].

Mutation and inactivation of adenomatous polyposis coli (*APC*) tumour suppressor gene is present already at the ACF stage and early stage in CRC [30]. Mutation at *APC* gene results in the activation of Wnt signalling which promotes the formation of small adenomas in the form of polyps[28]. Mutation at *KRAS* oncogene represents the second step in the adenoma carcinoma sequence, *KRAS* mutation leading to the activation of the Ras/Raf/MEK/ERK signalling pathway. Activation of this signalling pathway results in activation of genes that involved in cell proliferation, apoptosis, cyclin and cyclin dependent kinase[31,32]. Mutation in other oncogenes like *BRAF* is also found among adenomas[33]. At least 50% of large adenomas and 75% of carcinomas show loss of heterozygosity (LOH) at large arm chromosome 18. LOH at short arm chromosome 17 is also correlated with transition from benign adenoma to invasive cancer[29,34, 35]. Mutation in tumor suppressor gene *SMAD* 2/4 and *TP53* have also been identified[1]. P53 is a multifunctional protein essential for cell growth control and is also known as the ``guardian of the genome`` because it can block cell proliferation, when DNA damage is presence[36]. Inactivation of p53 is a key genetic step in the development of colorectal cancer and often coincides with the transition from large adenomas into invasive carcinomas[37]. The identification of these genetic changes has provided important information in the cellular process underlying tumorigenesis in the CRC.

Diagnosis and Treatment

CRC has not specific symptom until it reaches an advanced stage, but non-specific symptoms such as abdominal pain, change in bowel habits, weight loss and blood in feces are available. The diagnosis is made by fecal occult blood test, endoscopy, colonoscopy and CT colonography[38]. Once diagnosis is made, the disease should be staged. Staging is very important for making the best treatment and determining the patient prognosis. Two classification systems are being used for the staging of the CRC: Dukes classification and TNM system. Staging is usually done by the tumour-node- metastasis (TNM) staging system which was introduced in 1978 by UICC. In the TNM system patient are stratified according to depth of tumour (T), positive lymph node (N) and distance metastasis (M). Surgery and chemotherapy is widely used for treatment of all stage of CRC[1].

Tabel 1

TNM Classification (American Joint Commission on Cancer)				Dukes' Classification
Stages	T Main tumor	N Lymph nodes	M Metastatic disease	Stages
Stage 0	Tis	N0	M0	
Stage I	T1	N0	M0	A
	T2	N0	M0	
Stage II	T3	N0	M0	B
	T4	N0	M0	
Stage III	Any T	N1	M0	C
	Any T	N2	M0	
Stage IV	Any T	Any N	M1	D

TNM and Duke`s classification system[25]

Many of the molecular changes that are associated with cancer cells occur in cell signalling pathway that regulates cell proliferation and apoptosis. Therefor understanding the mechanism behind the cell cycle and apoptosis give us important information for the following action of a natural product compound or drug on cancer cells. In the following section a review of the basic concept of the cell cycle and apoptosis is given.

Cell cycle

The eukaryote cell cycle consists of two basic parts: interphase and mitosis (see figure 7). Interphase can further divided to G_1 phase, S phase and G_2 phases. During gap phase 1(G_1 phase), synthesis phase (S phase), and G_2 phase the cell grows, duplicates DNA and prepare for mitosis phase (M phase), in which one cell divided into two identical cells. The M phase can also divide further into pro-, meta-, ana- and telophase preceding the cytokinesis. During G_1 phase the cell metabolically active and grows but does not replicated its DNA. If DNA damage detected, G_1can be delayed to allow time for repair. $G_1$is follow by S phase (synthesis phase) which DNA replication takes place and cell increase in size. Then S phase follow by G_2 which cell grows, proteins are synthesized in preparation for mitosis. Depending on the type of the cell some cells come out of the cell cycle, while still remaining viable, this is known as G_0 phase. Cell in G_0 phase can continue towards proliferation when growth factors and nutrients are available or toward apoptosis if necessary. Through the cell cycle three different check point: start check point or G_1 check point, G_2 /M check point and metaphase anaphase checkpoint or M check point exist, where the cycle can be

arrested if for example defect in DNA synthesis[39]. During the cell cycle arrest repair mechanism is activated and preventing the defects to be inherited by daughter cells.

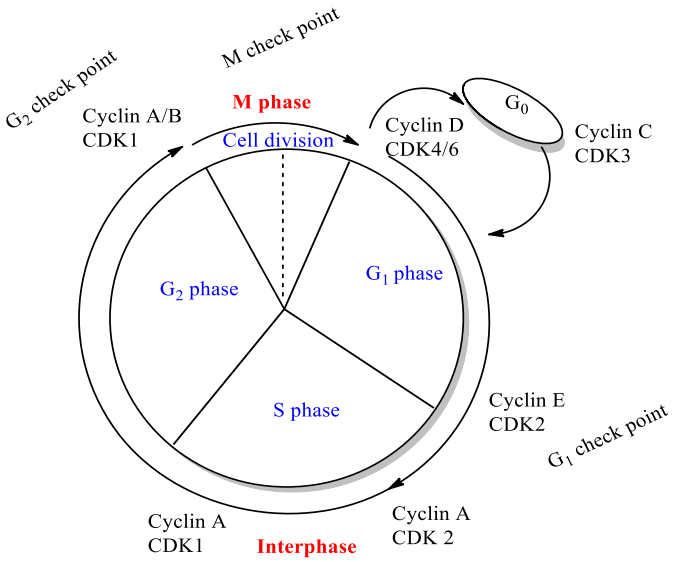

Figure 7

Cell in the G_0 enter G_1 when concentration of cyclin C increase and cyclin C is associated with Cdk3. Binding of Cyclin E to Cdk2 is necessary for transition from G_1 to S phase. Association of cyclin A with Cdk2 is required for passage into S phase while association with Cdk1 is required for completion of S phase and entry into G_2 phase. CyclinB-Cdk1 controls event and completion of mitosis. The G_2 phase provides a break between DNA synthesis and mitotic division. This is important because this gap can ensure DNA replication is correct. The gap phases separate two active phases allowing proper completion of the previous phase.

Cyclins & CDKs

The cellular checkpoints controls with different molecular mechanism such as cyclin and cyclin dependent kinase (CDK). Cyclins are a group of proteins that regulated the cell cycle, as these are formed and destroyed at specific time point. They named cyclin because of the cyclical concentration during the cell cycle[40]. Cyclins can be divided into four classes G_1/S cyclins, S cyclins, G_2 cyclins and M cyclins. They form complexes with cyclin dependent kinases (Cdks) which in contrast to cyclins have stable concentration during the cell cycle. Once they form complexes, Cdks become active kinases that phosphorylate target molecule such as retinoblastoma protein (pRb) which is an inhibitor of transcription factor E2F. Phosphorylation of Rb promotes release of transcription factor E2F and bring the cell from G_1 phase to S phase[41,42].

Table 2

Class	Cyclin	CDK
G1	D(1,2,3)	CDK4, CDK6
G1/S	E, D	CDK2, CDK4
S	A	CDK2, CDK1
M	B	CDK1

Cyclins can subdivided further, for example D1, D2 and D3[40] as shown in the table

Cyclins are not properly regulated during oncogenesis, specially cyclin D1 and E which are often overexpressed in human cancer cell [42 43 44 45].

CDK inhibitors

The activity of CDKs is also regulated by CDK inhibitors. CDK inhibitors are also proteins that can bind to CDK/cyclin complexes and cause inactivation of these complexes[40]. For example p 21, p27 and p57 are CDK inhibitory proteins that can bind to CDK2/cyclin E and A in order to inactivate them. As the result cell cannot go from G_1 to S phase and the cell cycle halted or cell G_1 arrested. In addition regulation of p21 is largely dependent on the presence of the p53, a transcriptional regulator that mediates cell cycle arrest after DNA damage. In the cell cycle arrest, DNA reparation system has time enough for reparation. Fail in the cellular repair mechanism or dysregulation in cellular checkpoint is observed in many cancer cells. For example in downregulation of p27 and CDK inhibitors, proliferation is increased and cell can easily go from G_1 to S phase. Upregulation of cyclins and CDK are common in human cancer cells. The knowledge of evets and mechanism in the cell cycle increase understanding of how a cell can be become cancerous and how we can fight better cancer cells.

Apoptosis

The term apoptosis from Greek origins (apo=for, ptosis=falling), was chosen to describe the cellular process of programmed cell death[46]. Apoptosis or programmed cell death is involved in the regulation of many physiological and pathological processes that occurs naturally during development of many tissues, since tissue homeostasis is the result of the balance between proliferation and apoptosis. Cell populations that have a high rate of proliferation, such as the

intestinal epithelium, depend upon apoptosis to maintain necessary number of cells. Apoptosis is a complex process involving different proteins with two major extrinsic and intrinsic pathways. Cancer cells are resistance to apoptosis, therefore a better understanding of the molecular mechanism that cause apoptosis provide a better understanding of cancer cells [47]. Beside apoptosis model of cell death, necrosis, autophagy, mitotic catastrophe and lysosomal cell death are also exists. In contrast to apoptosis, necrosis is not a genetically programmed function, it affect group of neighboring cells and produces as in inflammatory response[46].

Extrinsic pathway of apoptosis

Extrinsic pathway is activated when Fas ligand is released from surrounding cell, bind to Fas receptor and cause activation of FADD. The Fas receptor is a death receptor belong to the TNF receptor gene superfamily which are responsible for triggering extrinsic pathway. Fas is present on a variety of cell types including activated B cells and D cells. FADD is an adaptor protein that bridges Fas receptor to procaspase 8 and 10 to form the death inducing signaling complex known as DISC. As the result pro-caspase 8 becomes active, activate caspase 8 dimers leave DISC and releases into the cytosol. Here they activate pro-caspase- 3 and -7, resulting in nuclear protein cleavage and the initiation of apoptosis. [46, 47]

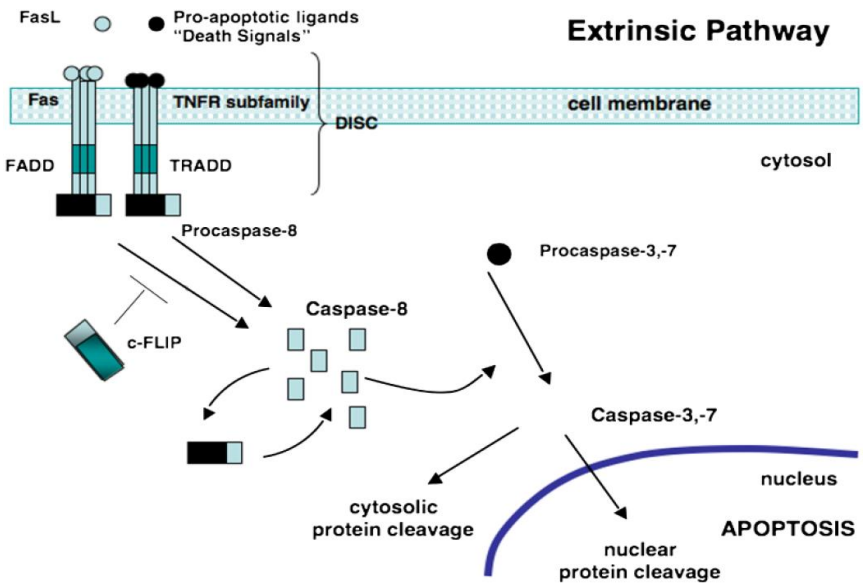

Figure 8

Extrinsic pathway of apoptosis [46]

Intrinsic pathway of apoptosis

Intrinsic pathway is also called mitochondrial pathway, because is associated with release of cytochrome c protein and Bcl-2 superfamily proteins such as Bid from mitochondrial into the cytoplasm. The Bcl-2 superfamily proteins are the second member of a range of proteins found in folicullar lymphoma. They are present on the outer mitochondrial membrane as dimer where they control membrane permeability in ion channel fashion or through creation of pores. They are subdivided into 3 groups based on structural similarities and functional criteria. Group I poses anti-apoptotic activity while group II and III promote cell death. The balance between pro and anti-apoptotic of this family determine whether or not a cell undergoes apoptosis. Intrinsic pathway is activated by mitochondrion as a result of intracellular stress such as DNA damage, radical oxygen species, radiation, chemotherapeutic agents, cytokines and glucocorticoids. In such situation p53 is activated and therefor becomes the key regulator of apoptosis. Activation of p53 leading to activation of other pro-apoptotic proteins such as Bax and Bak which leads to formation of pores and release of different substance such as cytochrome c from mitochondria. Cytochrome c is combines with Apaf-1 and procaspase 9 forming an apoptosome. Subsequently pro-caspase 3 and pro-caspase 7 are activated by caspase 9 which leading to apoptosis. A third type of pro-apoptotic activity found in inactive form in the cytoplasm. When activated by caspase 8, from the extrinsic pathway caused activation of cytoplasmic protein Bid. Activated Bid is referred to t-Bid allowing Bax to translocate into the mitochondria. This is one method or cross-talk that occurs between intrinsic and extrinsic pathways. Activation of Bax causes the release of several mitochondrial factors, such as Smac/DIABLO that inactivated IAP (inhibitors apoptosis protein)[46]. Caspases are essential in both apoptosis pathways, thus a short description of these proteins is given.

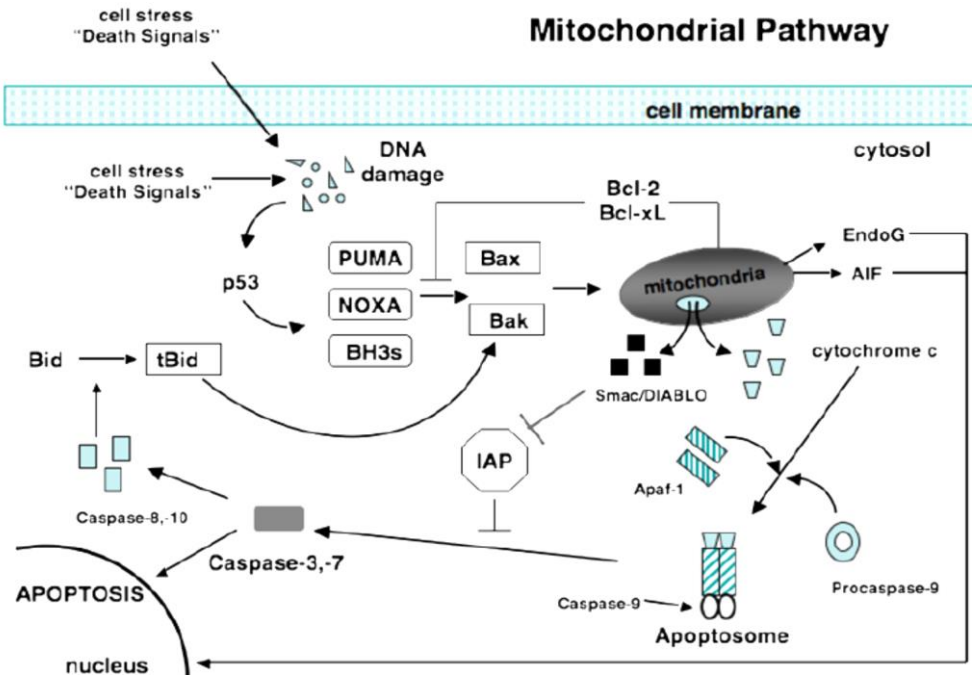

Figure 9

Intrinsic pathway of apoptosis [46]

Caspases

Caspase**s** or **c**ysteine **asp**artate-**s**pecific prote**ases** are a family of protease enzyme that playing central role in both apoptosis pathways. Caspases subdivided into two groups: initiator caspases and effector caspases. Caspases 8,9,10 are considered initiator caspase responsible for activation of effector caspases (3, 6, 7). Effector caspase have a range of cellular target in degradation process through a cascade mechanism. At least 14 caspases are known in mammalian (named from caspase 1 to caspase 14). They synthesized in inactive forms (zymogens) known as pro-caspases. The activities of caspases are regulated by inhibitors which bind to pro-caspases and inhibit activation of pro-caspases. Pro-caspases are cleaved by specific initiation mechanism which results in their activation[5]. The active caspase is a heterodimer with two active sites which can cleave selectively several substrates and other pro-caspases. The substrate for initiator caspases are the effector caspases and effector caspases cleaved a wide range of other proteins which is important in apoptosis cascade mechanism. For example caspase 6 and caspase 3are cleaved the nuclear mitotic apparatus protein. The cleavage mediates the shrinkage and fragmentation of nuclei and DNA. Caspase downregulation or deficiency has been identified as a cause of tumor development.

It is important to know based on measurement of caspase two pathways can distinguished from each other. The type I is caspase 8 dependent pathway and the type II is caspase 9 dependent pathway[10].

Polyphenols & Chemoprevention of cancer

From the name, it is clear compound that have more than one phenolic hydroxyl attached to one or more benzene rings are known as polyphenol. Polyphenolic compounds are the most studied of phytochemicals. The word phyto is derived from the Greek word phyto, which means plant. Phytochemicals are defined as bioactive, non- nutrient plant compounds that have been linked to reducing the risk of major chronic diseases[48]. The interest in polyphenol compounds is that many of them have anti-cancer properties and have health benefits for human. Fruits and vegetables are rich sources of polyphenols and consumption of food with polyphenols reduces the risk of different types of cancer [49]. These compounds can be classified based on the number of phenolic ring in their structure, the structural elements that bind these rings each other's and the substituents linked to the ring into two main groups of flavonoids and non-flavonoids. Flavonoids share a structure formed by two aromatic rings, linked together by three carbon atoms through an oxygenated heterocycle (see figure 10) [50].

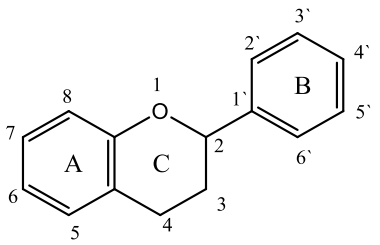

Figure 10

Flavonoid skeleton

Stilbenoids, such as resveratrol and pterostilbene are non-flavonoids polyphenolic compounds, known to have diverse pharmacologic activities including chemoprevention potential[7]. Chemoprevention is defined as non-toxic natural or synthetic compound that can prevent or halt carcinogenesis. Carcinogenesis is considered of three stages: tumour initiation, promotion and progression (see figure 11).

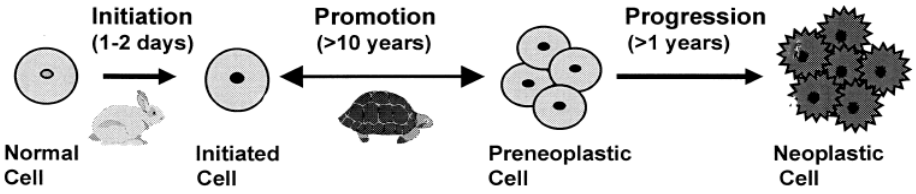

Figure 11

Initiation is a rapid and irreversible process. In contrast to initiation, tumour promotion is lengthy and reversible process. Progression involves the growth of the tumour with invasive and metastatic potential. [51]

Phytochemicals can interfere with different steps of this process. Lee Wattenberg, subdivided chemo preventive agents into two main categories: blocking agents and supressing agents.

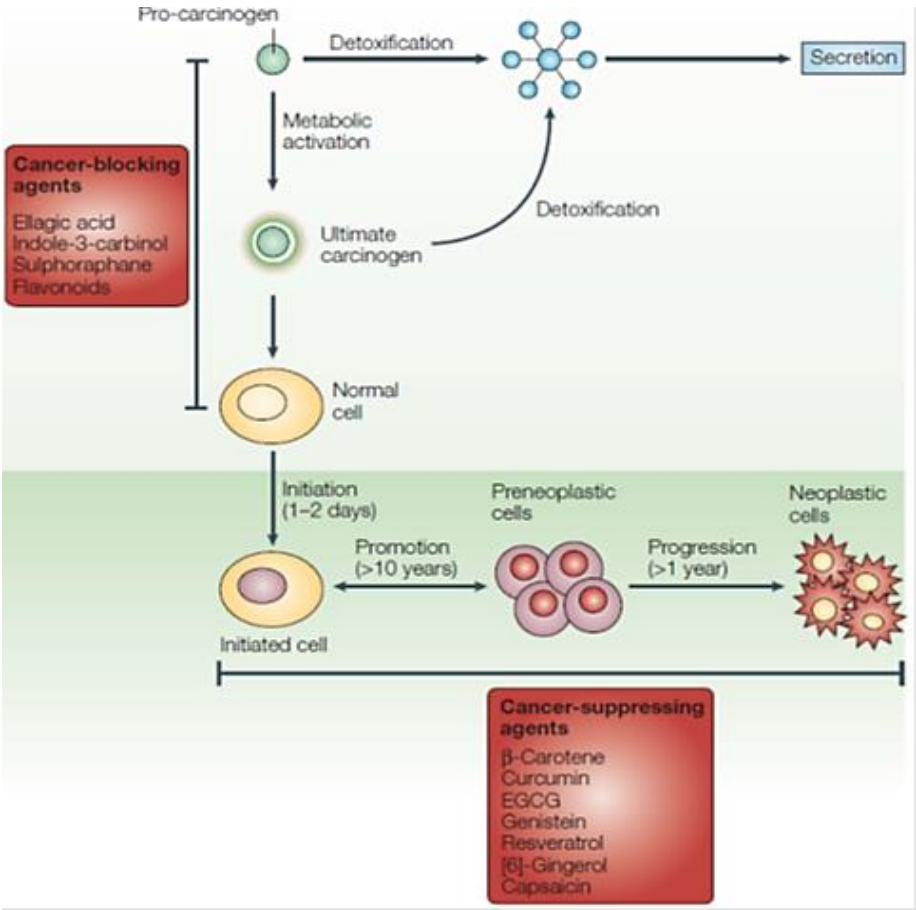

Figure 12

Blocking agents prevent carcinogens from reaching the target site, from undergoing metabolic activation or from subsequently interacting with crucial cellular macromolecules for example DNA, RNA and proteins. Suppressing agents, on the other hand, inhibit the malignant transformation of

initiated cells in either promotion or progression stage[52]. The cellular and molecular events that are affected or regulated by these chemopreventive phytochemicals include detoxification, DNA repair, cell cycle progression, cell proliferation, apoptosis, and activation of tumour suppressor genes[52]. Both RV and Pter have chemoprevention potential on different cancer cell lines[53, 54] by effect on different proteins or transcription factors, they can supress proliferation, induce apoptosis or both. For example Wolter et al. reported that RV can induce apoptosis by an increase in activity of caspase 3 of Caco-2 cell line[55]. Delmas et al. reported that RV at concentration 10µM to 100 µM activated various caspase and triggers apoptosis in human colon cancer cell line SW480[56].

Lesser studied stilbenoids, Pter has also shown to inhibit colonic cancer growth through apoptosis. Pter by inhibition production of inflammatory enzymes such as nitric oxide synthetase (iNOS) and cyclooxygenase-2(COX2) can inhibit grow of colonic cancer cells. Therefore Pter can diminish also inflammatory response in colon which is clinically important for both colon cancer and inflammatory bowel diseases[54]. Pter inhibit growth of colon cancer through downregulation of the anti-apoptotic Bcl-2 family and increase pro-apoptotic Bid, Bax and Bad. In vivo colon cancer study, Pter decrease the total number of aberrant crypt foci (ACF) in an azoxymethane induced colon cancer to a greater extent in compare with RV. [57]

Chemical property of RV & Pter

Resveratrol is a white powder, fat soluble compound with low solubility in water[9]. RV was originally isolated by Takado from the roots of white hellebore lily in 1940, and later, in 1963, from the roots of Japanese knotweed [58]. It is a stilbene with three hydroxyl groups. The name stilbene is derived from the Greek word stilbos, which means shining, because they show intense blue fluorescence under ultra violet light[59]. Stilbene or 1,2- diphenyl ethylene exists as two isomeric forms: (E) and (Z)-stilbene also known as trans and cis stilbene respectively [60].

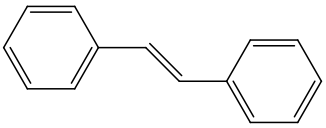

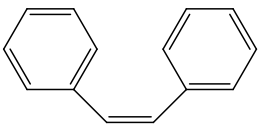

Figure 13

Trans-Stilbene Cis-Stilbene

The steric interaction of phenyl ring makes the cis isomer less stable. Trans-stilbene has a melting point of 125 °C, while the melting point of cis stilbene is around 6°C. [61]

Resveratrol contain both resorcinol and phenol moieties. The name was considered as resorcinol derivative coming from Vertatrum grandiflorum and therefore it called resveratrol[62].

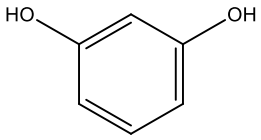

Figure 14

Resorcinol

Pter was originally isolated from the heartwood of red sandalwood (Pterocarpus santalinus) and is also found in blueberries and other berries[63]. Pter with two methoxy group and one hydroxyl group is more lipophilic than RV and has a higher potential for cellular uptake than RV with three hydroxyl groups. Pter has a higher bioavailability with a longer half-life than RV [54]. The structural formula and numbering carbon of RV, Pter and Pr.Pter are shown in the below.

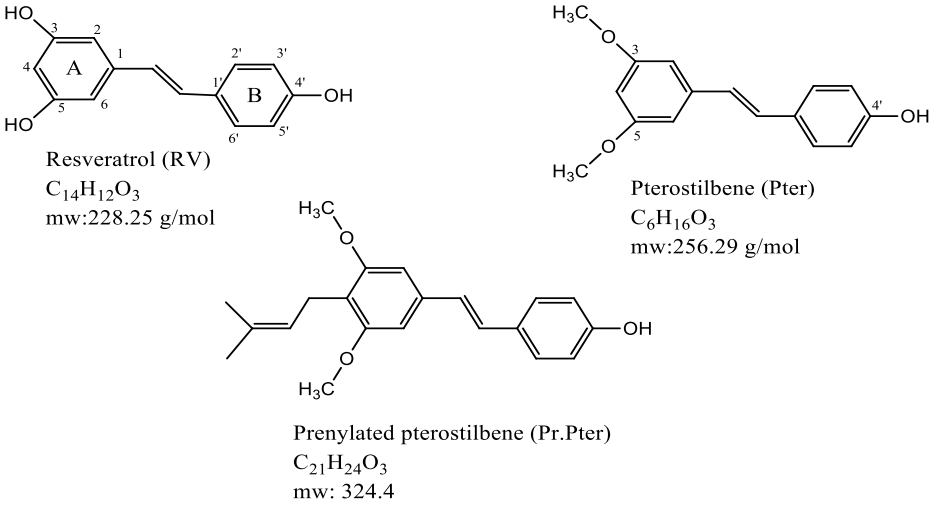

Figure 15

RV is named as trans-3,5,4′ trihydroxy stilbene. Pter as trans-3,5-dimethoxy-4′-hydroxy stilbene and Pr.Pter as 4-[(E)-2-[3,5-dimethoxy-4-(3-methylbut-2-en-1-yl)phenyl]ethenyl]phenol.

Synthesis of prenylated pterostilbene (Pr.Pter) was one of the purposes in this thesis. Therefor in the final part of this chapter a short description of prenyl and prenylation is given.

Prenyl & Prenylation

Prenyl or isoprene with IUPAC name 3-methyl-2-buten-1-yl and chemical formula C_5H_8 is a branched hydrocarbon with five carbon and a doubly bound as shown in figure 16.

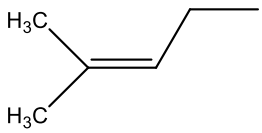

Figure 16

3-methyl-2-buten-1-yl (prenyl)

Based on the size of the carbon geranyl with ten atom carbons, farnesyl with 15 atom carbons and geranylgeranyl with 20 atom carbons are also identified [64]

Geranyl

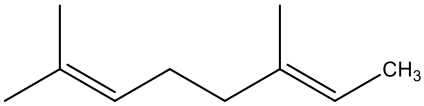

Farensyl

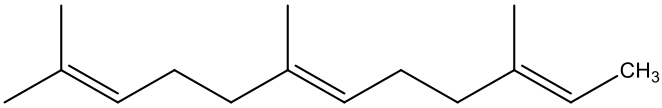

Geranylgeranyl

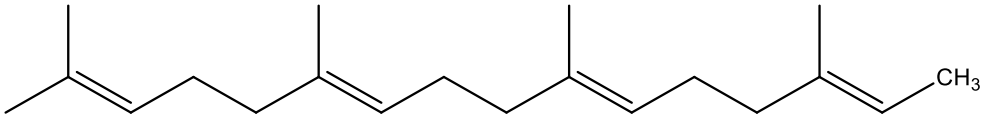

Figure 17

Prenylation is chemical or enzymatic addition of an isoprene side chain to another molecule [64] and plays a major role in the diversification of polyphenol compounds found in nature and often results in derivative with improve or modified pharmacological activity[65]. For example prenylated acridone alkaloids have more potent activity in compare to the non prenylated compounds against Epstein Bar virus in vitro[64].

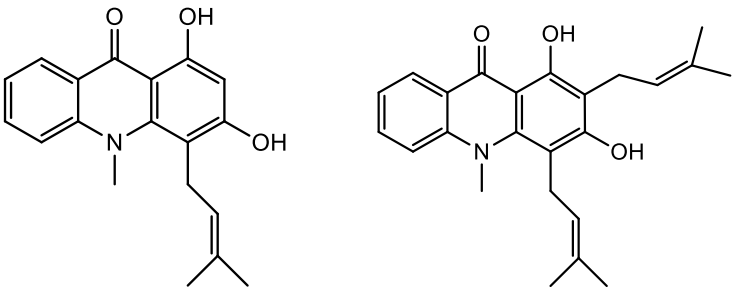

Figure 18

Prenylated acridone alkaloids are isolated from plants of the gerena Citrus[64]

Similarly the prenylated pyranoacridone showed more potent antitumor activity than non prenylated one. Prenylated flavonoids such as 8-prenylkaempferol and xanthohumol are other examples of prenylated natural product compounds, which have bioactivity in several vitro investigations [11 66 64]. These finding indicate that the isoprene side chain is an important structure feature and can be exploited in new drug development[14].

Chapter 2

Synthesis strategy

Synthesis natural product in the laboratory is an interesting subject for organic chemist and various attempts have been made to synthesize new derivatives of resveratrol to improve its biological activities. Before the onset of present study, Pr.Pter was synthesized with inspiration of Yong Rok Lee(see figure 19) [67]. Protected benzyl phosphonate (compound **8**) commercially unavailable and was also synthesized at three steps. HNMR and GC mass were used to validate product and determine its purity in each step.

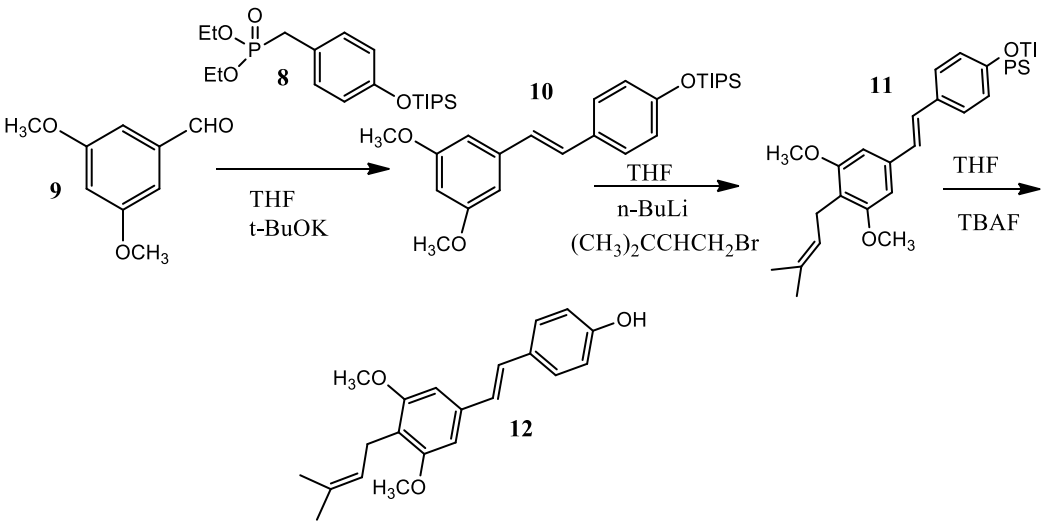

Figure 19

In order to synthesis protected benzyl phosphonate (compound 8) synthesis strategy was made as seen in figure 20. Although compound 8 was synthesized by another method and this method did not work for me, but the method is described in the following part of this thesis. Compound 8 can be made by three steps as shown in figure 20.

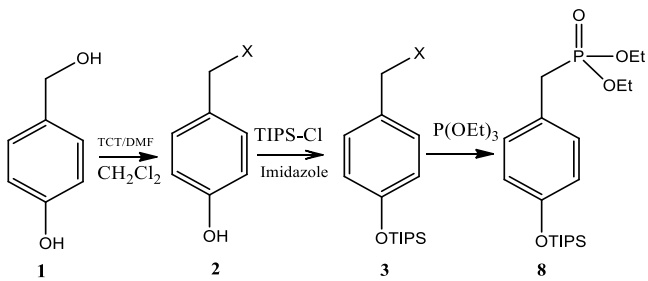

Figure 20

X=Br, Cl

Halogenation of 4-hydroxybenzyl alcohol in the first step converts the hydroxyl group to a better leaving group by a TCT/DMF system. The next step is protection of the phenolic hydroxyl with tri-isopropyl silyl chloride and finally synthesis of benzyl phosphonate ester from benzyl halide via Michaelis Arbuzov reaction.

Synthesis of 4-hydroxy benzyl bromide /chloride by TCT/DMF

A rapid and highly selective chlorination and bromination method has been developed by using of TCT and DMF. The use of TCT (2,4,6 trichloro-1,3,5-triazine) or cyanuric chloride has been reported for conversion of alcohol into alkyl halides[68].

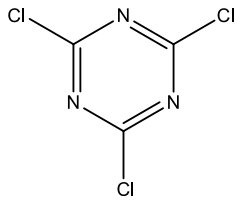

Figure 21

TCT or cyanuric chloride

TCT is a cheap reagent, already available in the RUC and conversion of alcohol to halide can be done without affecting the phenolic hydroxyl group. The method is based on the reaction between TCT and DMF at room temperature.

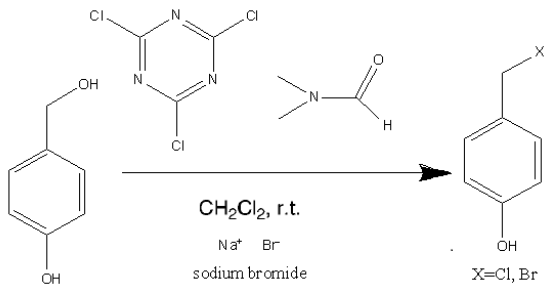

Figure 22

Both bromination and chlorination can be obtained by this method in a very simple way. Bromination can be obtained by addition of two equivalents of sodium bromide to the mixture of TCT and DMF, followed by addition of alcohol. Chlorination can be obtained by addition only of alcohol to the mixture of TCT and DMF[69].

Mechanism of TCT/DMF reaction

It is believed that in this reaction the iminium cation and cyanuric chloride is formed. The positive charge and small size of the iminium cation make it easy target for OH group. In the next step attack of the electron lone pair of oxygen to the iminium cation and finally by nucleophilic attack of halide ion product is formed.

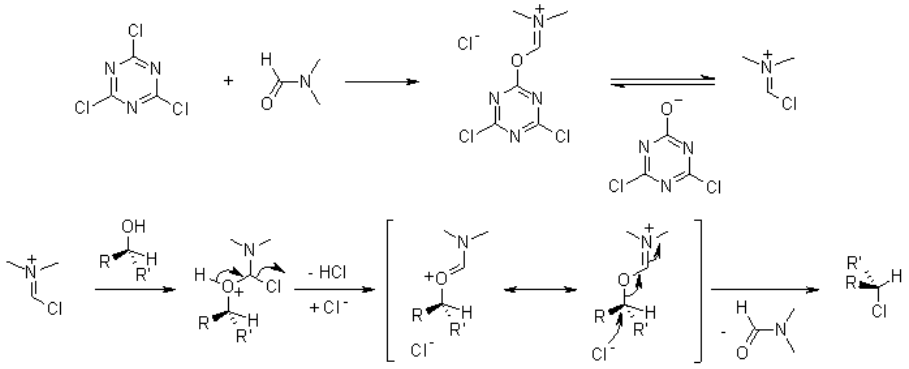

Figure 23

Possible mechanism [70]

Bromination with this method was unsuccessful. Bromination was tried twice without any formation of the product. Both brominated and chlorinated compound can also be used for the next step in the Michaelis Arbuzov reaction. Therefore chlorination was also tried by this method. Chlorination was done successfully, but because of impurity a new strategy was chosen.

New strategy

A new synthesis strategy must be designed for synthesis the target molecule. Different methods can be used for synthesis the target molecule. For example bromination by bubbling of HBr gas into the solution of p-metoxy-benzyl alcohol[71].

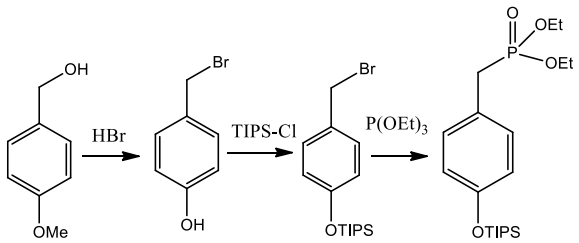

Figure 24

Bromination by HBr gas

Chloromethylation of phenol is another strategy. In this method $–CH_2Cl$ can introduce into phenol by chloromethyl methyl ether (CMME)[72, 73, 74].

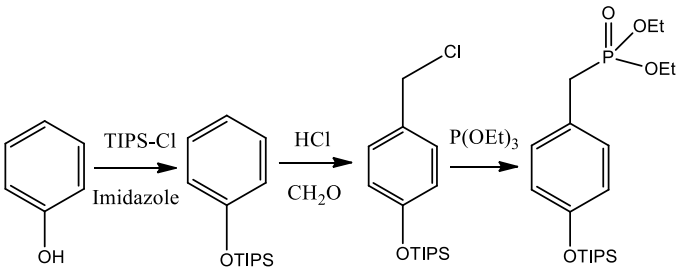

Figure 25

Chloromethylation of phenol by (CMME)

Among different methods, 4-hydroxy benzaldehyde was chosen as starting material for synthesis the target molecule (see figure 26), because it is cheap, safe and was already available in the Roskilde University.

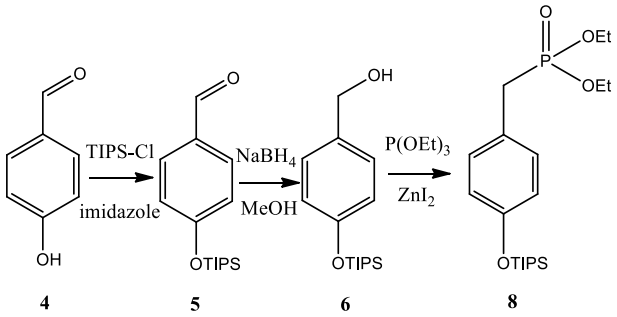

Figure 26

Steps in this strategy are protection of hydroxyl group by TIPS-chloride, reduction of aldehyde to alcohol by $NaBH_4$ and finally direct phosphonation of alcohol by tri ethyl phosphite and Zink Iodide. In the following part each step is described in details with its chemical mechanism.

The protection of phenolic alcohol by TIPS ether

A central problem in organic synthesis is to ensure that a specific hydroxyl group is protected from unwanted reaction. Therefor protecting groups plays an important role in multistep organic synthesis such as syntheses of natural products. Protection of hydroxyl group by the formation of silyl ether has been widely used in organic synthesis. Trialkylsilyls are usually used as protecting group of primary and secondary OH in organic synthesis since they can be installed and removed

under mild conditions[75]. A common strategy which was found by E.J. Corey was reaction of tert-butyldimetyl silyl chloride (TBDMS-Cl) with alcohol in the presence of imidazole[76].

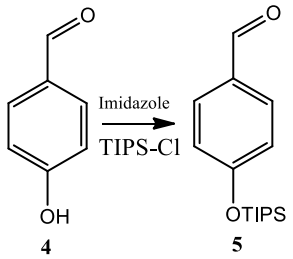

Figure 27

Tri-isopropyl chloride is sensitive to water and can hydrolyzed by water, therefor dry solvent and glassware was used. Molecular sieve was used for drying of dichloromethane. DCM is non hygroscopic solvent and easily was dried by molecular sieve[77].

Mechanism of the protection reaction

Corey assumed the reaction proceeds via formation of the reactive intermediate as seen in figure 28. Nucleophilic attack by lone pair N-3 imidazole to the electropositive silicon is the key of formation this intermediate. The silicon atom in the same group as carbon is more electropositive than carbon and more susceptible toward nucleophilic attack and substitution. Then lone pair attack of oxygen which has a greater affinity to silicon is the driving force in the next step. All silyl ethers can also be obtained in the same way. Generally, primary OH reacts faster than secondary OH and primary silyl ethers are cleaved easier than secondary silyl ethers [78] [76].

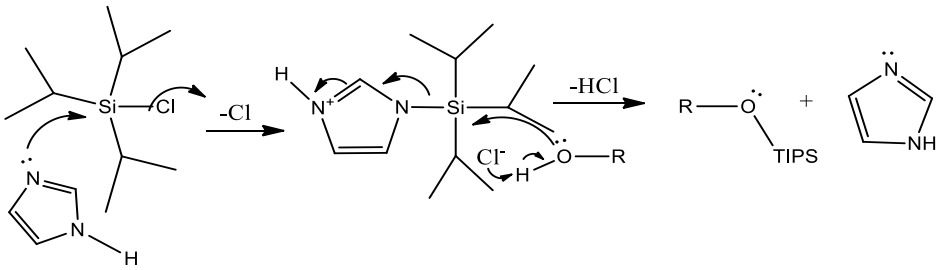

Figure 28

Silyl ether protecting group

There are many other of tri-alkyl silyl chloride reagents which can be used as hydroxyl protecting group, for example tri-methyl silyl- (TMS), tri-ethyl silyl- (TES), tert-butyhl dimethyl silyl- (TMDMS or TBS) and tri-isopropyl silyl- (TIPS) (see figure 29) [79].

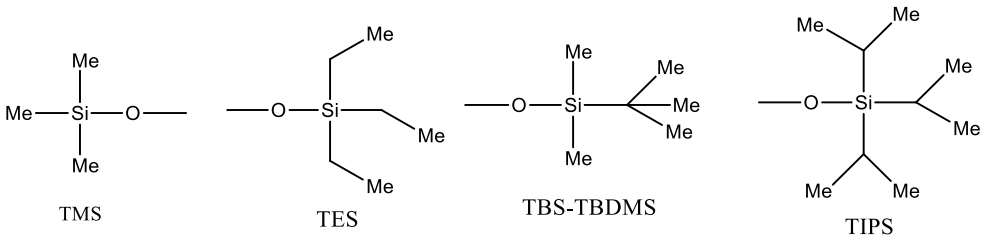

Figure 29

Some of silyl ether protecting groups, the bulky TIPS is the most stable under different conditions. In general bulkier the substituents on silicon atom make silyl ether more stable toward acidic and basic condition, therefore the bulky TIPS was used in the reaction.

Reduction of 4-OTIPS benzyl aldehyde to 4-OTIPS benzyl alcohol

In the next step protected benzyl aldehyde was reduced to alcohol by sodium borohydride, therefore a short description of sodium borohydride is given.

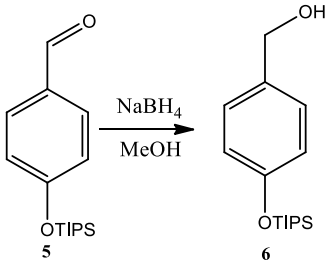

Figure 30

Sodium borohydride ($NaBH_4$)

Sodium borohydride ($NaBH_4$) is a cheap and mild reducing agent which use for selectively reduction of aldehyde and ketone to alcohol, without reduction of other functional group such as benzene or double bond[80]. This compound was discovered in the 1940s by H. I. Schlesinger[81]. Generally, aldehyde is more susceptible to reduction than ketones for both electronic and steric reason. Because of its selectivity and rapidity in aldehyde reduction is a useful reducing agent. $NaBH_4$ can hydrolysis by water to flammable hydrogen gas and sodium metaborate, therefor dry solvent and glassware was used in the reaction[82].

$$NaBH_4(s) + 2H_2O(l) \longrightarrow NaBO_2(s) + 4H_2(g)$$

Figure 31

Mechanism of the reduction reaction by $NaBH_4$

Sodium is slightly electronegative than boron. Therefor $NaBH_4$ is a source of hydride and the reaction begins with attack of nucleophile hydride to carbon of carbonyl, resulting C-H bond forms and carbonyl bonds breaks which makes oxygen negatively charged as seen in figure 32.

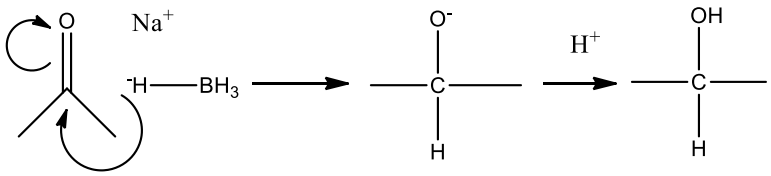

Figure 32

Mechanism of reduction reaction by $NaBH_4$

In the next step protonation by a source of proton (methanol or water) will convert anion oxygen to alcohol. Methanol was used in the reaction and sodium methoxy borohydride was formed $Na^+(BH_3OCH_3)^-$. This compound can also reduce three others carbonyl to alcohol and white solid $NaB(OMe)_4$ was formed which was removed by filtration. This reaction was done successfully and product was formed[83 84 82]

Phosphonation

In the next step benzylic phosphonate compound was synthesized and used as HWE reagent. Phosphonates are organophosphorus compounds with wide application in organic chemistry. Therefor a short review of phosphorous and organophosphorus is given.

A brief history of phosphorous

The name phosphorous is derived from the Greek phos meaning light and phorous meaning bearer. Phosphorous was discovered around 1669 by the German alchemist Hening Brandt on his search for the famed philosopher`s stone. After distillation of urine he found in the recipient a luminant matter that has since been called phosphorous [85]. Later phosphorous was also found in bones, other parts of various animals or plants and phosphorous become another important element of life. Phosphorous has several allotropes: white, red and black forms are the most common[85]. These names are derived from their appearance. All three forms contain phosphorus atoms in different arrangement and

connectivity[86]. Phosphorous can form bond with both metals and nonmetals such as oxygen and carbon. It forms strong bond with oxygen and formation of this bond is driving force in many reactions such as Arbuzov and Wittig reaction [87]. It can also form bond with different number of atoms in different coordination number, for example from 1 to 6.[88] Phosphorous can have a valence of 3 from the presence of 3 unpaired electrons in its valence shell. However it can also have a valence of 5 because of one electron pair and is usually found as a tri or pentavalent in nature.

Organophosphorus compounds

Organophosphorus compounds are chemical compounds containing carbon-phosphorous bonds. The nomenclature of these compounds is complicated to some extend by the overlap of inorganic and organic nomenclature. Some examples are given in figure 33 [89].

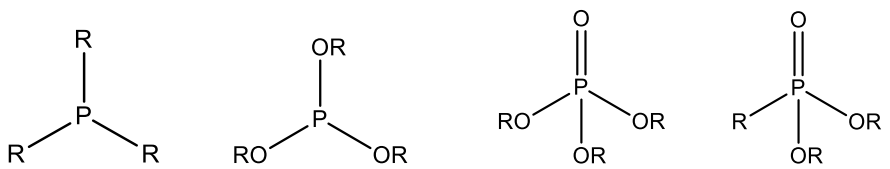

Phosphines Phisphites Phosphates Phosphonates

Figure 33

The structure of phosphonates compound includes a tetra coordinate phosphorous atom in the +5 oxidation state that is connected to two alkoxy group and a double bond to oxygen known as phosphoryl group (See figure 33). Phosphonates have been widely used in industry, medicine and chemistry. In industry they used as flame retardant, pesticides, and chelating agent. In medicine bisphosphonate is another class of phosphonates which used for treatment of osteoporosis. And in the chemistry are used as HWE reagents at the Horner-Wadsworth-Emmons reaction [90].

Synthesis of phosphonate compounds

Phosphonates are usually formed by the Michaelis Arbuzov reaction. In this reaction phosphonates are formed by reaction between a trialkyl phosphite for example tri ethyl phosphite with an organic halide.[91] [92]

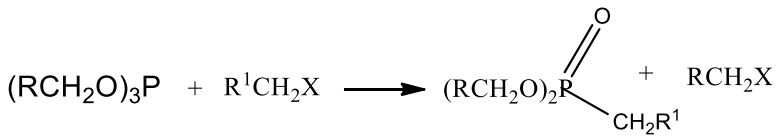

Figure 34

The general Michaelis Arbuzov reaction

The steps involves in the Arbuzov reaction is conversion of an alcohol to a better leaving group such as halide and then reaction with tri alkyl phosphite. As illustrated below, the first step of reaction involves a S_N2 nucleophilic attack by the lone pair of phosphorous on the electrophilic carbon of the alkyl halide to give a phosphonium intermediate. Then anion halide reacts with the phosphonium intermediate to give the desire phosphonate. It has been shown that if chiral phosphonium intermediates are produced, the halide substitution proceeds with inversion of configuration as expected by a S_N2 reaction[90 93].

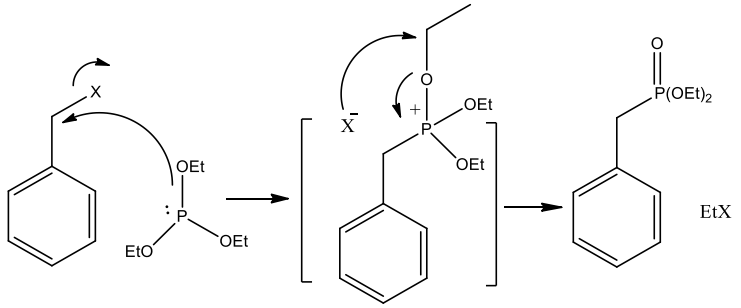

Figure 35

Mechanism of Arbuzov reaction illustrated with benzyl alcohol, the driving force in the Arbuzov reaction is the P=O bond formation [90 93]

Zink mediated phosphonation

Weimer and co-workers recently found an alternative method to the Arbuzov reaction with Zink iodide[94]. They obtained phosphonate compound in good yield based on treatment of alcohol with triethyl phosphite in the presence of ZnI_2 at reflux. Shorter reaction time, milder reaction condition and the lack of the halide intermediate are advantages of this reaction.

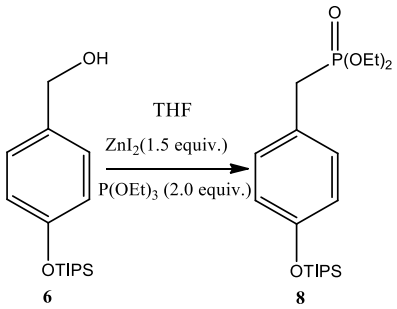

Figure 36

Synthesis of phosphonate by Zink mediated reaction

Both Zink iodide and tri ethyl phosphite are sensitive to water and oxygen[95], therefore dry THF and oven dried glassware was used. THF was dried by (20% w/v) molecular sieve as described in general experiment conditions. Triethyl phosphite is a trivalent organophosphorus compound and like other trivalent organophosphorus compounds is susceptible to oxidation by atmospheric oxygen, forming pentavalent phosphoryl compound. Therefor reflux condenser was flushed by nitrogen for 30 min. before reaction and flask containing triethyl phosphite was also flushed every time the flask was opened. The reaction was done first on 4-methoxy benzyl alcohol and then on 4-OTIPS benzyl alcohol. The byproduct Zink oxide (ZnO) was removed by washing with 1N sodium hydroxide.

$$ZnO + 2NaOH + H_2O \longrightarrow Na_2\left[Zn(OH)_4\right]$$

Figure 37

Sodium hydroxide reacts with byproduct Zink oxide and water soluble zincate is formed.

The product was purified by chromatography on silica gel with 50% ethyl acetate in 50% hexane as eluent. The phosphonate ester was formed by this method and the product was used for the next step in HWE reaction.

Mechanism of phosphonation by Zink iodide

Formation of Zink-phosphite complex was considered for the mechanism of the reaction by Weimer group. A tetra coordinate Zink complex is formed, followed by a formation of C-P bond through a process with Sn1 like character.

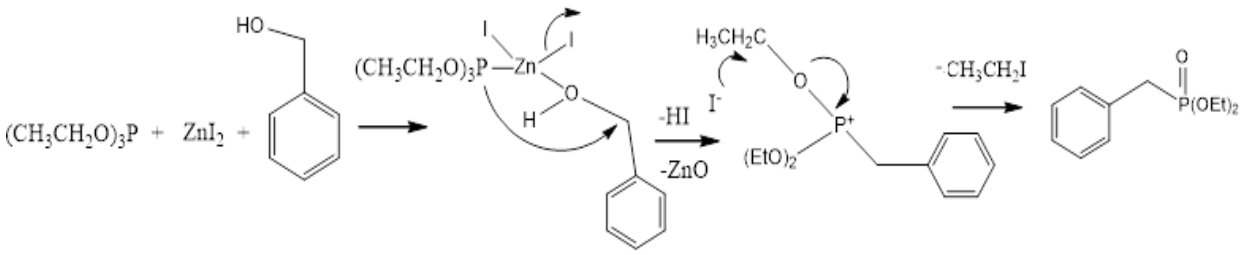

Figure 38

Possible mechanism of reaction[94]

The Horner-Wadsworth-Emmons (HWE) reaction

For the first time in 1953 Georg Wittig could synthesize alkene by using organophosphorus compound[96]. The typical reaction involves of chemical reaction between an aldehyde or ketone with a phosphonium ylide to give an alkene. Horner, Wadsworth and Emmons reaction (HWE) reaction is a modified Wittig reaction was first reported by Horner and later developed by Wadsworth and Emmons[97]. They used phosphonate carbanion instead of phosphonium ylide to produce olefins. The use of phosphonate in HWE reaction has some advantages over the Wittig reaction. The phosphonates carbanion are more nucleophile, stable and reactive than phosphonium ylide, therefor reaction is done in milder conditions. Another advantage of the HWE reaction is that the by product is water soluble and easily separate from product[98].

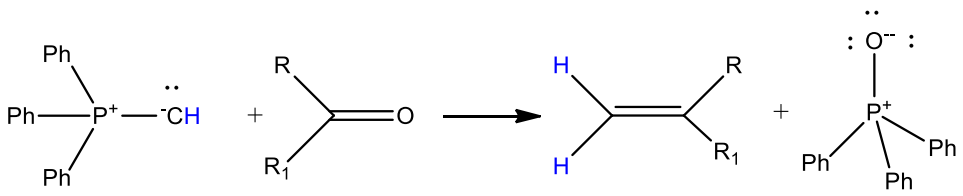

Figure 39

General Wittig reaction

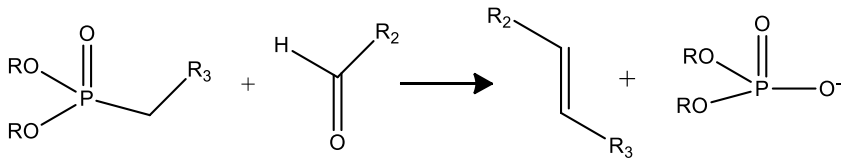

Figure 40

The general HWE reaction

The phosphonate mediate modification of the Wittig reaction is called HWE. In HWE reaction a phosphonate stabilized carbanion react with aldehydes or ketones to provide a trans-olefin product

The mechanism of the HWE reaction

The mechanism of the HWE reaction is similar to the Wittig reaction. The phosphonate ester will react with a base such as t-BuOK to give yilde or stabilized phosphonate carbanion, reactive enough to carry out the reaction [97]. Stabilized ylides are those that possess R substituent that is stabilizing anion by electron withdrawing group such as phenyl group. Such ylides are less reactive and usually only react with aldehydes to give E-alkene. In contrast, non-stabilized ylides possess R substituent that destabilizing anion by electron releasing group such as alkyl group. Such ylides are more reactive and can react with both aldehydes and ketones to give Z-alkene[99].

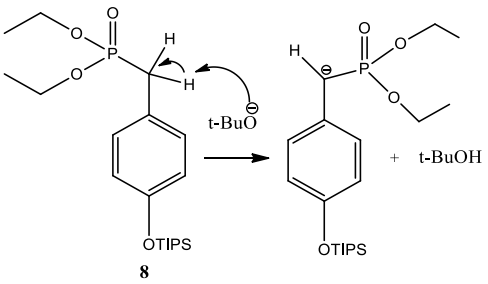

Figure 41

Phosphonate ester will react with a base such as t-BuOK to give phosphonate carbanion[99]

Nucleophilic addition of the phosphonate stabilized carbanion with an aldehyde producing betaine intermediate as shown in figure 42. Then another four membered cyclic intermediate (cis or trans-oxaphosphetanes) is formed. Decomposition of this intermediate via the syn-elimination can give E or Z-alkene and the phosphinate by-product which is water soluble and readily remove from the desire alkene.

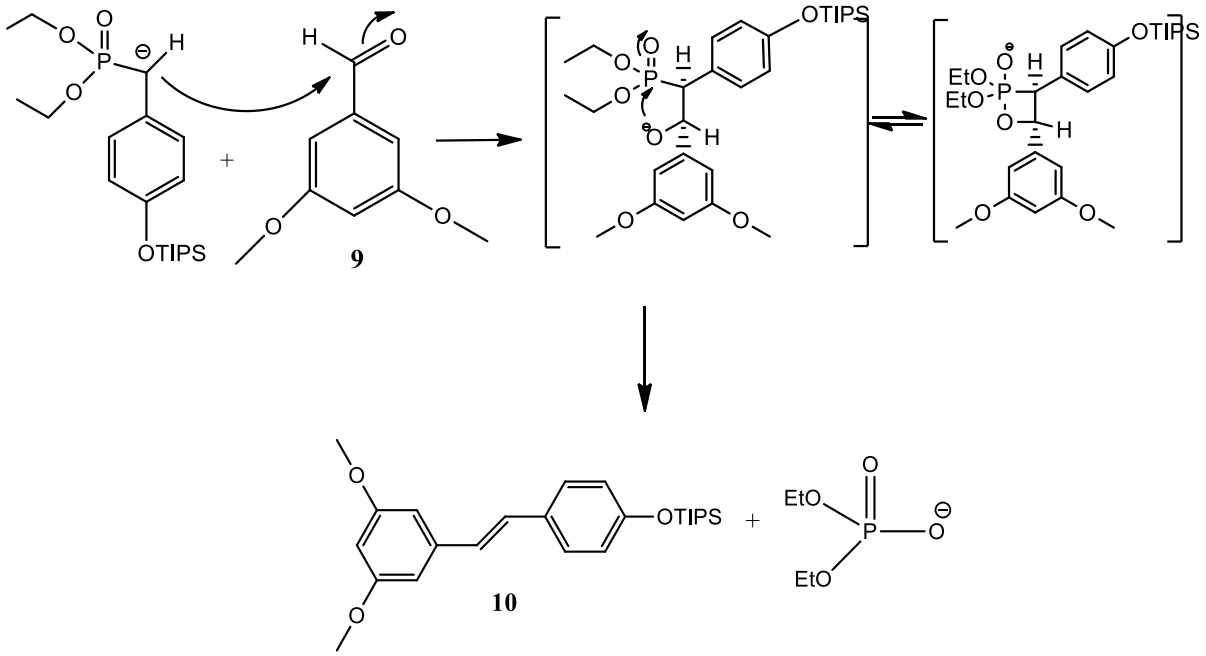

Figure 42

Mechanism of HWE reaction[100 101]

In general trans- olefin is favored over the cis olefin, but the factors that influence E and Z-steroselectivity are well understood and Z-selectivity can also be achieved. Depending on the type of the ylide, type of the carbonyl, type of the solvent and reaction conditions, the formation of the alkene can favor either the (Z) or (E) alkene. For example bulky substituent at the both phosphorous and the carbon adjacent to the carbanion favor formation of the E-alkene and primary aliphatic aldehydes favor Z-alkenes, while aromatic aldehydes favor E-alkenes specially in aprotic solvent such as THF[100].

C-Prenylation by DoM reaction

In this step prenyl with IUPAC name 3-methyl-2-buten-1-yl (see structure in fig. 16) was introduced into the molecule, between to methoxy group by an electrophilic substitution reaction. The classic electrophilic aromatic substitution (EAS) is not a good choose, because the regiochemistry observed is both ortho and para, when an aromatic ring is activated by activating group such as OCH_3 and multi-substitution of the ring can occurs. Isoprene side chain was introduced into the molecule by DoM reaction. DoM reaction is an attractive reaction because it is a regiospecific reaction and substitution is always ortho to a DMG group.

Directed ortho metalation (DoM) reaction

Wittig and Gilman was the first chemist who could ortho- lithiated anisole by n-BuLi[102]. The product of this reaction initiated a new methodology that is known as DoM reaction in chemistry. Directed ortho metalation (DoM) reaction which is an alternative to electrophilic aromatic substitution was used for synthesis the target molecule. In DoM reactions, the hydrogen ortho to a DMG group (directing ortho metalating group) such as methoxy on an aromatic ring is replaced with lithium and in the second step the lithiated carbon reacts with electrophilic compound such as prenylbromide. When two DMGs have a 1,3-position on an arene they will direct lithiation on the 2 position between them as shown in figure 43 [103].

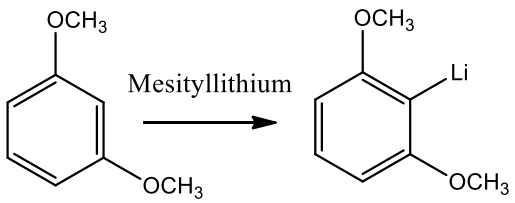

Figure 43

lithium atom enters at the position ortho to DMG group, for example resorcinol dimethyl ether is lithiated in the position 2, ortho to both methoxy groups [104].

Lithiation

Lithiation is an important method for the introduced many substitutions in organic synthesis. Because the electronegativity difference between carbon-lithium bonds makes this bond polar, nucleophilic carbon generated and therefor lithiated organic compound is very reactive toward a wide range of electrophilic compounds.

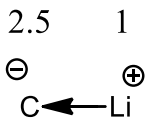

Figure 44

Lithiation (metal-hydrogen exchange) depends on the acidity of the hydrogen, stability of the carbanion and the reaction aided with DMG groups such as methoxy or MOM which are present ortho to the site of metal-hydrogen exchange. Organolithium compounds are used for lithiation. In order to understand their stability, reactivity and safe handling of organolithium compounds, a short review of these compounds is also given.

Organolithium compounds

Commercially available of organolithium compounds are made by oxidative insertion reaction of lithium metal with alkyl halide[105].

$$MeCl \xrightarrow{2\ Li} MeLi + LiCl$$

Figure 45

Organolithium compounds are used as reagents for making other useful organolithium compounds. They need to be kept absolutely free from moisture and oxygen because they act as strong base, and is protonated to form its conjugated acid for example methane in the case of methyl lithium. The electronegativity difference between carbon and lithium suggests ionic character for this bond, but alkyl lithium compound are soluble in hydrocarbon such as hexane and in ether solvents such as THF. This is because a percentage of covalent character is associated with this bond[106]. The most common organolithium compounds which use in organic synthesis are methyl lithium, n-butyl lithium and tert-butyl lithium.

Aggregation of organolithium compounds

Aggregation is common for organolithium compounds and organolithium compounds exhibit varying degree of polymerization depending on the solvent, concentration and temperature[107]. For example n-BuLi is hexamer in nonpolar hydrocarbon solvent such as hexane and in equilibrium between dimer and tetramer in THF.

Figure 46

3 oligomeric structure for n-Buli, a hexamer in nonpolar hydrocarbon solvent and equilibrium between dimer and tetramer in THF [108]

Tetramers and hexamers are common in hydrocarbon solution while tetramers and dimmers are common in electron donor solvent such as THF[109]. Aggregation number is important because the reactivity of organolithium compounds is strongly depended on the aggregation number. Lower aggregates tend to be more reactive, therefor the hexamer form of the alkyl lithium should be deoligomerized to the tetramer and dimer form before reaction. Polar solvent such as ether and THF can cleave the aggregated form compound to the less aggregation number such as dimer or tetramer. But organolithium are not stable in ethereal solvent and it should be storage in a hydrocarbon solvent such as hexane in the cold condition[108 110].

Stability of organolithium compounds

All organolithium compounds are pyrophoric, thermally unstable and sensitive to water and oxygen. Therefor they should storage in a sealed bottle with an inert gas such as nitrogen in the cold condition. Most organoliithium compounds decompose on heating to lithium hydride and an unsaturated molecule. For example butyl lithium decomposes to lithium hydride, 1-butene and n-butane.

$$\text{n-BuLi} \xrightarrow{\text{Heat } 50°\text{C}} \text{LiH} + \text{CH}_2{=}\text{CHCH}_2\text{CH}_3$$

Figure 47

Organolithium compounds are thermally unstable[111]

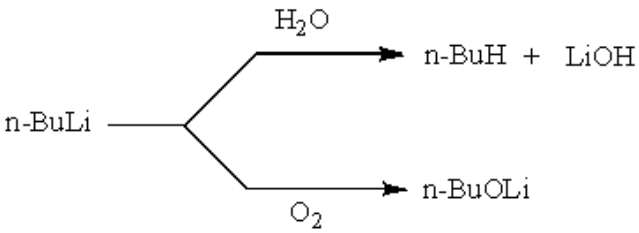

Figure 48

Contact with oxygen or water cause loose of organolithium compound[111]

Mechanism of Directed ortho metalation (DoM) reaction

The steps involves in DoM reaction are insertion of lithium into C-H bond, ortho to a pre-existing substituent. Then the molecule is further treated with another reagent (electrophile) such as prenyl bromide. The proposed mechanism for DoM reaction may be viewed as three steps: 1-coordination of the alkyl lithium compound to a hetero atom of DMG group (1.2 in the below figure). This is a kind of acid base reaction since lithium is acid and DMG group such as $-OCH_3$ is a base. Then deprotonation of the proton in the nearest position to DMG group gives lithiated compound (1.3 in the below figure) which after reaction with an electrophile, di-substituted aromatic product is obtained[112].

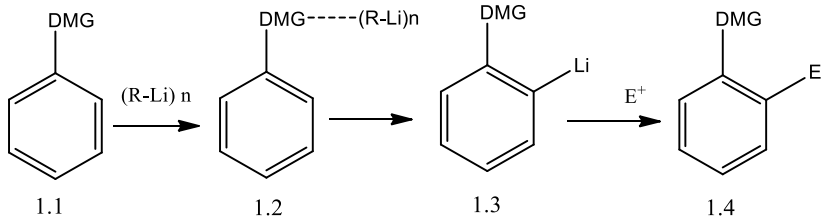

Figure 49

Lithiation of an aromatic ring adjacent to a substituent, which acts as a direct metalation group (DMG), is called ortho metalation. Several groups such as methoxy acts as DMG group, these groups can increase acidity of the ortho-hydrogen. Then the lithiated product can reacts as nucleophile with alkyl bromide such as prenyl bromide and a new C-C bond (prenylation) is generated. The DoM reaction was done after second attempt. In the third attempt, THF was dried by sodium/benzophenone system.

Deprotection reaction by TBAF

The final step was de-protection reaction by tetra-n-butyl ammonium fluoride[67]. Tetra-n-butyl ammonium fluoride is a quaternary ammonium salt with the chemical formula $(C_4H_9)_4NF$.

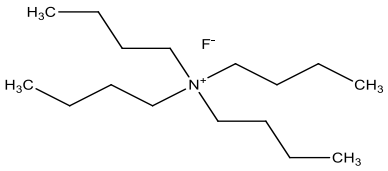

Figure 50

TBAF commercially is available as the white solid and as a solution in THF

Mechanism of desilylation reaction

It is believed the reaction occur by nucleophilic attack of small fluoride ion to silicon. As the result strong Si-F bond and a pentavalent intermediate are formed[113]. Then de-protected product is obtained by elimination neutral silane as shown in figure 51.

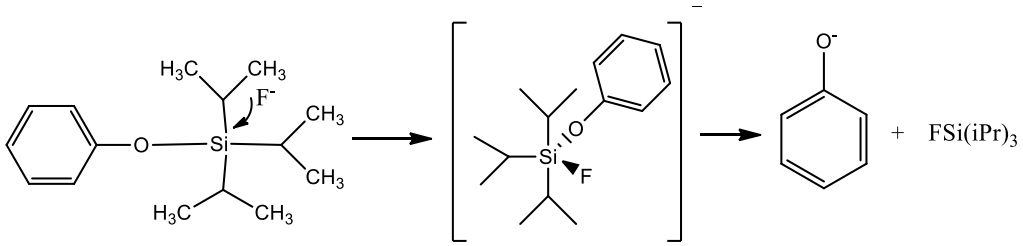

Figure 51

The Product (Pr.Pter) was obtained after two times chromatography.

Chapter 3

Experimental procedure

The following chapter describes the work in the laboratory, use of chemicals, reagents and treatment of DLD-1 cells. The chapter also describes in detail methods and setups for determination of cell number, cell viability, cell cycle progression and cell death.

Chemicals

The chemical used were mainly obtained from Sigma-Aldrich without further purification. This include: TCT (CAS 108-77-0), THF(CAS 109-99-9), 4-hydroxy benzyl alcohol (CAS 623-05-2), 4-hydroxy benzaldehyde (CAS 123-08-0), tri isopropyl silyl chloride (CAS 13154-24-0), imidazole (CAS 288-32-4), silica gel 60 Å, 70-230 mesh (CAS 112926-00-8), $NaBH_4$(CAS 16940-66-2), methanol (CAS 67-56-1), tri ethyl phosphite (CAS 122-52-1), 4-methoxy benzyl alcohol(CAS 105-13-5), diethyl ether, 99.99 anhydrous Zink iodide(CAS 10139-47-6), 3,5-dimethoxy benzaldehyde(CAS 7311-34-4), Potassium t-butoxide (CAS 865-47-4) NH_4Cl(CAS 12125-02-9), 1.6M n-BuLi in hexane (CAS 109-72-8), benzophenone(CAS 119-61-9), sodium in petroleum (CAS 7440-23-5), prenylbromide (CAS 870-63-3, d:1.29 g/ml), sodium bromide (CAS 76-47-15-6) and TBAF(CAS 87749-50-6).

There were also chemical used from other suppliers: n-Hexane (CAS 110-54-3), ethyl acetate (CAS 141-78-6) from Th. Geyer, DMF (CAS 68-12-2) from lab scan, TLC silica gel 60 F254, aluminum sheets 20 x 20 and dichloromethane (CAS 75-02-09) from Merck.

General experimental conditions

As described in the methods most of the reactions were sensitive to water and oxygen. Therefor dry solvent was used. THF and DCM were dried over 20 % m/v 3 A° or 4A° activated molecular sieve. Molecular sieve is cheap, non- toxic and effective for drying of the most common solvents special non-hygroscopic solvent such as DCM. They must fully activated special in reactions which are very sensitive to water such as in the reaction with n-BuLi. DCM is not particularly hygroscopic and has low water content, therefore simple storage for 24 hr. of the solvent over 10% m/v activated 3Å or 4Å is enough to reduce water content to 0.1 ppm[77].

However in the prenylation reaction molecular sieve was not effective for drying of THF, therefor THF was dried by sodium/ benzophenone system which was effective[114]. All glassware was dried in an oven at 100 °C -110 °C for minimum 20 minutes before reaction. TLC was performed for each reaction and visualized under UV lamp. Column chromatography was performed using silica gel as the stationary phase with hexane and ethyl acetate. The compositions of eluents are further detailed in each step.^{1}HNMR were recorder with a Bruker Avance III (400 MHz) HD NMR spectrometer and chemical shift were reported in parts per million (ppm) relative to tetra methylsilane (δ_H = 0.00ppm). Mass spectra were obtained with a Finnigan Trace Ultra-DSQ II (Thermo Co.) system equipped with an Agilent J&W capillary column. All ^{1}HNMR and GC-MS data are available in appendix.

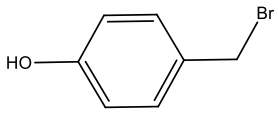

1

Synthesis compound 1 by TCT/ DMF

To a 200 ml Erlenmeyer flask which containing magnetic stir bar was added 10 g (54 mmol) of TCT followed by11ml DMF. The mixture was stirred at room temperature until white solid compound was formed. The reaction was monitored by TLC (1:1 hexane /ethyl acetate) on the white solid compound until TCT was disappeared. Then 125 ml of dichloromethane was added. The white solid compound was dissolved. Then 11.4 g (110 mmol) of Sodium bromide was added. This mixture was stirred for 10 h. Then 6.4 g (52 mmol) of 4-hydroxybenzyl alcohol was added. The reaction mixture was monitored by TLC. After 2 h starting material was disappeared. Then the mixture was filtered through Celite with vacuum to remove excess of sodium bromide. The yellowish organic layer was washed with 30 ml distilled water to dilute and remove excess of DMF and TCT. Then organic layer which was laid under water phase washed by 30 ml 1M HCl (2 x 15 ml) to remove DMF and washed with brine (2 x 15 ml). The organic layer was dried over sodium sulfate at 0°C for about 30 minute to remove excess of water and the solvent evaporated by rotary evaporator to 1.81 g of yellow oily compound. ^{1}HNMR ($CDCL_3$, 400 MHz) analysis showed product was not formed. A second attempt was done without success. A white yellowish solid compound was obtained in the second attempt, which was insoluble in d-chloroform and d^6-DMSO. Therefor ^{1}HNMR analysis was impossible. ^{1}HNMR was run (DMSO-d^6, 400 MHz) on the water phase fraction. Based on ^{1}HNMR and yellowish color of water phase can be concluded that some of the starting material or the product were end up in the water phase.

However the desire product could not be obtained and the reaction pathway was changed to chlorination of alcohol. Because both brominated and chlorinated product can be used in the Michaelis Arbuzov reaction.

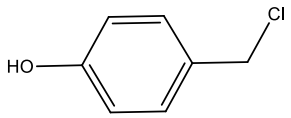

1'

Synthesis compound 1´ by TCT / DMF

To an Erlenmeyer flask which containing magnetic stir bar was added 3.5 g (19 mmol) of TCT and 4 ml DMF and stirred at room temperature until white solid compound was formed. TLC (1:1 hexane /ethyl acetate) was done on the white solid compound until TCT was disappeared. Then 50 ml of DCM was added and the resulting the white solid compound was dissolved. Then 2.3g (18.5 mmol) of 4-hydroxy benzyl alcohol was added. The reaction mixture was stirred at room temperature and monitored by TLC until completion (2 h). Then 40 ml water was added to the reaction mixture and organic layer was washed with 30 ml of saturated solution of Na_2CO_3 followed by 30 ml 1N HCl and 30 ml brine. The organic layer was dried by sodium sulfate to remove excess of water and solvent evaporated by rotary evaporator to 1.65 g (72%) of oily product. ^{1}HNMR (DMSO-d^6, 400 MHz) showed product was formed, but with some of impurities. It was tried to remove impurity with rotation evaporator, but without success. However TCT/DMF method did not work for me.

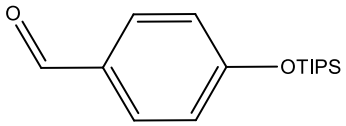

5

Synthesis compound 5

DCM was dried by molecular sieve as described in general experimental conditions. To an Erlenmeyer flask contains magnetic stir bar was added 3.13 g (25.62 mmol) of 4-hydroxy benzaldehyde in 60 ml anhydride CH_2Cl_2 at 0°C. The solution was stirred for 30 min. at 0 °C. Then 4g (21 mmol) TIPS-Cl was added to the solution, followed by 3.13 g (46mmol) imidazole. A yellowish solution was obtained. The reaction mixture was stirred overnight at room temperature. The reaction mixture was quenched with 60 ml water and washed with 125 ml DCM. The organic layer was dried over sodium sulfate, and DCM was removed by rotary evaporator to give 11.13 g of the product as pale yellow oil. 1HNMR was run (CDCl3, 400 MHz) a doublet at 1.09, 1.12ppm, a multiple at 1.26- 1.34ppm, two doublet at 6.97- 7.78ppm and a singlet at 9.88ppm showed

formation of product but another small signal at 9.83ppm, showed also starting material(see figure 52). TLC analyze (8:2 hexane / ethyl acetate) showed also two spots with R_f 0.27 and 0.8 which were related to starting material and the product, respectively. 4-hyddroxy benzaldehyde has a pKa value of 7.61 and in PH higher than 7.61, OH group is mostly deprotonated and more water soluble. Therefore starting material was removed by washing with basic solution of 20% sodium carbonate (Na_2CO_3) (PH=11-12) in distilled water. Then by washing with 100 ml water excess of Na_2CO_3 was removed and solution was neutralized. TLC and HNMR showed starting material was removed and this led to improvement of the reaction.

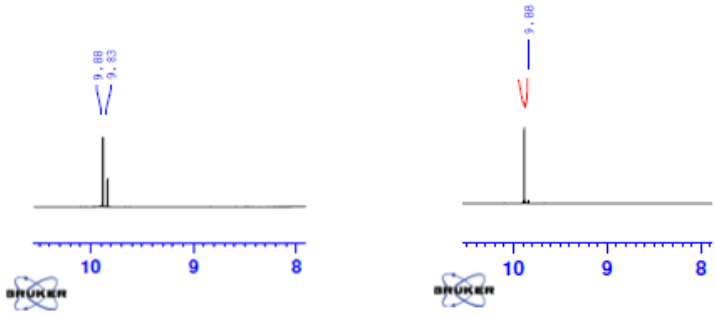

Figure 52

^{1}HNMR before and after washing with Na_2CO_3 solution, small singlet signal at δ 9.83 was disappeared

The product was not used for the next step and instead another batch was made. In the second batch organic layer was washed first with basic solution of 20% sodium carbonate as described. In the second batch 6.02 g (84.5%) of product as a pale yellow oil was obtained. The product was more pure and with higher yield than the first attempt.

^{1}HNMR (CDCl3, 400 MHz) was run singlet at 9.88 ppm (1H), doublet at 7.78-7.80 ppm (2H), doublet 6.98-7.00 ppm(2H), multiple at 1.26-1.34 ppm (3H) and sharp doublet at1.10-1.12 ppm (18H) confirmed formation of product.

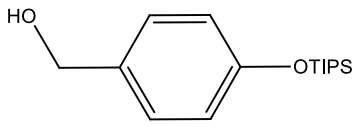

6

Synthesis compound 6

Dry solvent (DCM) was also used in this step. To an Erlenmeyer flask containing a magnet stir bar 5.057 g (18 mmol) of compound **5** was dissolved in 50 ml dry CH_2Cl_2 followed by 6 g of silica gel. At 0°C (using an ice bath) 0.8 g (21 mmol) of NaBH4 was added and the mixture was stirred for 1

hr. Then 10 ml of methanol was added and the reaction mixture was stirred for another 1 h at room temperature. Silica gel and tetra methoxy borate was removed by filtration. Evaporation of solvent by rotary evaporator gave 4.66 g (91.5%) of oily product. TLC analysis (8:2 hexane / ethyl acetate) showed one spot with R_f value 0.4.

^{1}HNMR was run (CDCl3, 400 MHz) doublet at 7.20-7.22ppm (2H), doublet at 6.85-6.87ppm (2H), singlet at 4.59ppm(2H), broad signal at 3.5 ppm, multiple at 1.22-1.27 ppm and doublet at 1.09-1.11ppm confirmed formation of product.

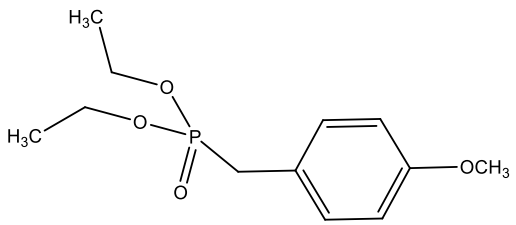

7

Synthesis compound 7

This compound was synthesized for training purpose and the product was not used in synthesis of the target molecule (Pr.Pter). Dry THF was used in this reaction and THF was dried by molecular sieve. A three- necked round bottomed flask containing a magnetic stirrer bar, fitted with a reflux condenser and two glass stoppers in the side necks, was flushed by nitrogen for 30 minutes (see figure 53). Then 60 ml dry THF was added to it and then 5 g (15.6mmol) anhydrous ZnI_2 was dissolved in THF. Then 5.5 ml (32 mmol) tri ethyl phosphite was added, followed by 1.4 ml (11mmol) of 4-methoxy benzyl alcohol. The reaction mixture was heated using an oil bath for 20 hrs. Then the reaction mixture was allowed to cool to room temperature and THF was removed by rotary evaporation. Then residue was transferred to a 500 ml separatory funnel with diethyl ether (2 x10 ml) and 1N sodium hydroxide (2 x 10 ml). White precipitate was formed and then reaction mixture was diluted by 90 ml diethyl ether. Then the organic phase was washed by 200 ml 1N sodium hydroxide, resulting the solution became colourless without any white precipitate. Water phase was washed twice with 100 ml diethyl ether and the combined organic phase was dried over magnesium sulphate. Then Magnesium sulphate was removed by filtration and 6.86 g of colourless oil was obtained, after evaporation of solvent by rotary evaporator. The residue was purified by chromatography with 45% ethyl acetate in hexane and 2g of product with (67%) yield was obtained. 1HNMR was run (CDCl3, 400 MHz) doublet at 7.20-7.23ppm, doublet at 6.84-6.86ppm, multiple at 3.98-4.03ppm, singlet at 3.80ppm, doublet at 3.07-3.12ppm, and triplet at 1.21-1.27 ppm confirmed formation of product.

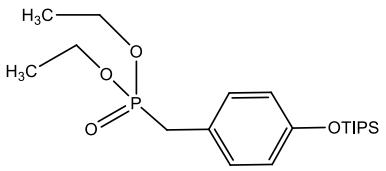

8

Synthesis compound 8

A three- necked round bottomed flask containing a magnetic stirrer bar and fitted with a reflux condenser, was flushed by nitrogen for 30 minutes (see figure 53).

Figure 53

Then 60 ml dry THF was added and 5 g (15.6mmol) ZnI_2 was dissolved in THF, followed by 4 ml triethyl phosphite (d; 0.969 g/ml, 23mmol, 1.5 eq.) using a disposable syringe. Finally 4.1 g (14.6 mmol) of compound **6** was added to the reaction mixture. The reaction mixture was heated using an oil bath at reflux for 24 hrs. Then the reaction mixture was allowed to cool to room temperature and THF was removed by rotary evaporation. Then residue was transferred to a 500 ml separatory funnel with diethyl ether (2 x10 ml) and 1N sodium hydroxide (2 x 10 ml). White precipitate was formed. Then Reaction mixture was diluted by 90 ml diethyl ether and organic phase was washed by 250 ml 1N sodium hydroxide. Solution became colourless without any white precipitate. Water phase was washed with diethyl ether (2 x 100 ml) and the combined organic phase was dried over magnesium sulphate. $MgSO_4$ was removed by filtration and the solvent was removed by rotary evaporation. The product was purified by chromatography with 45% ethyl acetate in hexane and finally 2.68 g (46%) of colourless oil with sweet smell was obtained.

^{1}HNMR was run (CDCl3, 400 MHz) doublet at 7.14-7.16 ppm, doublet at 6.81-6.83ppm, multiple at 3.94-4.00ppm, doublet at 3.05-3.11ppm, triplet at 1.21-1.26 ppm, and doublet at 1.08-1.09 ppm.

Synthesis compound 10 by HWE reaction

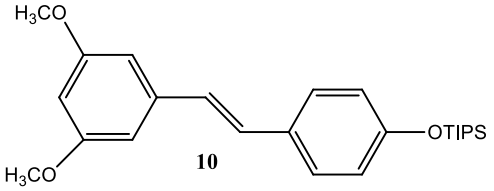

An oven dried 250 ml round bottom flask equipped with a magnetic stir bar was flushed by N_2 for 5 minutes. Then 60 ml dry THF was added to it, followed by 2.1 g (5mmol) of compound **8** at 0 °C (using an ice bath). Then 0.875 g (5mmol) of commercially available 3,5- dimethoxy benzaldehyde was added to the flask, followed by 1.63 g (14 mmol) of potassium tert-butoxide. The colour was changed from yellow to brown. The reaction mixture was monitored by TLC. After one hour, TLC analysis showed the product with R_f 0.80 was formed, but 3,5dimethoxy benzaldehyde with R_f 0.67 could be also seen. After 3 hours, TLC analysis showed another component with R_f 0.3. After 7 hours, TLC analysis showed still the presence of three components in reaction mixture (see figure 54) and finally the reaction was quenched by 60 ml water.

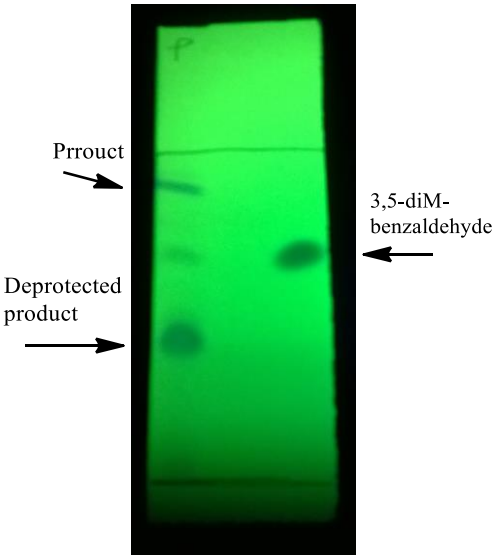

Figure 54

Starting material, product and de-protected product are shown on TLC

Product was extracted by ethyl acetate (3 x 60 ml). Then the combined organic layer was washed first by 60 ml 5% aq. NH_4Cl, then 60 ml distilled water, 60 ml brine and dried over anhydrous magnesium sulphate. Then magnesium sulphate was removed by filtration and residue was concentrated by rotary evaporator. Purification by column chromatography over silica gel with hexane in ethyl acetate (4:1) gave 0.67 g (15.5%) of product with 0.65 g of another compound. ^{1}HNMR analysis showed the other compound with R_f 0.3 was belonging to de-protected product.

^{1}HNMR was run (CDCl3, 400 MHz) doublet at 7.36-7.38 ppm, doublet at 7.04-7.0 ppm, doublet at 6.91-6.88 ppm, doublet at 6.87-6.85 ppm, triplet at 6.37ppm, doublet at 6.64, singlet 3.83 ppm, doublet 1.05-1.07 ppm and multiple at 1.21-1.29 ppm, showed the product was formed.

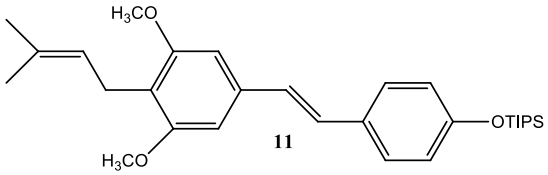

Synthesis of (O-TIPS) Pr.Pter

As described before n-BuLi is very sensitive to water and oxygen. Therefor dry solvent and glassware was used. An oven dried round bottom flask containing a magnetic stir bar was flushed with a balloon filled with nitrogen, while the top of the flask was closed with a septum and a needle was inserted through the septum to allow air in the flask flushed out. This is called an exit needle. The setup is shown in figure 55.

Figure 55

Setup for synthesis compound **11**

When balloon was deflated, exit needle was removed, balloon was refilled with nitrogen and the flask was flushed for a second time. The flask was flushed three times by N_2. Then exit needle was removed and 40 ml dry THF was added to the flask using a disposable syringe. Syringe was also flushed by N_2 3 times before use. Then 0.48 g (1.1mmol) of compound **10** was dissolved in THF at 0°C (using an ice bath). Then 1 ml (10 mmol) of 1.6M n-BuLi in hexane was added dropwise by disposable syringe to the reaction mixture. The yellow colour of the reaction mixture was changed

to green after addition n-BuLi. The reaction mixture was stirred for 2 h and then 0.15ml (1.29 mmol) of prenyl bromide was added dropwise to it. The reaction mixture was stirred overnight at room temperature. Then the reaction mixture was quenched by 20 ml saturated NH_4Cl and extracted with ethyl acetate (3×30 ml). The combined organic layer was washed with 30 ml water and dried over $MgSO_4$. Evaporation of solvent by rotary evaporator and chromatography on silica gel by hexane /ethyl acetate (5:1) gave 0.34 g (62%) oily product with R_f 0.9. This reaction was done after two failed attempts and 0.20 g of starting material was loose during the first and second attempt.
^{1}HNMR was run (CDCl3, 400 MHz) doublet at 7.36-7.38 ppm, doublet at 7.01-6.97 ppm, doublet at 6.94-6.90ppm, doublet 6.87-6.85 ppm, singlet at 6.65 ppm, triplet at 5.21 ppm, singlet at 3.86 ppm, doublet at 3.80-3.82 ppm, singlet at 1.77 ppm, singlet at 1.66 ppm, multiple at 1.22-1.29 ppm and doublet at 1.06-1.08 ppm showed formation of the product.

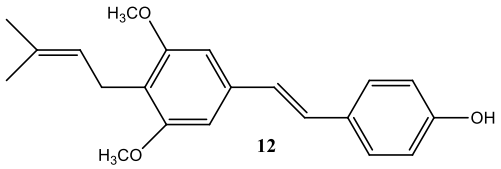

12

Synthesis of Pr.Pter

0.3 g (0.624mmol) of compound **11** was dissolved in 20 ml THF, followed by 0.393 g (1.24 mmol) of TBAF at 0°C (using an ice bath). The reaction mixture was stirred at room temperature for 24 hrs. Then the reaction mixture was quenched by 30 ml saturated NH_4Cl and extracted by ethyl acetate (3 x 30 ml). The organic layer was washed with 50 ml water and then dried over anhydrous sodium sulphate. The product was concentrated by rotary evaporator and the product was purified by column chromatography over silica gel with hexane/ethyl acetate (4:1). 0.14 g compound was obtained. TLC analysis (hexane/ ethyl acetate 4:1) showed two components A: (R_f 0.56) and B: (R_f 0.39). Therefore another eluent was developed for separation of these two components (A, B) and another column chromatography was run with hexane/ ethyl acetate (6:2). Finally 18 mg Pr.Pter (9%) with R_f 0.47 was obtained. In addition 16 mg of compound A was also obtained. Some of the collected fractions was containing both A and B, therefore calculated yield should be higher than 9%. ^{1}HNMR was run (CDCl3, 400 MHz) doublet at 7.40-7.42 ppm, doublet at 7.03-6.99 ppm, doublet at 6.95-6.91 ppm, doublet 6.83-6.85 ppm, singlet at 6.68 ppm, triplet at 5.18-5.20 ppm, singlet at 3.88 ppm, doublet at 3.65-3.68 ppm, singlet at 1.78 ppm, singlet at 1.67 ppm and a broad signal at 1.38-1.5 ppm. GC MS showed an intense peak at 324.13m/z which was related to the product with molecular formula $C_{21}H_{24}O_3$ (see page 98).

Materials and Methods

McCoy`s 5A medium obtained from Lonza, resveratrol, pterostilbene, phosphate buffer saline (PBS), Thiazolyl blue Tetrazolium bromide (MTT), penicillin/streptomycin and DMSO from Sigma-Aldrich, Hanks balance salt solution (HBSS) and trypsin-EDTA from Gibco, fetal bovine serum (FBS) from Biochrom , and T-175 flasks, 24 well plate and 96 well plate obtained from Nunc Roskilde-Denmark. Resveratrol, pterostilbene and Pr.Pter were diluted in DMSO to 60 mM and kept at -20 °C.

Cell line and treatments

Frozen human colon cancer cells line DLD-1 from American type culture collection with passage number 8 to were thawed in McCoy`s 5A medium containing 20% FBS and 2% pen/strep. The following day media was changed to McCoy`s 5A medium containing 10% FBS and 2% pen/strep and this was the standard growth media cultured in T-175 flask with McCoy`s 5A medium which containing 10% fetal bovine serum (FBS) and 2 % pen/strep. The cells were grown in an incubator with humidity of 95% at 37°C, 5%CO_2 atmosphere and sub-cultivated twice per week when they reached 80% confluence. Sub cultivation was done by removing of old media with aspiration and washing the cells twice with 15 ml phosphate buffer (PBS) without calcium and magnesium. The cells were detached by adding 2 ml of 0.05% trypsin+ 0.02% EDTA in PBS followed by incubation for 4 minutes in incubator. Finally by adding 8.5 ml of McCoy`s 5A medium trypsinization stopped and cells re-suspended to single cells. Then 1 to 2 ml of the cells suspension is transferred to a new T-175 flask which containing suitable amount of fresh medium and new passage was made. The cells were only used up to passage 30.

Statistical analysis

To analyse the effects of Pr.Pter on the cells growth, proliferation, viability, and cell cycle Coulter counter assay, MTT assay and FACS was used. Each experiment was performed three times with similar results and results were expressed as means with standard deviation represented by bars. Analyses were made in Graphpad Prism version 6.0. The Data was statistically analysed by one way ANOVA and value of $P \leq 0.05$ was considered significant.

Coulter counter

A coulter counter is an instrument for counting of particles or cells and analysing of their size [115]. In this method cells suspended in an electrolyte solution for example sterile filtered 0.9% sodium chloride and pass through a microchannel or small hole with two electrodes between them that have an electrical current, while the resistance of the microchannel is measured. Because the cells block part of the hole, the resistance will increase if the cell is in the solution.

These changes can be used to estimate both size and number of the cell by software in computer. This technique introduced in the mid-1950s by the Coulter brothers and theory behind is known as Coulter principle [116]. Today fully automated Coulter counter for laboratorial and industrial use exist. The Beckman Coulter Z model was used to determine the number and size of the cells in this investigation. Particles less than 10.5 µm were considered as debris and usually cells between 10.5 µm and 28 µm will be included. A single count can be made in less than one minute and a size distribution curve of particles is obtained by multisizer software on monitor as shown in the below. The Coulter counter data were extracted and exported to an excel file, were counts were transformed to cells/ml using dilution factor.

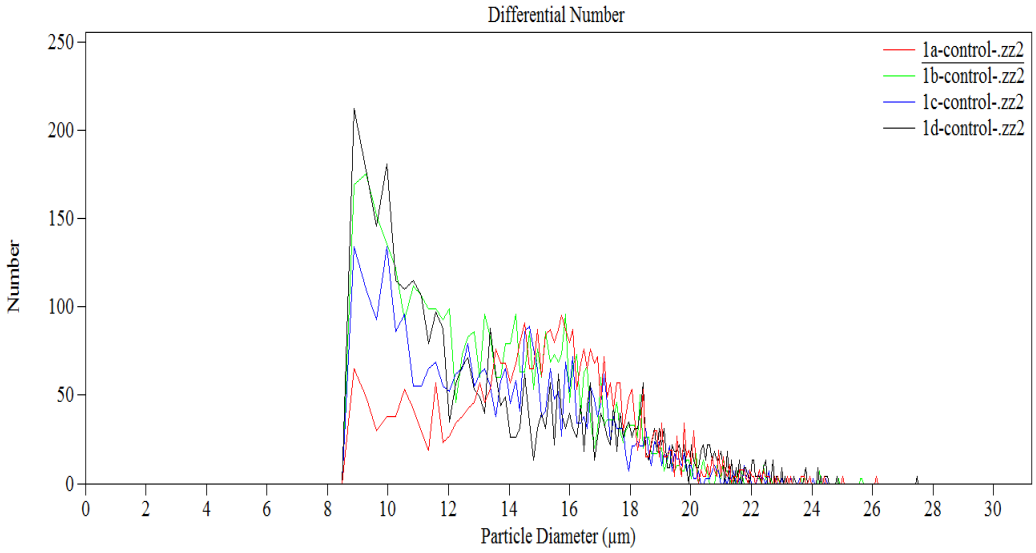

Figure 56

An Example of four samples of control cells as output from coulter counter.

Measurement of cell growth and proliferation

As described in methods, Coulter counter assay is a simple method to investigate the time and dose dependent effect of a compound on a specific cell line such as DLD-1. The time dependent and dose dependent effect of Pr.Pter at 24, 48 and 72 hour was done as in the following setup. Cells were plated in 24 well plate with $5*10^4$ cells in each well. The cells attached by incubation at 37 °C with 5% CO_2 during overnight. The next day, medium was replaced with 1ml medium containing increasing concentration of Pr.Pter (15 µM, 30 µM and 60 µM). McCoy`s medium containing 0.1% DMSO was used as control. Two other columns were used for 30 µM RV and 30 µM pterostilbene as shown in figure 57.

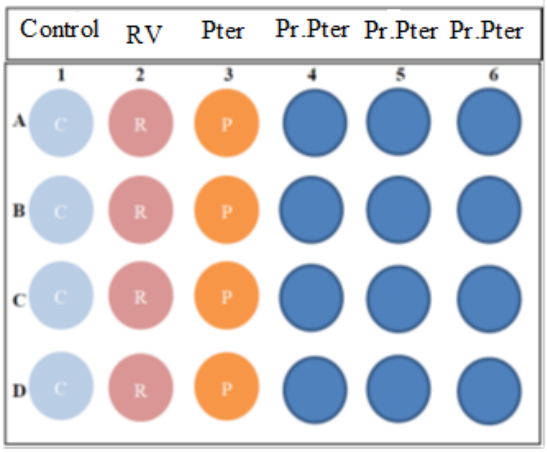

Figure 57

Coulter counter (CC) set up

The plates incubated for 24, 48 and 72 hours with incubator. At the time of analyse the media was removed and each well was washed with 1ml PBS and incubated for 20 minutes with 200 µL 0.05% trypsin. Then 800 µl of PBS was added to each well to stop action of trypsin. Then the cells were re-suspended to single cells and finally 800 µl of the cell solution from each well was transferred to a cuvette containing 10 ml of sterile filtrated 0.9% sodium chloride. The cells were counted by Coulter counter. In order to avoid settling effect cuvette was gently mix before each measurement. The result of each counting was saved in computer as Z2 files. Finally the result from each counting was exported to a excel file and time dependent and dose dependent curve was made from this excel fil which is found in the result part.

FitterBJ03 Software

Base on the coulter counter data it is possible to estimate cell diameter by using Java based software program Fitter BJ developed by Benjamin Toft, Aarhus University. The data for each sample from Coulter counter are transmitted to the FitterBJ03 program. The fitter BJ03 estimates the median cell diameter from each sample by fitting a polynomial graph.

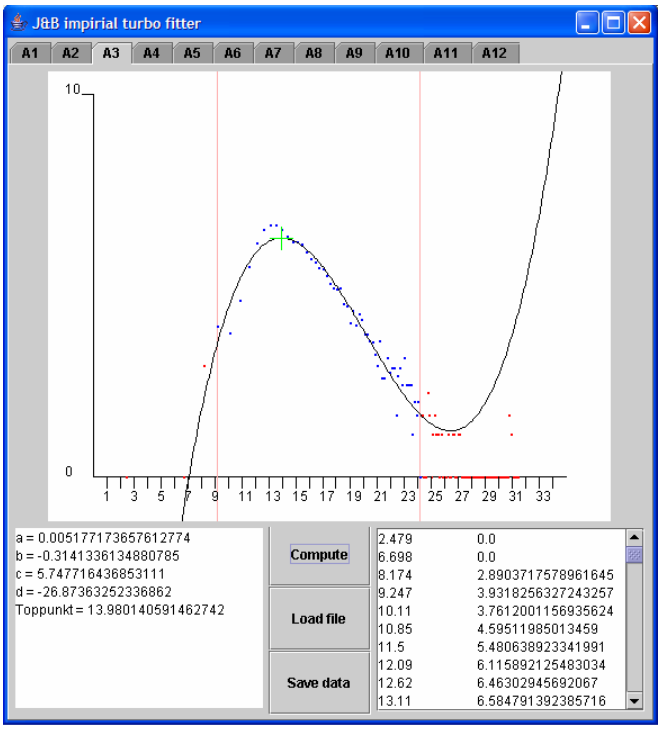

Figure 58

An example of fitted polynomial

Phase contrast microscopy

The cells were photographed at 20X and picture was taken from each well by using phase contrast microscope, Leica DMIRB with a DFC 450 C digital camera system for morphological study. Before counting the cells from each well, picture of cells were obtained using a x20 magnifying microscope with a camera attached. Pictures were taken from middle of the well, were the contrast was highest. These pictures are shown in the result. Then imajeJ program version 1.32j was used to measure the cell area from phase contrast images. The mean area of 10-15 random cells was determined from the pictures using ImageJ software. Then an average of estimates from four measurement of each time and concentration were calculated.

MTT assay

MTT assay is a colorimetric assay, which is used to determine the cell viability [117]. In this assay yellow coloured tetrazolium salt is taken up and cleaved by metabolically active cell to purple, water soluble formazan as shown in the below.

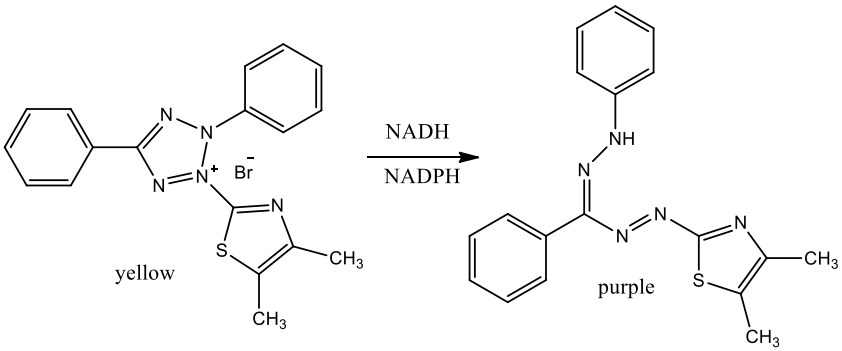

Figure 59

Tetrazolium salts are a large group of heterocyclic organic compound that are highly colored. The first tetrazolium salt was synthesized by Von Pechmann and Runge in 1894. They are widely used as dye and analytical reagents, where their deep color makes them good indicator for redox reactions[118 119]. MTT is reduced by active actively growing cells to produce a blue formazan product. Berridge & Tan observed that the most cellular MTT reduction occurs outside the mitochondrial inner membrane and involves the pyridine nucleotides cofactors NADH and NADPH[120121117]. In other word cell metabolism is used as an indicator for cell survival: more cells means more metabolism activity and more tetrazolium salt is reduced therefore darker purple is appear as shown in figure 60.

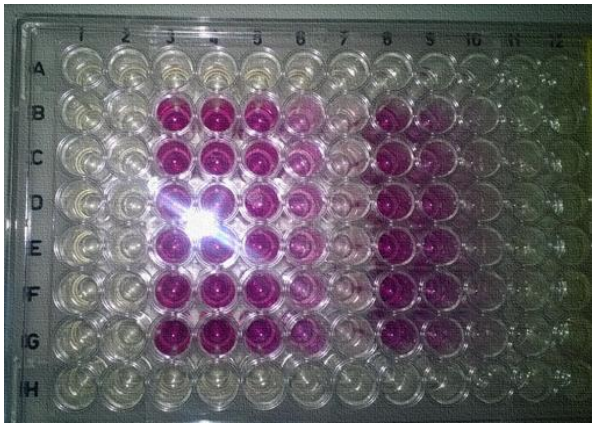

Figure 60

Column 6, 7, 10 and 11 appear brighter than others. Because of the less cellular activity which is related to more concentration of Pter and Pr.Pter.

Solubilized formazan has a maximum absorbance near 570 nm. Absorbance of solubilized formazan at 570 and 620 nm was measured by a Bio-Tech Synergy HT Multi-Mode microplate reader. Results are exported to an excel file where absorbance OD calculates with the below formula. OD is optical density for each well and OD blank is optical density for well without cells.

$$OD = (aveOD_{570} - aveODblank_{570}) - (aveOD_{620} - aveODblank_{620})$$

Then percent of cytotoxicity (H %) or grow inhibition can calculated from below equation

$$H(\%) = \frac{O_{DC} - O_{TN}}{O_{DC}}$$

O_{DC}= OD average value of control cells

O_{TN}=OD value of each well with treated cells

H% is usually between 0 and 100% where 0% indicates the same grow as in control and100% indicates all cells are dead and negative H % means more cells than in control.

Determination of optimal cell density

A serial dilution of cell concentrations ranging from 50.000 cells/ml to 391 cells/ml were prepared in McCoy`s medium and incubated for 24 hour in a 96 well plate as shown in figure 61.

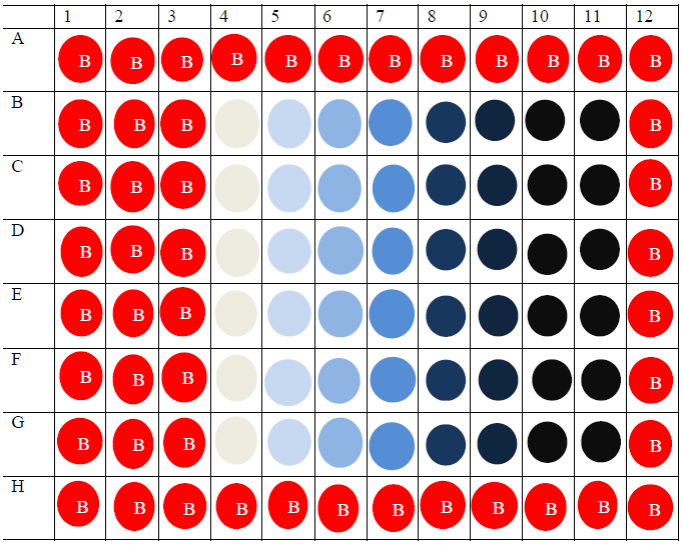

Figure 61

The red wells are wells without cells (blank), column 11 with 50,000 cells /ml or 5000 cell/100 µl has highest cell density and column 4 with 3901 cells /ml has lowest cell density.

Then absorbance was measured by a Bio-Tech synergy HT multi- mode micro plate reader. Plotted Absorbance against number of cells provided a curve. The optimal cell density was considered as $3*10^4$ cells /ml, since it was laid within the linear portion of the plot.

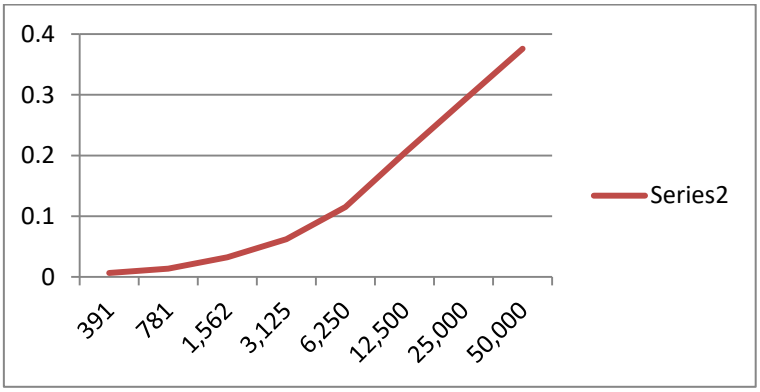

Figure 62

The optimal cell number 30.000 cells /ml or 3000 cells/100 µL was chosen.

Measurement of cell viability

In order to carry out assay, cells were grown in McCoy`s medium for 24 h, then exposed to increasing concentration of Pr.Pter (15, 30, 45, 60 µM), Pter (15, 30, 60 µM) and RV (30 µM). Control received 0.1% DMSO and a column was used as blank (medium without any cells) as shown in figure 63.

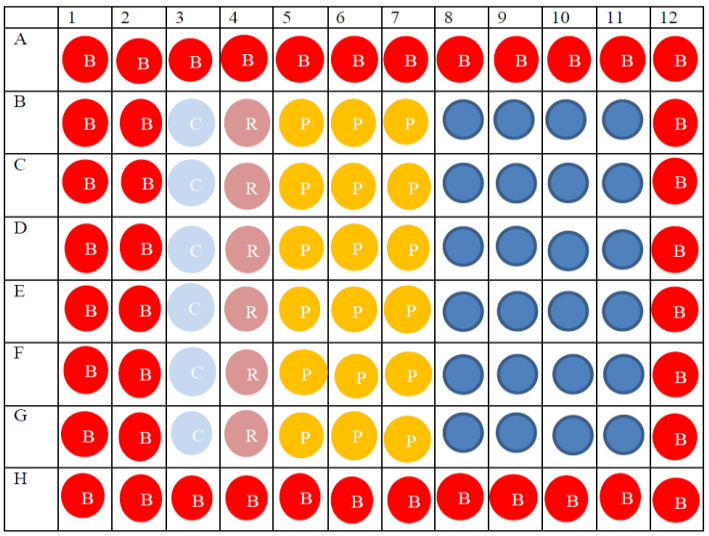

Figure 63

MTT set up

Dark blue are Pr.Pter, red are blank, bright blue are control, yellow are Pter and purple is RV.

The cells were incubated at 37°C in the 5% CO_2 incubator for 24h, 48h and 72 h. Then medium was removed by gently inverting the plate on a sterile paper and replaced by 100 µL of 0.5 mg/ml of 3-(4,5 dimethylthiazol-2-yl)-2,5-diphenyl-2H tetrazolium bromide in HBSS solution and incubated at the same condition for 4 h. Then MTT solution in each well was removed by gently inverting the plate on a sterile paper and replaced with 100 µL DMSO to dissolve purple formed crystal. Then the plate was covered by aluminium foil and was left on the plate shaker for10 min. When all formazan crystal was completely dissolved, the optical density was read at 570 nm and 620 nm by Bio-Tech synergy HT multi- mode micro plate reader. The result was saved and exported to excel fil. Then absorbance can be converted to related cell number by some simple calculation as described in methods.

Fluoresces Activated Cell Sorters (FACS)

Fluoresces activated cell sorters (FACS) which works based on the principle of flow cytometry is a helpful method for quantitative measurements on a single cell level in cell biology. The word cytometry means the measurement and analysing of scattered light or fluoresces, while particle or cells pass through a beam of light or a laser beam. The basic component of FACS consists of a flow cell that forces cell into the middle of a fluidic sheath, a laser source of light, detector, a photomultiplier to amplify the signal and a computer as shown in figure 64.

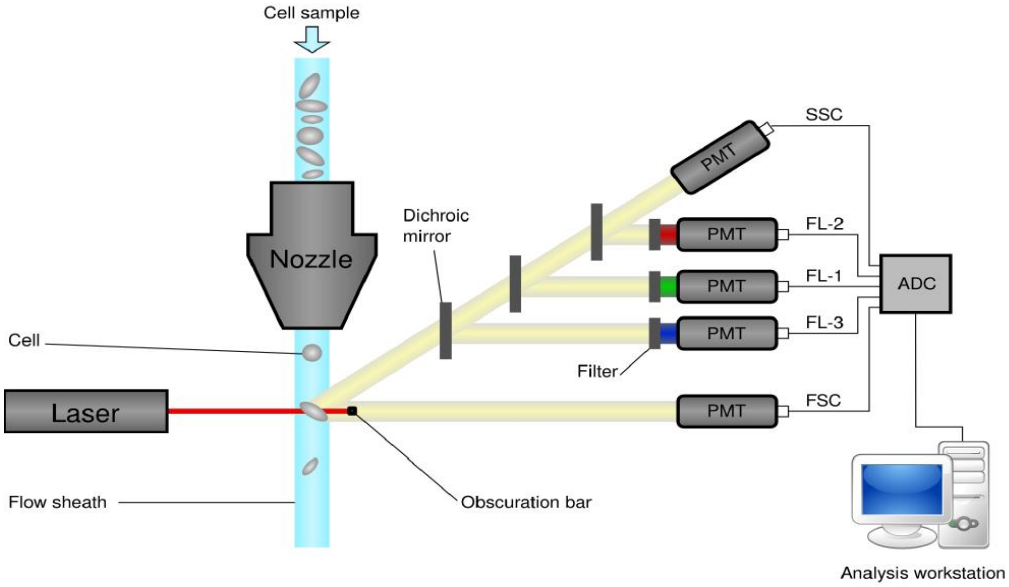

Figure 64

Schematic diagram of a flow cytometry, showing the flow sheath, laser, photomultiplier tubes (PMTs), analogue to digital converter (ADC) and analysis workstation (computer)[122]

The cells are passed through a laser light beams. As the laser beam hits the cells, the light beam is scattered in a forward (FSC) and side (SSC) direction. The Forward scatter provides information about cell size and side scatter provides information about granularity or complexity. Fluorescence can also be detected if fluorescently labelled cells are used. Scattered light or fluorescence is captured and directed to photodetector for conversion to electronic signals. The electronic in the flow cytometry amplify the signal and convert the analog data to digital data, which can be analysed by computer software programs. Measured particles can be cells, chromosomes or other particles that can be suspended in the fluid[123 122].

The cell cycle analysis by FACS

As it mentioned before during the cell cycle a cell undergoes dramatic change in both size and DNA content. For example the amount of DNA is lowest in G_0/G_1 phase and cells are diploid (2n). In the S phase DNA is synthesized and amount of DNA increase from 2n to 4n until the cell enter the G_2 phase where it now has twice amount of DNA as in G_0/G_1 phase. These changes make possible to determine the cell cycle distribution by FACS. This can be done by using a flurochrome such as propidium iodide (PI) that has high specificity for DNA. Fluorescence of the PI stained cell and then DNA content is measured by FACS. The DNA histogram appears as a relatively simple data set with three distinct populations that are related to G_1, S and G_2 phase as shown in figure 65.

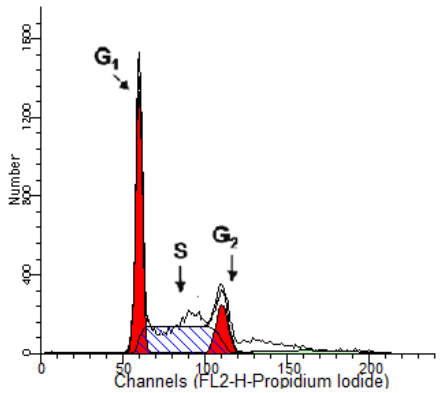

Figure 65

Typical DNA content frequency histogram provided by software program

Cell cycle analysis by FACS

The Effect of Pr.Pter, Pter and RV on the cell cycle was examined by FACS at 24, 48 and 72 hours. Experiment was performed with 10 cm dish according to the protocol which is exists in the Ole's Lab.$5*10^4$ DLD-1 cells were seeded in 10 cm dish one day before to RV, Pter and Pr.Pter treatment. At the day of treatment medium was changed to medium containing 30 µM RV, 30 µM Pter and 30 µ Pr.Pter. After incubation at the designate times, the growth medium containing dead cells was transferred in 50 ml Eppendorf tube for apoptosis analysis. Then the cells were washed with 10 ml PBS and transferred to the same Eppendorf tube. Then the cells were detached by 1 ml trypsin followed by incubation for 10-15 minutes. Then 4.5 ml PBS was added and collected in the same Eppendorf tube. The cell suspension was pelleted by centrifuge for 6 min. (300 g or 1800 rpm at 4°C). Then supernatant was discarded and the cells were washed in 10 ml PBS and were pelleted as before. The supernatant was discarded again and the cells re-suspended in 5 ml PBS. Then the cells were counted by Coulter counter and $2*10^5$ cells were transferred to FACS tube. The cells were pelleted and supernatant was discarded as before. Finally, the cells re-suspended in 200 µl PBS and fixed by slowly adding 2 ml ice cold 70% ethanol, while mixed by vortex mixer. The FACS tubes were incubated for 30 min on the ice before storage at -20°C.

For FACS analysis samples from freezer were pelleted and supernatant was discarded.

The cells re-suspended at 400µl PBS. 50 µl RNase (1mg/ml) and 50 µl PI (0.4 mg/ml) was added and the cells were incubated in the dark at room temperature for 30 min. Then the cells were pelleted for the last time, supernatant discarded and re-suspended in 2 ml PBS. Finally cells were analyzed by FACS. The FACS files were opened in Modfit software. The resulting percentage-wise distribution of cells in phases was given from a model fitted by the software.

Chapter 4

Results

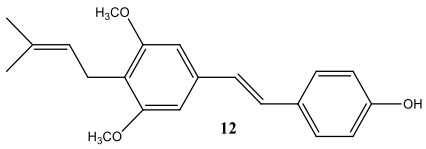

Pr.Pter (Compound **12)** was obtained as colorless oil after purification via column chromatography. This compound was synthesized after 6 steps and has not been synthesized before. Pr.Pter was synthesized with 9% yield and verified by HNMR and GC-MS. In the following part chemical structure and ^{1}HNMR of each step and final product is shown. Protons are labeled as (a) to (k).

Step 1 (Compound 5)

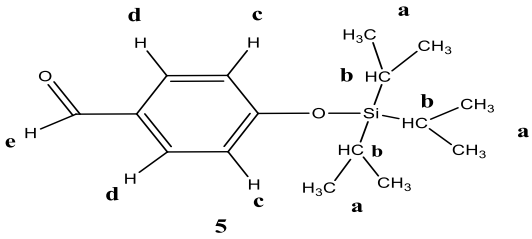

Compound **5** was obtained with 84.5% yield and R_f value 0.8 as a yellow pale oily which was verified by HNMR and GC-MS. Proton H_e appear downfield as singlet at 9.8.8 ppm, indicated the presence of an aldehyde. Protons (Hc, Hd_c) are down fielded as doublet at7. 80- 7.78 and 7.0-6.98 ppm, indicated the presence of a para-substituted benzene ring. Protons (H_b) are up fielded as multiple at 1.26-1.34. Protons ($H_{\mathbf{a}}$) are up fielded as doublet at 1.1 ppm, indicated the presence of a TIPS group.

NMR SPECTROSOPIC DATA FOR COMPOUND **5** IN $CDCl_3$

Proton(s)	Chem. Shift (δ)	Splitting	Integration & j coupling
e	9.88	singlet	1H
d	6.98-7.00	doublet	8 Hz (2H)
c	7.78-7.80	doublet	8 Hz (2H)
b	1.26-1.34	multiple	-
a	1.10-1.12	doublet	8 Hz

Step 2 (Compound 6)

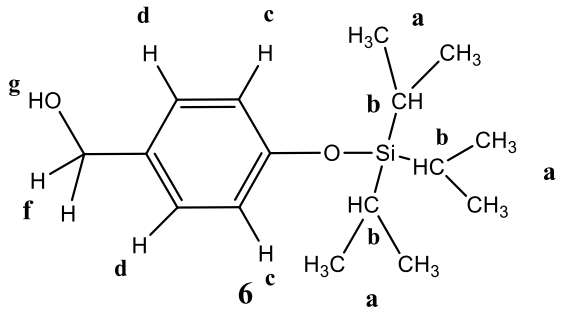

Compound **6** was obtained as yellow oil with high yield 91.5 % and verified by ^{1}HNMR. This compound with R_f 0.4 was obtained after filtration. Proton (H_g) appeared as broad at 3.50 ppm, indicated the presence of OH group. Protons (H_f) appeared as singlet at 4.59 ppm, indicated the presence of a methylene group. Protons (H_c, H_d) are down fielded as doublet at 7.20 and 6.85 ppm, indicated the presence of a para-substituted benzene ring. Protons (H_a, H_b) are related to TIPS group appeared as doublet and multiple at 1.11-1.09 and 1.22-1.27 ppm, respectively.

NMR SPECTROSOPIC DATA FOR COMPOUND 6 IN $CDCl_3$

Proton(s)	Chem. Shift (δ)	Splitting	Integration & j coupling
g	3.50	broad	1H
f	4.59	singlet	2H
c	6.85-6.87	doublet	8 Hz (2H)
d	7.20-7.22	doublet	8 Hz (2H)
b	1.22-1.27	multiple	
a	1.09-1.11	doublet	8 Hz

Step 3 (Compound 8)

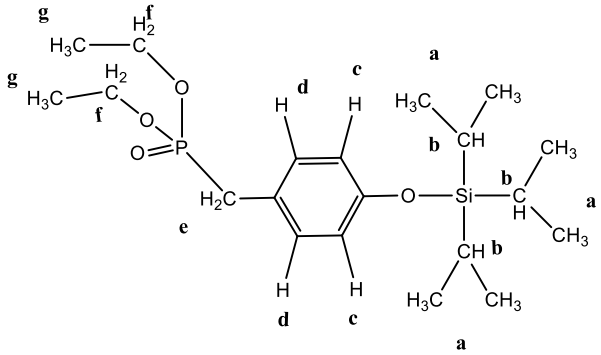

8

Compound **8** was obtained as colourless oil with **46%** yield. This compound with R_f 0.3 was verified by ^{1}HNMR. Protons (Hg) are up fielded as triplet at 1.21 ppm and overlapped with protons H_b since they have the same chemical shift. Protons (H_f) appeared as multiple at 4.00 ppm, indicated the presence of methylene group. Protons (H_e) appeared as doublet at 3.05 because of coupling with phosphorous. Protons (Hc, H_d) as in compound 5 down-fielded as doublet at 7.16 and 6.83ppm are related to benzene ring. Protons H_a as doublet at 1.09 ppm indicated the presence of methyl group.

NMR SPECTROSOPIC DATA FOR COMPOUND **8** IN $CDCl_3$

Proton(s)	Chem. Shift (δ)	Splitting	Integration & j coupling
g	1.21-1.26	triplet	-
f	3.94-4.00	multiple	4H
e	3.05-3.11	doublet	24Hz (2H)
d	6.83-6.81	doublet	8 Hz (2H)
c	7.16-7.14	doublet	8 Hz (2H)
b	1.08-1.09	doublet	4 Hz
a	1.20-1.24	multiple	-

Step 4 (Compound 10)

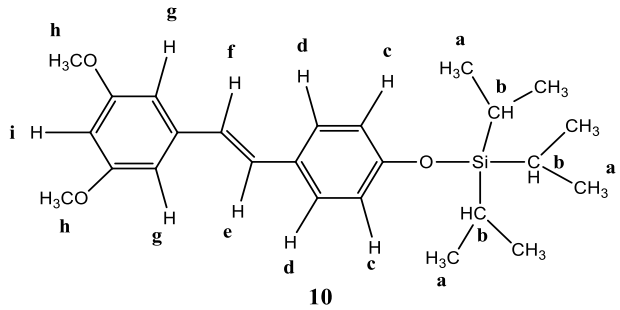

Compound **10** was obtained as oil after column chromatography with 15.5% yield. This compound with R_f 0.8 was verified with HNMR and GC-MS. Protons (H_a) are up fielded as doublet at about 1 ppm and protons (H_b) appeared as multiple at 1.21 ppm, indicated TIPS group. Protons (H_c, H_d) appeared down fielded as doublet at 7.36 and 6.85 ppm, indicted the presence para-substituted benzene ring. Protons (He, H_f) appeared down fielded as doublet at 6.91 and 7.00 with j=16Hz indicated trans- stilbene. Protons H_g appeared as doublet because of ortho coupling with (H_i) at 6.64 ppm, indicated the presence of aromatic ring. Protons (H_i) appeared as triplet because of ortho coupling with (H_g) at 6.37 ppm.

NMR SPECTROSOPIC DATA FOR COMPOUND **10** IN $CDCl_3$

Proton(s)	Chem. Shift (δ)	Splitting	Integration & j coupling
a	1.05-1.07	doublet	-
b	1.21-1.29	multiple	3H
c	7.36-7.38	doublet	8Hz (2H)
d	6.87-6.85	doublet	8 Hz (2H)
e	6.91-6.88	doublet	16 Hz (1H)
f	7.04-7.00	doublet	16 Hz (1H)
g	6.64	doublet	1H
h	3.83	singlet	6H
i	6.37	triplet	1H

Step 5 (Compound 11)

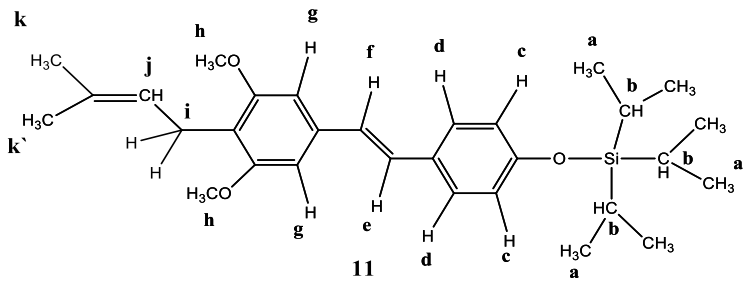

Compound **11** was obtained as colorless oil after column chromatography with 62% yield. This compound with R_f 0.9 was verified by HNMR and GC-MS. Protons (H_a) are up fielded as doublet at 1.06 ppm and protons (H_b) appeared as multiple at 1.22-1.20 ppm, indicated TIPS group. Protons (H_c, H_d) are down fielded as doublet at 7.36-7.38 and 6.87-6.85 ppm, indicated the presence of para-substituted benzene ring. Protons (He, H_f) are down fielded as doublet at 7.01-6.97 and 6.94-6.90 ppm with j=16 Hz, indicated the presence of trans-stilbene. Protons (H_g) appeared as singlet at 6.65 ppm, are related to benzene ring. Protons (H_i) appeared as doublet at 3.80-3.8 ppm, indicated the presence of methylene group. Protons (H_j) appeared as triplet at 5.17-5.21 ppm, indicated the presence of methine group. Protons (H_k, H_k`) appeared as singlet at 1.77 and 1.66 ppm, indicated the presence of methyl group.

NMR SPECTROSOPIC DATA FOR COMPOUND **11** IN $CDCl_3$

Proton(s)	Chem. Shift (δ)	Splitting	Integration & j coupling
a	1.06-1.08	doublet	8 Hz
b	1.22-1.29	multiple	-
c	7.36-7.38	doublet	8Hz (2H)
d	6.87-6.85	doublet	8 Hz (2H)
e	6.90-6.94	doublet	16 Hz (1H)
f	7.01-6.97	doublet	16 Hz (1H)
g	6.65	singlet	1H
h	3.86	singlet	6H
i	3.80-3.82	doublet	8 Hz (2H)
j	5.17-5.21	triplet	-
k	1.66	singlet	-
k`	1.77	singlet	-

Step 6 (Compound 12)

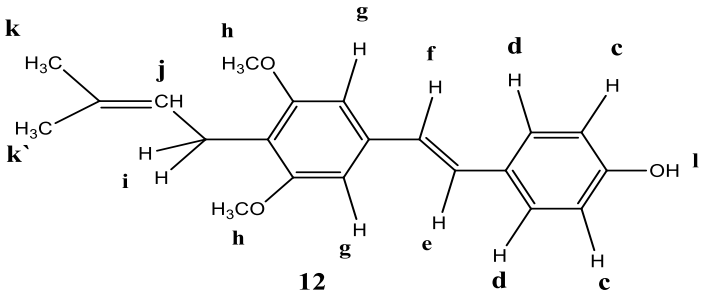

Compound **12** or Pr.Pter was obtained as colorless oil after 2 times column chromatography with 9% yield. This compound with R_f 0.47 was verified with ^{1}HNMR. Protons (H_a) are appeared as broad at 1.38-1.5 ppm, indicated OH group. Protons (H_c, H_d) appeared down fielded as doublet at 7.42-7.40 and 6.85-6.83 ppm, indicated para-substituted benzene ring. Protons (H_e, H_f) appeared down fielded as doublet at 7.03-6.99 and 6.95-6.91 ppm with *J*=16 Hz, indicated trans-stilbene. Protons (H_g) appeared as singlet at 6.68 ppm, indicated benzene ring. Protons H_h appeared as singlet at 3.88 ppm, indicated methoxy group. Protons (H_i) appeared as doublet at 3.68-3.65 ppm, indicated methylene. Proton (H_j) was appeared as triplet at 5.18-5.20 ppm, indicated methane group. Protons (H_k, $H_{k'}$) are appeared as singlet at 1.78 and 1.67 ppm, indicated methyl group.

NMR SPECTROSOPIC DATA FOR COMPOUND **12** IN $CDCl_3$

Proton	Chem. Shift (δ)	Splitting	Integration& j coupling
l	1.38-1.5	broad	2H
c	7.40-7.42	doublet	8Hz (2H)
d	6.85-6.83	doublet	8Hz (2H)
e	7.03-6.99	doublet	16 Hz (1H)
f	6.95-6.91	doublet	16 Hz (1H)
g	6.68	singlet	1H
h	3.88	singlet	6H
i	3.65-3.68	doublet	12Hz (2H)
j	5.18-5.20	triplet	1H
k	1.67	singlet	--
k′	1.78	singlet	--

The Effect of on cell number

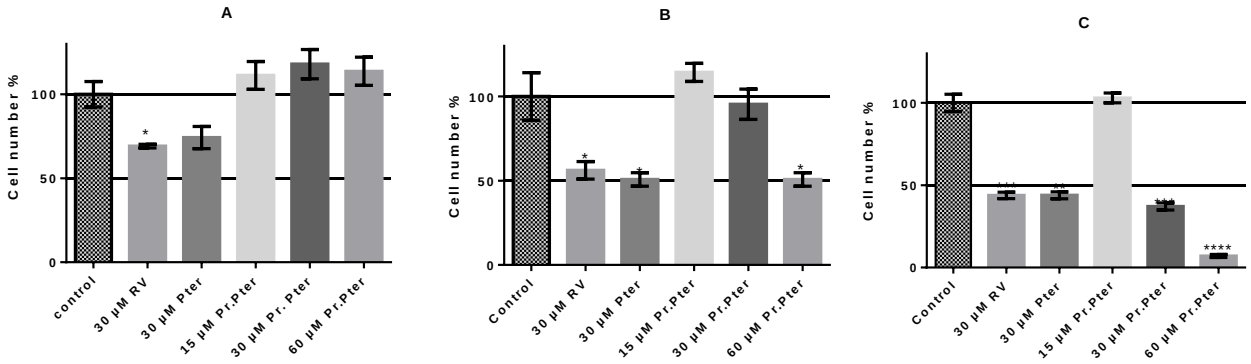

Cell number for DLD-1 cells exposed to (15, 30 and 60 µM) Pr.Pter, 30 µM Pter and 30 µM RV, after 24h: (A), 48h: (B) and 72 h: (C). The values are the mean of the result from three similar experiment and the bars represent the standard deviation of these values.*: P≤0.05, **:P≤0.01, ***:P≤0.001, ****:P≤0.0001 vs. control values. The cell number is relative percentage to control.

To analyse the effect of Pr.Pter on DLD-1cells growth, cell number was determined by Coulter counter. The cells were counted at 24, 48, 72 hours after treatment with 30 µM RV, 30 µM Pter, 15, 30 and 60 µM Pr.Pter. The results were analysed by considering the control cells at 24, 48, 72 hours. The data shows that after 24 h treatment with three concentration of 15, 30 and 60 µM Pr.Pter cell number was slightly increased. While 48 h treatment with 30 µM Pr.Pter caused 5% decrease in cell number and 60 µM Pr.Pter caused significantly decrease in cell number (50% compared to control). Treatment with 15 µM Pr.Pter did not change the cell number. 72 h treatment with 30 µM Pr.Pter caused significantly decrease in cell number (63 %) and treatment with 60 µM Pr.Pter caused the cell number strongly reduced (93% compared to control). Treatment with 15 µM Pr.Pter did not change the cell number.

24 h treatment with 30 µM RV caused significantly decrease in cell number (31% compared to control). 24 h treatment with 30 µM Pter caused 26% decrease in cell number, but it was not statistically significantly different from the control. 48 treatment with 30 µM RV and 30 µM Pter caused significantly decrease to about 50% in cell number.

72h treatment with 30 µM RV and 30 µM Pter showed significantly decrease in cell number (57%). It was also observed that although RV and Pter treatment strongly reduced the cell number compared to control, the cell number was still higher compared to the numbers at the setup, whereas the treatment with (30 and 60 µM) Pr.Pter caused a lower cell number compare to set up after 48 h and the cell number was further decreased.

IC_{50} was determined by Coulter counter. IC_{50} decreased overtime (48 to 72h) from 54.8 to 25.5. An IC_{50} was not obtained at 24 h and it was not possible to obtain an IC_{50} for Pter and RV treated cell, because one concentration of them used.

IC_{50}(µM)	48 hours	72 hours
Pr.Pter	54.8 ± 1.8	25.5 ± 2.17

IC_{50} of Pr.Pter found by Coulter counter assay. The values are the mean of three experiments with percentage of the standard deviations.

The effect on cell Diameter

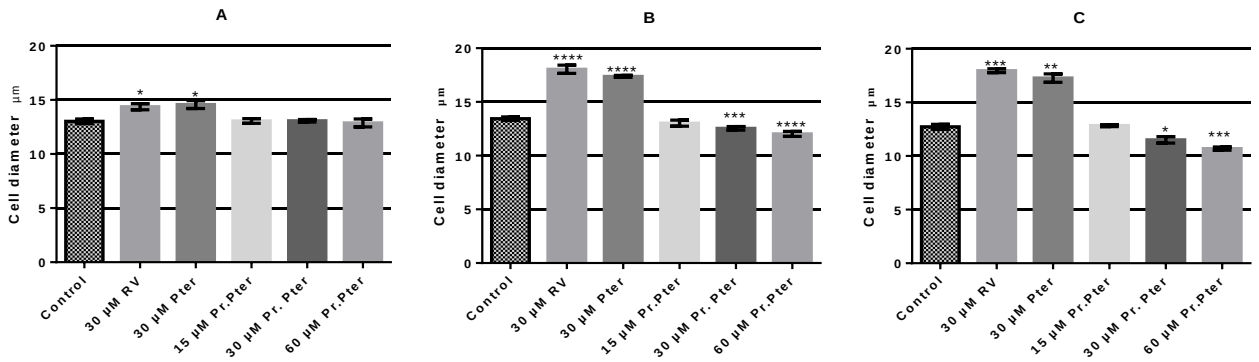

Cell diameter for DLD-1 cells exposed to (15, 30 and 60 µM) Pr.Pter, 30 µM Pter and 30 µM RV, after 24h: (A), 48h: (B) and 72 h: (C) treatment. The values are the mean of the result from three similar experiment and the bars represent the standard deviation of these values, *: P≤0.05, **:P≤0.01, ***:P≤0.001, ****:P≤0.0001 vs. control value.

After 24 h treatment with 15, 30 and 60 µM Pr.Pter cell diameter did not change, while after 48 h treatment with 30 and 60 µM Pr.Pter cell diameter decreased significantly to about 12 µm. 72 h treatment with 30 and 60 µM Pr.Pter caused a significantly decrease in the cell diameter to about 11 µm compared to control. It was also observed that the cell diameter did not change after treatment with 15 µM Pr.Pter at 24, 48 and 72 h.

After 24 h treatment with 30 µM RV and 30 µM Pter cell diameter increased significantly to 14.5 µm and after 48 h treatment cell diameter increased significantly to 18 µm. 72 h treatment with 30 µM RV and 30 µM Pter caused cell diameter increased significantly compared to control, but the cell diameter did not change compared to 48 h and increase in the cell diameter was reached a plateau after 48 hrs.

The effect on Cell Morphology

For morphological study, cells were viewed with phase contrast microscope and images were taken with 20X magnification. From the images it was clear that fewer cells are presented in cells treated with 30 µM Pr.Pter, 30 µM Pter and 30 µM RV. Furthermore cells appeared larger and flatter after treatment with RV and Pter and some cells had grown very large with an appearance of a fried egg. In contrast Pr.Pter treated cells appeared smaller, rounded and with less contact between cells. The effect was observed after 24, 48 and 72 hrs. It was also noticed that RV treated cells adhered more tightly to surface of the dish than control or Pr.Pter treated cells when trypsinized.

a) Untreated cells after 24 h

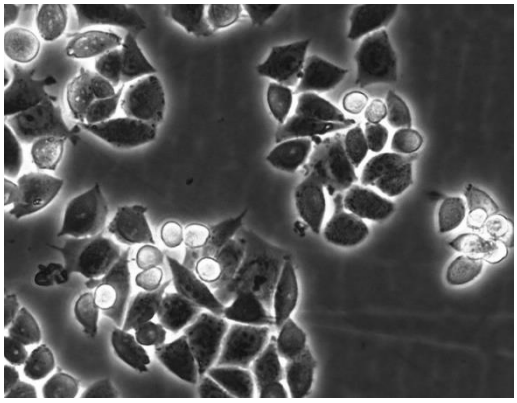

b) Cells with 30 µM RV after 24 h

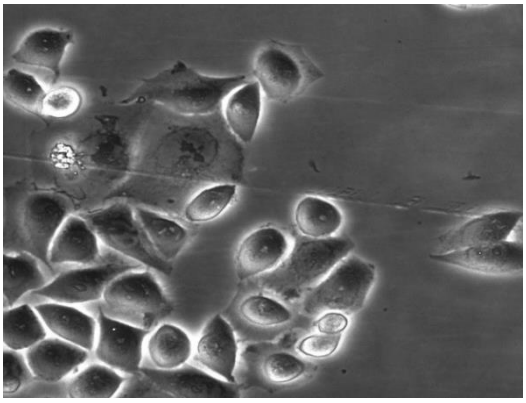

c) Cells with 30 µM Pter after 24 h

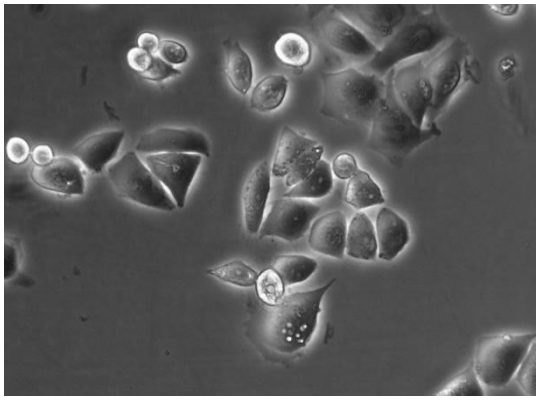

d) Cells with 30 µM Pr.Pter after 24 h

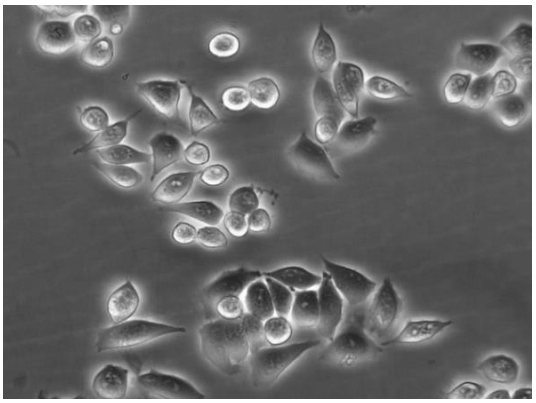

e) Untreated cells after 48 h

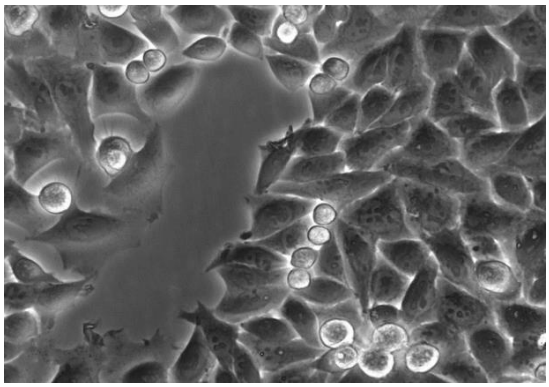

f) Cells with 30 µM RV after 48 h

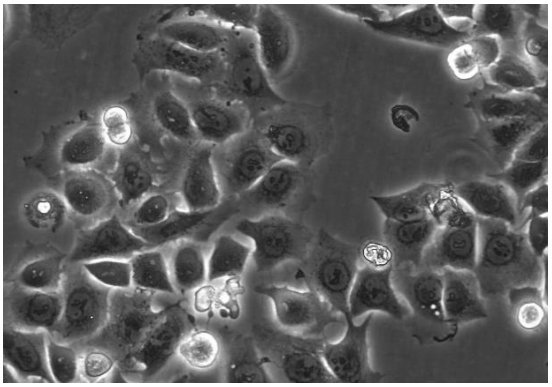

g) Cells with 30 µM Pter after 48 h

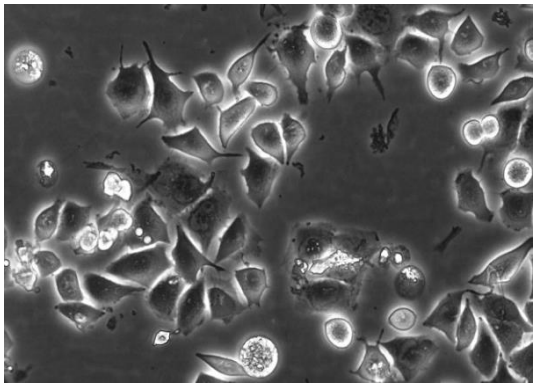

h) Cells with 30 µM Pr.Pter after 48 h

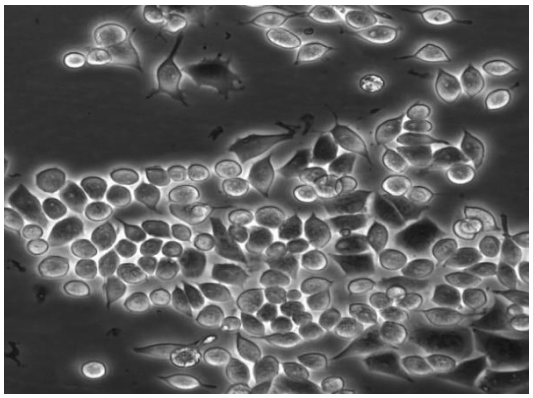

i) Untreated cells after 72 h

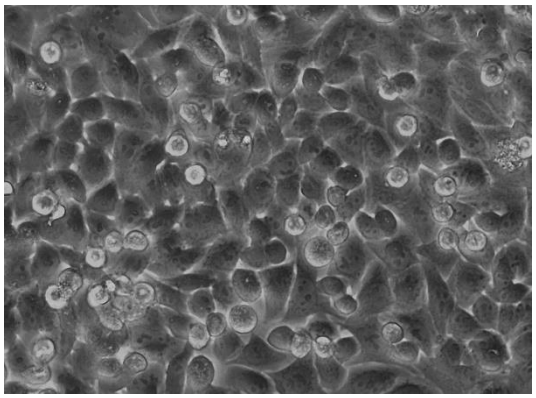

j) Cells with 30 µM RV after 72 h

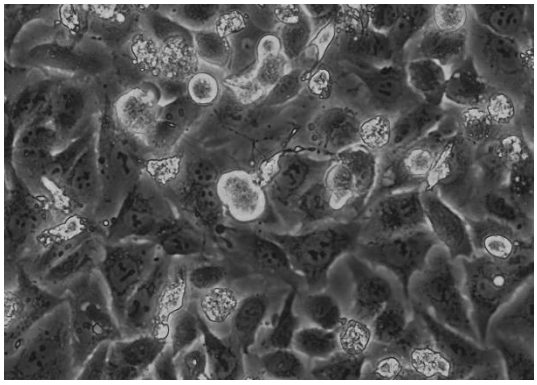

k) Cells with 30 µM Pter after 72 h

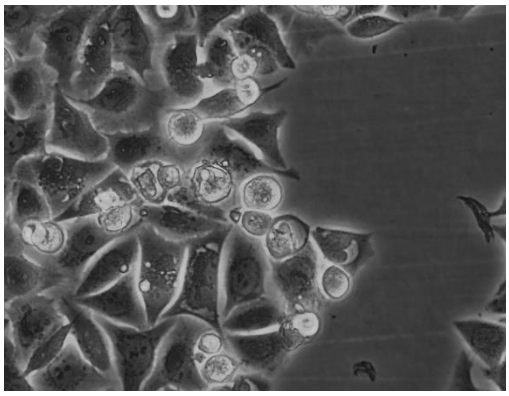

l) Cells with 30 µM Pr.Pter after 72 h

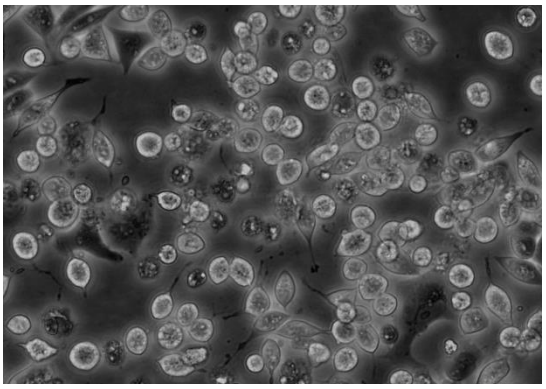

The effect on cell area

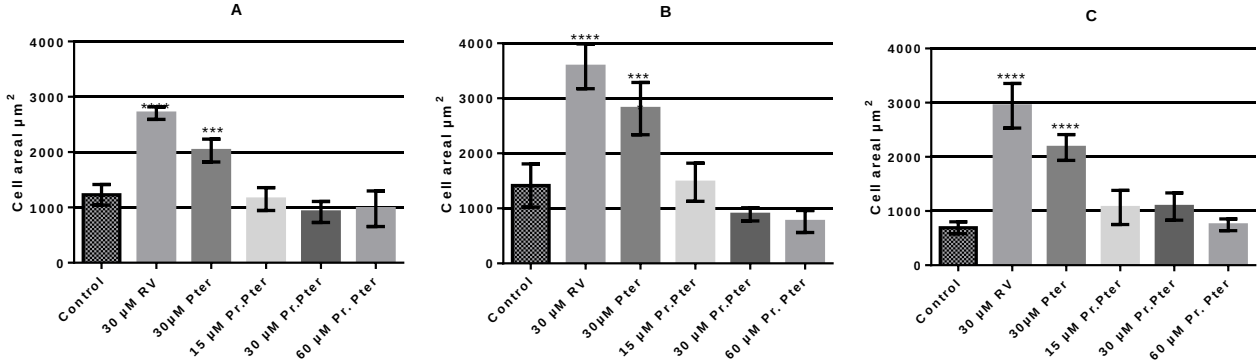

Cell area for DLD-1 cell exposed to (15, 30 and 60 µM) Pr.Pter, 30 µM Pter and 30 µM RV, after 24h: (A), 48h: (B) and 72 h: (C). The values are the mean of the result from three similar experiment and the bars represent the standard deviation of these values, *: P≤0.05, **:P≤0.01, ***:P≤0.001, ****:P≤0.0001 vs. control value.

The cell area of Pr.Pter treated cells did not differ much from the control, although the cell area was slightly reduced after 48 h treatment with 30 and 60 µM Pr.Pter. After 24 and 48 h treatment with 30 µM RV and 30 µM Pter, the cell area significantly increase from 1000-1200µm^2 to 3000-3500 µm2. After 72 h treatment with 30 µM RV and 30 µM Pter the average cell area decreased slightly.

The effect on cell viability

This experiment was done to investigate the effects of Pr.Pter on cell viability and compare its effect with Pter and RV.

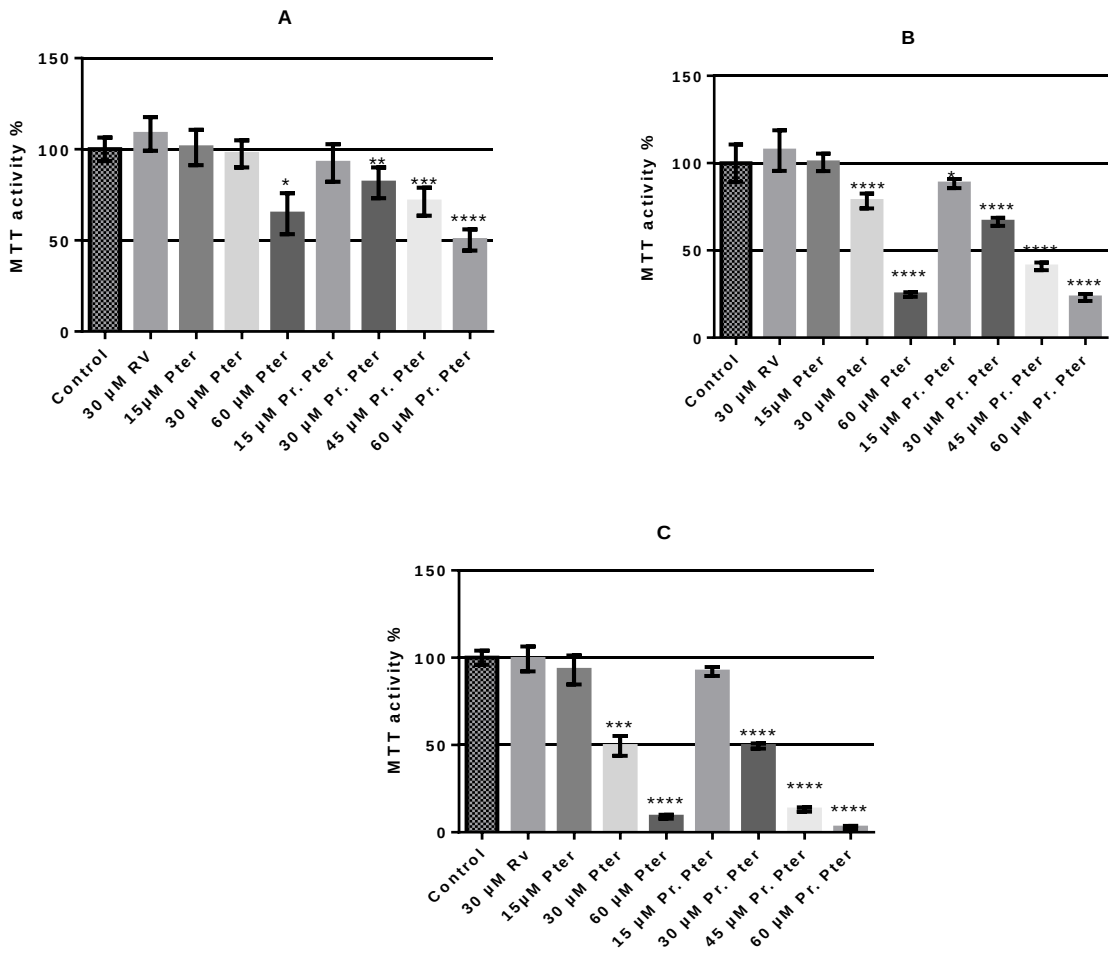

Cell viability for DLD-1 cells exposed to (15, 30 and 60 µM) Pr.Pter, 30 µM Pter and 30 µM RV. Cell exposed for 24h: (A), 48h: (B) and 72 h: (C) The values are the mean of the result from three similar experiment and the bars represent the standard deviation of these values, *: P≤0.05, **:P≤0.01, ***:P≤0.001, ****:P≤0.0001 vs. control value.

Data shows that after 24 h treatment with 15 µM Pr.Pter, MTT activity decreased (8%) but difference is not significantly compared to control, while treatment with 30, 45, 60 µM caused significantly decrease of 20%, 30%, 50%, respectively. 48 h treatment with 15, 30 and 60 µM Pr.Pter caused significantly decreased of 22%, 34%, 77% respectively, in MTT activity. 72 h treatment with 30, 45 and 60 µM Pr.Pter caused significantly decreased of 57%, 87%, and 97% respectively in MTT activity. After 72 h treatment with 15 µM Pr.Pter MTT activity decreased, but difference in not significant.

After 24 h treatment with 30 µM RV, 15 and 30 µM Pter MTT activity did not change, but 60 µM Pter caused 35% decrease in MTT activity. After 48 h treatment with 30 µM RV and 15 µM Pter MTT activity did not change. 48 h treatment with 30 and 60 µM Pter showed significantly decrease of 22% and 76% respectively in MTT activity. MTT activity did not change after treatment with 30 µM RV. After 72 h treatment with 15 µM Pter caused slightly decrease in MTT activity. Treatment with 30 and 60 µM Pter showed significantly decrease of 51% and 91 % respectively in MTT activity.

IC_{50} was calculated by MTT. IC_{50} decreased overtime (48 to 72h) from 39.6 to 29.7µM for Pr.Pter and from 42.7 to 30.3 for Pter. An IC_{50} was not obtained at 24 h.

IC_{50}(µM)	48 hours	72 hours
Pr.Pter	39.6 ± 14.9	29.7 ± 11.3
Pter	42.7 ± 12.7	30.3 ± 16.3

IC_{50} of Pter and Pr.Pter found by MTT assay. The values are the mean of three experiments with percentage of the standard deviations.

The effect on Cell death

To investigate the effect of Pr.Pter, Pter and RV on the cell cycle phases and cell death, FACS analyse was performed. Cells in the sub- G_1 marker windows were considered to be apoptotic. It was observed that induction of the cell death was increased over time to about 28% for both Pr.Pter and RV treated cells after 72 h. It was also observed that induction of cell death was reached to 19% for Pter treated cells after 72 hrs.

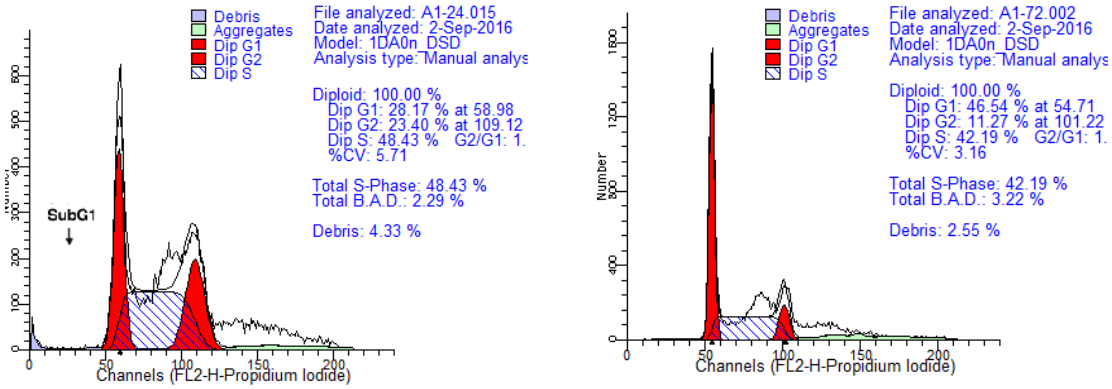

a) Histogram of control after 24 and 72 hrs.

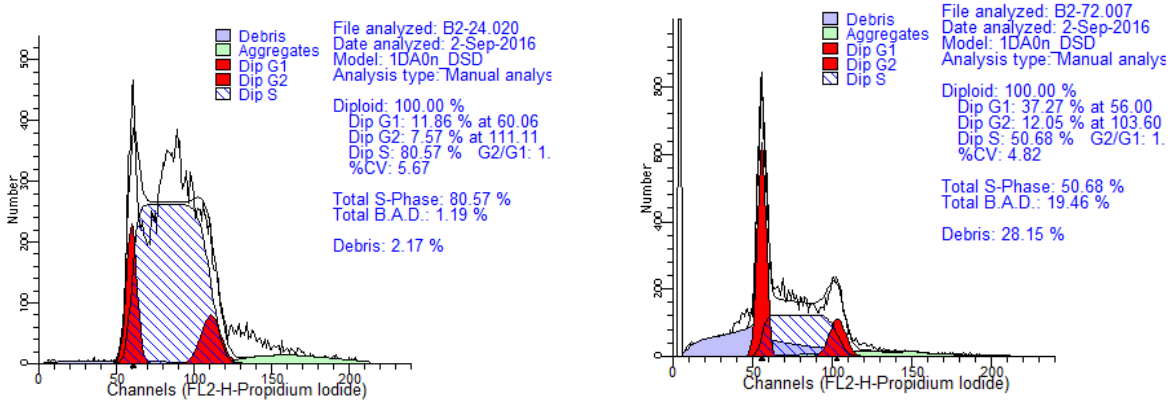

b) Histogram of RV treated cells after 24 and 72 hrs.

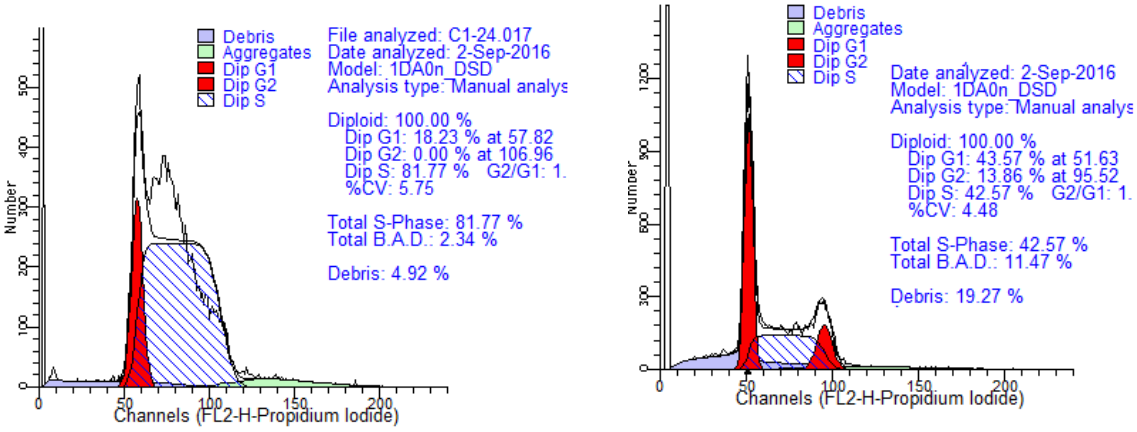

c) Histogram of Pter treated cells after 24 and 72 hrs.

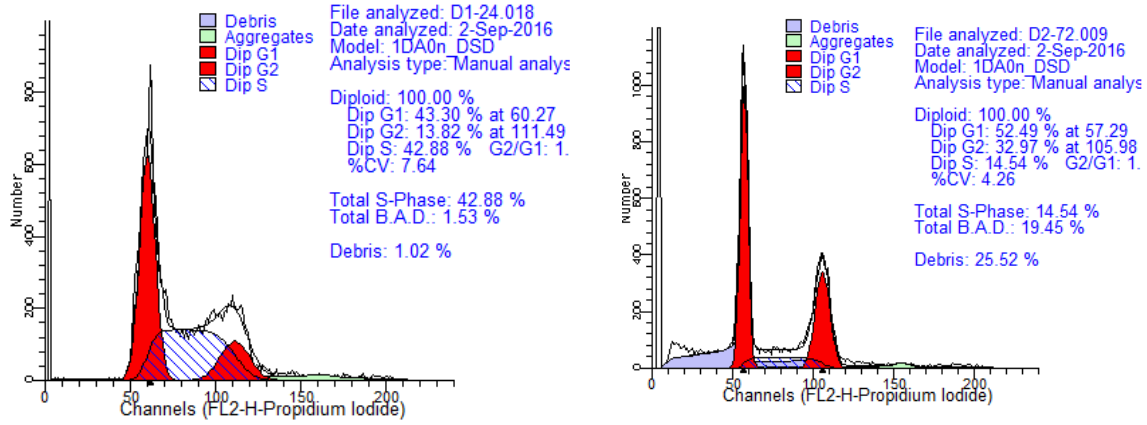

d) Histogram of Pr.Pter treated cells after 24 and 72 hrs.

The effect on the cell cycle

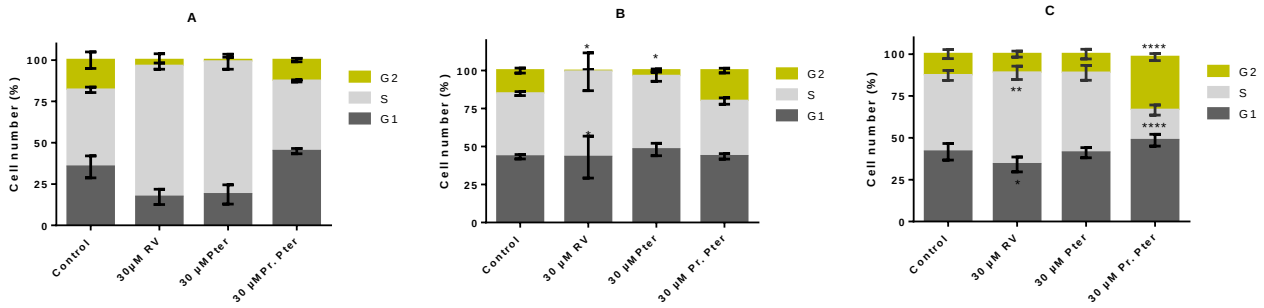

DLD-1 cells were treated with medium containing 30 µM Pr.Pter, 30 µM Pter and 30 µM RV at 24h: (A), 48h: (B) and 72 h: (C). The values are the mean of the results from three similar experiment and the bars represent the standard deviation of these values. *: P≤0.05, **:P≤0.01, ***:P≤0.001, ****:P≤0.0001 vs. control value.

The data showed that Pr.Pter induced cell cycle accumulation in G_1 phase, while both RV and Pter induced cell cycle accumulation in S phase after 24 hrs. However difference in not significant compared to control. 48 h treatment with RV and Pter induced cell cycle accumulation in S phase resulting in a significantly decrease in G_2 phase, while Pr.Pter has almost did not change cell cycle phases compared to control. After 72 h treatment both RV and Pter induced significantly cell cycle accumulation in S phase, resulting in a significantly decrease in G_1 phase. Pter induced also cell cycle accumulation in S phase, but the difference is not significantly from the control. Pr.Pter induced a significantly accumulation in G_2 phase resulting in a significantly decrease in S phase.

Discussion

Compound **12** (Pr.Pter) has not been synthesized before and can be subjected for further biological evaluation. Except in the first step (compound **5**), no attempt was made to optimize yields. ^{1}HNMR was carried out and confirmed formation of major desire product with a minor part of impurities which could not further separated and identified. Therefor the percentage of impurities was not calculated, but the major compound was the desire product and was pure enough to be tested in vitro. Mass spectroscopy confirmed formation of the product. Compound **5** was obtained with high yield of 84.5% versus 96% reported in similar reaction in literature[124]. Compound **6** was obtained with high yield of 91.5% versus 97% reported in similar reaction in literature[124]. Compound **7** was obtained with moderate yield of 67% versus 85% reported in literature[125]. The discrepancy between

the 67% yield in this study and 85% yield made by Rebekah may be explained by different method used for drying of THF. Compound **8** was obtained with moderate yield of 46% versus 43% reported in similar reaction in literature[90]. In synthesis of compound **7,** 3 equivalent of tri ethyl phosphite was used. ^{1}HNMR signal and smells of the reaction mixture showed this amount was too much, therefor for synthesis compound **8** (1.5 eq.) tri ethyl phosphite was used. This led to improve purification. In synthesis compound **10** a longer reaction time was detrimental to the reaction yield and therefor yield was not high enough (15.5%) compared to similar reaction in literature with 82% yield[67]. Compound **11** was obtained with 62% yield after 2 failed attempts. In the third attempt, THF was dried by sodium/benzophenone. This is because n-BuLi is very sensitive to water and THF is hygroscopic. Although molecular sieve are more efficient than sodium benzophenone for drying of solvent, but they are required full activation special in reactions which are very sensitive to water such as in reaction with n-BuLi[77]. Compound **12** was obtained with low yield of 9% versus 75% reported in similar reaction in literature[67]. A low yield could be explained through an increase in side reaction or lose of the product during purification.

The effect of Pr.Pter on cell growth, cell proliferation and cell cycle arrest was examined and compared with Pter to clarify the effect of isoprene side chain. No studies have examined before the effect of Pr.Pter on human cancer cells.

Effect on cell proliferation

DLD-1 cell numbers were reduced after treatment with Pr.Pter, Pter and RV in a dose and time dependent manner. Both Pter and RV showed almost the same manner at 24 hrs 48 and 72 hrs, which is in agreement with other studies [7]. Pr.Pter treated cells showed also reduction in the cell numbers, but first after 48 hrs at 60 µM and then after 72 hrs, a stronger response was observed compared to control. This is may be because of cellular metabolism which takes time to convert Pr.Pter to another compound or may be because Pr.Pter operates on another target molecule which can explained by structural differences. The decrease in the cell number could be due to reduced cell division or increased cell death. In contrast to RV, Pr.Pter treated cells caused a lower cell number compared to set up after 48 h and the number was further decreased. This indicates that Pr.Pter has a stronger inhibitory effect or maybe an irreversible effect on DLD-1 cells. Studies have shown that anti-proliferative of RV is reversible, when replenishing RV treated cells with fresh medium without RV[126]. However this needs to be investigated.

Effect on cell morphology & cell diameter

Based on the result from the cell diameter, it was concluded that Pr.Pter, Pter and RV showed indications of a time and dose dependent effect on the cell diameter. Pr.Pter showed a reduction of 11% in cell diameter after 48 hrs at 30 and 60 µM, while RV and Pter exposed DLD-1 cells were enlarged with maximum effect of 38% at 30 µM. Increase in cell diameter with RV treated cells is in agreement with other studies in the RUC and other articles where showed RV caused cell diameter enlargement.[126, 127]. No study has examined the effect of Pr.Pter on the cell diameter, but other studies have shown that mammalian cell will enlarge if m-TOR and S6K overexpressed or m-TOR inhibitors suppressed or if cell division is inhibited and arrested in S phase[128 129]. M-TOR pathway is involved in cell growth, cell proliferation, protein synthesis and cell size control through the mechanism that are not well defined[130]. Fingar et.al reported that mammalian cell size regulated by m-TOR and PI3K pathways[131 132]. Therefor a decrease in the cell diameter by Pr.Pter treated cells may be linked to inhibition of m-TOR pathway. Increase in the cell diameter by RV and Pter treated cells showed, even though the cell cycle was blocked, cell growth were not affected and they did not inhibit the cell growth or protein synthesis, resulting in larger cells[131].

Pr.Pter treated cell has no significantly effect on cell area, while RV and Pter treated cells caused cell area enhancement compared to control. Increase in the cell area could be linked to an increase in the cell attachment and arrangement of actin cytoskeleton which is regulated by mTORC2[133]. Study showed that eukaryote cells will reduce in size if they arrested in G_1 phase and will increase in size if they arrested in S phase[134]. Therefor it could speculate that Pr.Pter caused cell cycle arrest at G_1 phase, while RV and Pter caused cell cycle arrest in S or G_2 phase. In other word they have different targeting molecule. Altogether, it was found that Pr.Pter, Pter and RV were able to induce morphological changes in DLD-1 cells. It is thought that observed morphological change is related to changes in the adherence function of the cells[127].

Effect on cell viability

Based on the result from MTT, it was concluded that Pr.Pter and Pter showed indications of a time and dose dependent effect on cell viability. Pr.Pter treated cells showed a very strong response in MTT activity and cell viability significantly decreased after 24 h. 51% of cell viability was inhibited with 60 µM, while cell viability did not change with Pter treated cells after 24 hrs. As Pr.Pter was able to reduce the cell number in Coulter counter, it would be expected the same effect in MTT but

MTT showed a very strong response. This was may be some of the counted cells in Coulter counter were already dead. The cell viability did not change when they was exposure to RV at 24, 48, 72 hrs. This finding is in agreement with the observed result by Bernhard[135]. This is may be because 30 µM RV is not sufficient for induce apoptosis and reduction in cell numbers was related to reduction in cell growth. This is in agreement with observed result by Duranton .Duranton et al. reported that 25 µM RV can reduce proliferation of Caco-2 cells, but cannot induce apoptosis[136].

IC_{50} values decreased overtime (48 to 72h) from 39.6 to 29.7 µM for Pr.Pter and from 42.7 to 30.3 µM for Pter which is comparable with IC_{50} values in Coulter counter. IC_{50} values was also decreased overtime (48 to 72) from 54.8 to 25.5µM for Pr.Pter treated cells in Coulter counter. This indicates that Pr.Pter was toxic for DLD-1 cells and less amount of Pr.Pter was needed when cells were exposed for a longer time. Furthermore, it showed that DLD-1 cells were not able to detoxify or maintain resistant to Pr.Pter. IC_{50} values were slightly lower for Pr.Pter compared to Pter treated cells; this also showed a better inhibitory effect for Pr. Petr.

Effect on cell cycle

Base on the result from FACS, Pr.Pter treated cell caused accumulation in G_1 phase after 24 hrs compared to control. This is may be linked to decrease expression of cyclin D [55]. Cyclin D is responsible for transition from G1 to S phase. After 48 hours, this G_1 phase accumulation was no longer observed compared to the control. But after 72 h a strong accumulation in G_2 phase was observed. This could be a result of the death of some G1 arrested cells. Other studies have also observed a shift in phase distribution, for example from S phase to G_2 phase, when increasing exposure time from 48 to 72 h [137]. Accumulation of cells in G_1 or S phase caused cells are spending longer time in these phases than normal, resulting the reduced proliferation.

RV and Pter treated cells caused a large S phase accumulation after 24, 48 and 72 h compared to the control. These observations confirm the evidence in the literature[138 137 55 139]. Accumulation in S phase can be due inhibition of DNA polymerase α and δ[4, 55].

FACS analysis revealed also an increase of sub-G_1 for Pr.Pter, Pter and RV treated cells after 72 h. Therefor Pr.Pter, Pter and RV were able to induce cell death in a time dependent manner. Other studies have also showed Pter and RV can induce apoptosis in different cell line[126 140]. Pr.Pter treated cells led to greater extent (28%) of cell death than Pter treated cells (19%).

Conclusion

In conclusion synthesis Pr.Pter was accomplished through the HWE reaction in 6 steps. Attempt to employ TCT/DMF system was met with problems, which were overcomes through the Zink mediated phosphonate synthesis. The HWE reaction was not complicated, but some of the product was lost through de-protection reaction and this make other steps challenging with so little product to work it. The DoM reaction was another challenging step, because the environment of reagents has to be kept free from oxygen and water, which was difficult to obtain by molecular sieve and 0.20 g of compound 11 was lost in the first and second attempt. However, formation of Pr.Pter was achieved and many of its biological activities were explored. Pr.Pter was shown to inhibit the growth of DLD-1 cells in a dose and time dependent manner in vitro. MTT analysis showed a very strong effect (51%) after 24 h and IC_{50} showed a better activity of Pr.Pter compared with Pter. FACS analysis revealed that Pr.Pter arrested cells at G_1 phase after 24 h and G_2 after 72 h. FACS analysis showed also Pr.Pter caused induction of cell death (25.5%) after 72 h versus 19.3% of Pter treated cells. These finding indicated that prenylation might improve the cancer prevention effect of Pter, however further investigations are needed.

Perspective

This study has demonstrated anti-cancer activity of Pr.Pter in the DLD-1 cells in vitro. It is still unknown which pathways were involved in the reduction of the cell growth and inducing of the cell death. Further research in this area could be done. In future studies it would be interesting to examine its effect on the other cancer cells or on the normal cells. This study was performed in vitro and an important stage in further research would be study in vivo.

References

Front Background is showing DLD-1 cells after 72 h treatment with 60 µM Pr.Pter

1. Sameer AS. Colorectal cancer: molecular mutations and polymorphisms. *Front Oncol*. 2013;3(May):114. doi:10.3389/fonc.2013.00114.

2. Vegetables V. Chemoprevention of Cancer. 1996;(September):96-99.

3. Rimando AM, Suh N, Products N, Brunswick N. Biological / Chemopreventive Activity of Stilbenes and their Effect on Colon Cancer. 2008:1635-1643. doi:10.1055/s-0028-1088301.

4. Lines C, Joe AK, Liu H, et al. Resveratrol Induces Growth Inhibition , S-phase Arrest , Apoptosis , and Changes in Biomarker Expression in Several Human Cancer. 2002;8(March):893-903.

5. Gosslau A, Chen KY. Nutraceuticals, apoptosis, and disease prevention. *Nutrition*. 2004;20(1):95-102. doi:10.1016/j.nut.2003.09.017.

6. Saiko P, Szakmary A, Jaeger W, Szekeres T. Resveratrol and its analogs: Defense against cancer, coronary disease and neurodegenerative maladies or just a fad? *Mutat Res - Rev Mutat Res*. 2008;658(1-2):68-94. doi:10.1016/j.mrrev.2007.08.004.

7. Suh N, Paul S, Hao X, et al. Cancer Susceptibility and Prevention Pterostilbene , an Active Constituent of Blueberries , Suppresses Aberrant Crypt Foci Formation in the Azoxymethane-Induced Colon Carcinogenesis Model in Rats. 2007;13(1):350-355. doi:10.1158/1078-0432.CCR-06-1528.

8. Soleas GJ, Diamandis EP, Goldberg DM. The world of resveratrol. *Adv Exp Med Biol*. 2001;492:159-182.

9. Murtaza G, Latif U, Najam-Ul-Haq M, et al. Resveratrol: An active natural compound in red wines for health. *J Food Drug Anal*. 2013;21(1):1-12. doi:10.6227/jfda.2013210101.

10. Aggarwal BB, Bhardwaj a, Aggarwal RS, Seeram NP, Shishodia S, Takada Y. *Role of Resveratrol in Prevention and Therapy of Cancer: Preclinical and Clinical Studies*. Vol 24.; 2004.

11. Botta B, Botta B, Vitali A, Menendez P, Misiti D, Delle G. Prenylated Flavonoids : Pharmacology and Biotechnology Prenylated Flavonoids : Pharmacology and Biotechnology. 2005;(February 2016). doi:10.2174/0929867053202241.

12. Yang DS, Wei JG, Peng WB, et al. Cytotoxic prenylated bibenzyls and flavonoids from Macaranga kurzii. *Fitoterapia*. 2014;99:261-266. doi:10.1016/j.fitote.2014.10.003.

13. Yang T, Fang L, Rimando AM, Sobolev V, Mockaitis K, Medina-Bolivar F. A Stilbenoid-Specific Prenyltransferase Utilizes Dimethylallyl Pyrophosphate from the Plastidic Terpenoid Pathway. *Plant Physiol*. 2016;171(4):2483-2498. doi:10.1104/pp.16.00610.

14. W??tjen W, Weber N, Lou Y j., et al. Prenylation enhances cytotoxicity of apigenin and liquiritigenin in rat H4IIE hepatoma and C6 glioma cells. *Food Chem Toxicol*. 2007;45(1):119-124. doi:10.1016/j.fct.2006.08.008.

15. Hanahan D, Weinberg R a, Francisco S. The Hallmarks of Cancer Review University of California at San Francisco. 2000;100:57-70.

16. Favaloro B, Allocati N, Graziano V, Ilio C Di, Laurenzi V De. Role of Apoptosis in disease. 4(5):330-349.

17. Bergers G, Benjamin LE, Francisco S. TUMORIGENESIS AND THE. 2003;3(June):1-10. doi:10.1038/nrc1093.

18. Chiang AC. Molecular Basis of Metastasis. 2008.

19. Shay JW, Zou Y, Hiyama E, Wright WE. Telomerase and cancer. 2001;10(7):677-686.

20. Cancerregisteret. Nye kræfttilfælde i Danmark - 2014. 2014:1-51. http://www.esundhed.dk/sundhedsregistre/CAR/CAR01/Sider/Tabel.aspx.

21. Bardhan K, Liu K. Epigenetics and colorectal cancer pathogenesis. *Cancers (Basel)*. 2013;5(2):676-713. doi:10.3390/cancers5020676.

22. Sinclair P, Singh A, Riaz AA, Amin A. An unsolved conundrum: The ideal follow-up strategy after curative surgery for colorectal cancer. *Gastrointest Endosc*. 2012;75(5):1072-1079. doi:10.1016/j.gie.2012.01.004.

23. Brenner H, Kloor M, Pox CP. Colorectal cancer. In: *The Lancet*. Vol 383. ; 2014:1490-1502. doi:10.1016/S0140-6736(13)61649-9.

24. Nedrebø BSO. Colorectal Cancer in Norway. 2013.

25. Johns Hopkins medicine. https://gi.jhsps.org/GDL_Disease.aspx?CurrentUDV=31&GDL_Cat_ID=AF793A59-B736-42CB-9E1F-E79D2B9FC358&GDL_Disease_ID=B329650A-F196-4B6E-89D2-1D9BAE11538B.

26. Takuji Tanaka. Colorectal carcinogenesis: Review of human and experimental animal studies. *J Carcinog*. 2009:5. doi:10.4103/1477-3163.49014.

27. Wargovich MJ, Brown VR, Morris J. Aberrant crypt foci: The case for inclusion as a biomarker for colon cancer. *Cancers (Basel)*. 2010;2(3):1705-1716. doi:10.3390/cancers2031705.

28. Mcintyre RE, Buczacki SJA, Arends MJ, Adams DJ. Mouse models of colorectal cancer as preclinical models. *BioEssays*. 2015;37(8):909-920. doi:10.1002/bies.201500032.

29. Vogelstein B, Fearon ER, Hamilton SR, et al. Genetic alterations during colorectal-tumor development. *N Engl J Med*. 1988;319(9):525-532. doi:10.1056/NEJM198809013190901.

30. Leslie a, Carey F a, Steele RJC. The colorectal adenoma ± carcinoma sequence. *Br J Surg*. 2002:845-860. doi:10.1046/j.1365-2168.2002.02120.x.

31. Kim EC, Lance P. Colorectal polyps and their relationship to cancer. *Gastroenterol Clin North Am*. 1997;26(1):1-17. doi:10.1016/S0889-8553(05)70280-6.

32. Roberts P, Der C. Targeting the Raf-MEK-ERK mitogen-activated protein kinase cascade for the treatment of cancer. *Oncogene*. 2007;26:3291-3310. doi:10.1038/sj.onc.1210422.

33. Baldus SE, Schaefer KL, Engers R, Hartleb D, Stoecklein NH, Gabbert HE. Prevalence and heterogeneity of KRAS, BRAF, and PIK3CA mutations in primary colorectal adenocarcinomas and their corresponding metastases. *Clin Cancer Res*. 2010;16(3):790-799. doi:10.1158/1078-0432.CCR-09-2446.

34. Spencer DS, Robbins RJ, Naftolin F. The New England Journal of Medicine Downloaded from nejm.org at DTU Library on October 30, 2013. For personal use only. No other uses without permission. Copyright © 1992 Massachusetts Medical Society. All rights reserved. *N Engl J Med*. 1992;327(22):1541-1548.

35. Devilee P, Cornelisse CJ, Devilee P. Ever since Knudson. 2001;17(10):569-573.

36. Lane DP. Cancer. p53, guardian of the genome. *Nature*. 1992;358(6381):15-16. doi:10.1038/358015a0.

37. Baker SJ, Preisinder AC, Jesus JM, Paraskeva C, Markowitz S, Wilson JK, Hamilton S VB. P53 Gene Mutations Occur in Combination With 17P Allelic Deletions As Late Events in Colorectal Tumorigenesis. *Cancer Res*. 1990:7717-7722.

38. Labianca R, Beretta GD, Kildani B, et al. Colon cancer. *Crit Rev Oncol Hematol*. 2010;74(2):106-133. doi:10.1016/j.critrevonc.2010.01.010.

39. Stewart ZA, Westfall MD, Pietenpol JA. Cell-cycle dysregulation and anticancer therapy. *Trends Pharmacol Sci*. 2003;24(3):139-145. doi:10.1016/S0165-6147(03)00026-9.

40. Whitaker M. Cell Cycle. 1996:240. doi:10.1080/15384101.2015.1044188.

41. Nevins JR. The Rb / E2F pathway and cancer. 2001;10(7):699-704.

42. Gautschi O, Ratschiller D, Gugger M, Betticher DC, Heighway J. Cyclin D1 in non-small cell lung cancer: A key driver of malignant transformation. *Lung Cancer*. 2007;55(1):1-14. doi:10.1016/j.lungcan.2006.09.024.

43. Takahashi-Yanaga F, Sasaguri T. GSK-3?? regulates cyclin D1 expression: A new target for chemotherapy. *Cell Signal*. 2008;20(4):581-589. doi:10.1016/j.cellsig.2007.10.018.

44. Maddika S, Ande SR, Panigrahi S, et al. Cell survival, cell death and cell cycle pathways are interconnected: Implications for cancer therapy. *Drug Resist Updat*. 2007;10(1-2):13-29. doi:10.1016/j.drup.2007.01.003.

45. Musgrove E a. Cyclins: roles in mitogenic signaling and oncogenic transformation. *Growth Factors*. 2006;24(March 2006):13-19. doi:10.1080/08977190500361812.

46. O'Brien MA, Kirby R. Apoptosis: A review of pro-apoptotic and anti-apoptotic pathways and dysregulation in disease. *J Vet Emerg Crit Care*. 2008;18(6):572-585. doi:10.1111/j.1476-4431.2008.00363.x.

47. Riedl SJ, Shi Y. MOLECULAR MECHANISMS OF CASPASE REGULATION DURING APOPTOSIS. 2004;5(November). doi:10.1038/nrm1496.

48. Liu RH. Nutrition , and Cancer Potential Synergy of Phytochemicals in Cancer Prevention : Mechanism of Action 1. 2004:3479-3485.

49. Liu RH. Health benefits of fruit and vegetables are from additive and synergistic combinaions of phytochemicals. *Am J Clin Nutr*. 2003;78:3-6.

50. de la Rosa L.A., Alvarez-Parrilla E. G-AG. *Fruit and Vegetable Phytochemicals: Chemistry, Nutritional Value, and Stability*. 1st ed. Wiley J. & Sons; 2010. http://197.14.51.10:81/pmb/AGROALIMENTAIRE/0813803209 PhytochemicalsA.pdf.

51. Surh YJ. Molecular mechanisms of chemopreventive effects of selected dietary and medicinal phenolic substances. *Mutat Res - Fundam Mol Mech Mutagen*. 1999;428(1-2):305-327. doi:10.1016/S1383-5742(99)00057-5.

52. Surh Y-J. Cancer chemoprevention with dietary phytochemicals. *Nat Rev Cancer*. 2003;3(10):768-780. doi:10.1038/nrc1189.

53. Fulda S. Resveratrol and derivatives for the prevention and treatment of cancer. *Drug Discov Today*. 2010;15(17-18):757-765. doi:10.1016/j.drudis.2010.07.005.

54. Wang Y-J, Chen R-J. *Pterostilbene Protection and Bladder Cancer Cells*. Elsevier; 2014. doi:10.1016/B978-0-12-405205-5.00027-1.

55. Wolter F, Akoglu B, Clausnitzer A, Stein J. Downregulation of the cyclin D1/Cdk4 complex occurs during resveratrol-induced cell cycle arrest in colon cancer cell lines. *J Nutr*. 2001;131(8):2197-2203. http://www.ncbi.nlm.nih.gov/pubmed/11481417.

56. Delmas D, Rébé C, Lacour S, et al. Resveratrol-induced Apoptosis Is Associated with Fas Redistribution in the Rafts and the Formation of a Death-inducing Signaling Complex in Colon Cancer Cells. *J Biol Chem*. 2003;278(42):41482-41490. doi:10.1074/jbc.M304896200.

57. Mccormack D, Mcfadden D. Pterostilbene and Cancer : Current Review. *J Surg Res*. 2012;173(2):e53-e61. doi:10.1016/j.jss.2011.09.054.

58. Planas JM, Colom H, Juan ME. Resveratrol : A polyphenol with multiple effects. *Recent Adv Pharm Sci*. 2011;661(2):101-120. http://diposit.ub.edu/dspace/bitstream/2445/21369/1/256197.pdf.

59. Chromatography OF. Ow. 32:323-336.

60. Of A, Diffusa C, Br WNE, Part A. Academic Sciences. *Int J Pharm*. 2013;5(2):3-6.

61. Gertz Likhtenshtein. Stilbenes. Applications in Chemistry, Life Sciences and Materials Science. In: WILEY-VCH Verlag GmbH; 2009:1.

62. Takaoka M. Resveratrol, a new phenolic compound, from Veratrum grandiflorum. *J Chem Soc Japan*. 1939;60:1090-1100.

63. Chemistry T. Extractives from Hardwoods. Part X I I I . 3693 742. The Chemistry. 1953;(I):3693-3697.

64. Alhassan AM, Abdullahi MI, Uba A, Umar A. Prenylation of aromatic secondary metabolites: A new frontier for development of novel drugs. *Trop J Pharm Res*. 2014;13(2):307-314. doi:10.4314/tjpr.v13i2.22.

65. Yazaki K, Sasaki K, Tsurumaru Y. Prenylation of aromatic compounds, a key diversification of plant secondary metabolites. *Phytochemistry*. 2009;70(15-16):1739-1745. doi:10.1016/j.phytochem.2009.08.023.

66. Chen C, Tsai P, Wei B, Chiou W. 8-Prenylkaempferol suppresses inducible nitric oxide synthase expression through interfering with JNK-mediated AP-1 pathway in murine macrophages. 2008;590:430-436. doi:10.1016/j.ejphar.2008.05.018.

67. Park BH, Lee HJ, Lee YR. Total Synthesis of Chiricanine A, Arahypin-1, trans-Arachidin-2, trans-Arachidin-3, and Arahypin-5 from Peanut Seeds. *J Nat Prod*. 2011;74(4):644-649. doi:10.1021/np100696f.

68. De Luca L, Giacomelli G, Porcheddu A. An efficient route to alkyl chlorides from alcohols using the complex TCT/DMF. *Org Lett*. 2002;4(4):553-555. doi:10.1021/ol017168p.

69. Nieddu G, De Luca L, Giacomelli G. A Chemoselective, Easy Bromination of

(Hydroxymethyl)phenols. *Synthesis (Stuttg)*. 2008;2008(24):3937-3940. doi:10.1055/s-0028-1083247.

70. Mokhtari B, Azadi R, Azhdari A. 2,4,6-Trichloro-1,3,5-triazine/dimethylformamide as an efficient reagent for one-pot conversion of alcohols into N-alkylphthalimides. *Chinese Chem Lett*. 2010;21(2):171-174. doi:10.1016/j.cclet.2009.10.006.

71. Viswanatha V, Hruby VJ. Synthesis of [3',5'-13C2]tyrosine and its use in the synthesis of specifically labeled tyrosine analogs of oxytocin and arginine vasopressin and their 2-D-tyrosine diastereoisomers. *J Org Chem*. 1979;44(16):2892-2896. doi:10.1021/jo01330a014.

72. Publication A. Monochloromethyl Ether. *Org Synth*. 1929;9(September):58. doi:10.15227/orgsyn.009.0058.

73. June, 1963 853. 1963;I(11):1963.

74. DeHaan FP, Djaputra M, Grinstaff MW, et al. Electrophilic Aromatic Substitution. 13. Kinetics and Spectroscopy of the Chloromethylation of Benzene and Toluene with Methoxyacetyl Chloride or Chloromethyl Methyl Ether and Aluminum Chloride in Nitromethane or Tin Tetrachloride in Dichloromethane. The . *J Org Chem*. 1997;62(9):2694-2703. doi:10.1021/jo961064o.

75. Rucker C. The Triisopropylsilyl Group in Organic Chemistry : Just a Protective Group , or More ? 1995:1009-1064.

76. Naegeli P, Oppolzer W, Vorburggen H, et al. the Editor. 1972;1490(1971):6190-6191.

77. Williams DBG, Lawton M. Drying of organic solvents: quantitative evaluation of the efficiency of several desiccants. *J Org Chem*. 2010;75(24):8351-8354. doi:10.1021/jo101589h.

78. Bartoszewicz A, Kalek M, Nilsson J, Hiresova R, Stawinski J. A new reagent

system for efficient silylation of alcohols: Silyl chloride-N-methylimidazole-iodine. *Synlett*. 2008;2(1):0037-0040. doi:10.1055/s-2007-992379.

79. Wiley J, Groups PGMP, Organic I, York SN. Protective Groups – Silicon-Based Protection of the Hydroxyl Group. 2007:1-26.

80. Applied W, Journal S. Chemoselective Reduction of Carbonyl Compounds Corresponds to Alcohols by Sodium Borohydride Adsorbed in Silica Lipid Substrate as a Novel Chemical Agent. 2015;(November).

81. General BI, Finholt a E, Horvitz LEO, Earl K. New Developments i n the Chemistry. 1953;219:186-190.

82. Vilarinho-Franco T, Tenu R, Delmas J, Heitzmann M, Capron P, Goutaudier C. Lifetime analysis of a hydrogen generator by hydrolysis of sodium borohydride. *Energy Procedia*. 2013;36(4):1192-1201. doi:10.1016/j.egypro.2013.07.135.

83. William H. Brown and Lawrence S. Brown. *Organic Chemistry*. 6th ed. Cengage Learning; 2011.

84. Melorose J, Perroy R, Careas S. Reduction of Ketones by Sodium Borohydride. *Statew Agric L Use Baseline 2015*. 2015;1:1108-1109. doi:10.1017/CBO9781107415324.004.

85. Ashley K, Cordell D, Mavinic D. A brief history of phosphorus: From the philosopher's stone to nutrient recovery and reuse. *Chemosphere*. 2011;84(6):737-746. doi:10.1016/j.chemosphere.2011.03.001.

86. Engel, Robert-Cohen JI. *Synthesis of Carbon–Phosphorus Bonds*. 2nd ed. New York: CRC Press; 2003.

87. Statistik BP. Phosphorus. In: *Katalog BPS*. Vol XXXIII. ; 2014:81-87. doi:10.1007/s13398-014-0173-7.2.

88. D.E.C. Corbridge. *Phosphorus: An Outline of Its Chemistry, Biochemistry, and*

Technology. 4th ed. New York: Elsevier; 1990.

89. Murphy PJ. *OrganoPhosphorus Reagents*. Oxford: Oxfor university press; 2004.

90. Richardson RM. New synthesis and reactions of phosphonates. 2012. http://ir.uiowa.edu/etd/3375/.

91. Bhattacharya A, Thyagarajan G. The Michaelis-Arbuzov Rearrangement. *Chem Rev*. 1981;81:415-430. doi:10.1021/cr00044a004.

92. Hudson HR, Powroznyk L. Some new observations on an old reaction: disproportionation and the formation of P-O-P intermediates in the Michaelis-Arbuzov reaction of triaryl phosphites with alkyl halides. *Arkivoc*. 2004;2004(9):19-33. doi:10.3998/ark.5550190.0005.905.

93. Rajeshwaran GG, Nandakumar M, Sureshbabu R, Mohanakrishnan AK. Lewis Acid-Mediated Michaelis - Arbuzov Reaction at Room Temperature : A Facile Preparation of Arylmethyl / Heteroarylmethyl Phosphonates. *Org Lett*. 2010;13(6):1270-1273.

94. Barney RJ, Richardson RM, Wiemer DF. Direct conversion of benzylic and allylic alcohols to phosphonates. *J Org Chem*. 2011;76(8):2875-2879. doi:10.1021/jo200137k.

95. Reaction ADR. Synthesis of Zinc Iodide Revisited. *J Chem Educ*. 2003;80(7):796-798.

96. Nicolaou KC, Harter MW, Gunzner JL, Nadin A. The Wittig and Related Reactions in Natural Product Synthesis *. *Liebigs Ann Chem*. 1997:1283-1301. doi:10.1002/jlac.199719970704.

97. Wadsworth WS, Emmons WD. The utility of phosphonate carbanions in olefin synthesis. *J Am Chem Soc*. 1961;83(7):1733-1738. doi:10.1021/ja01468a042.

98. Steinbach T, Wahlen C, Wurm FR. Poly(phosphonate)-mediated Horner–Wadsworth–Emmons reactions. *Polym Chem*. 2015;6(7):1192-1202. doi:10.1039/C4PY01365D.

99. Boutagy J, Thomas R. Olefin synthesis with organic phosphonate carbanions. *Chem Rev*. 1974;74(1):87-99. doi:10.1021/cr60287a005.

100. Kokin K, Iitake K-I, Takaguchi Y, Aoyama H, Hayashi S, Motoyoshiya J. a Study on the Z-Selective Horner-Wadsworth-Emmons (Hwe) Reaction of Methyl Diarylphosphonoacetates. *Phosphorus Sulfur Silicon Relat Elem*. 1998;133(1):21-40. doi:10.1080/10426509808032451.

101. Almond HR, Whittle RR, Olofson RA. Stereochemistry and Mechanism. 1986;(6):7664-7678.

102. Reaction TH. Chem 115. 2011:4133-4135.

103. Krawczuk P. Baran Group Meeting Directed Metalation : A Survival Guide Baran Group Meeting Other Metalation Considerations Directed Metalation : A Survival Guide Nature of the Base and Solvent Paul Krawczuk Reactivity of Metalated Arenes. *Current*. 2007.

104. Mallan M, Bebb RL. Organolithium compounds 3. *Chem Rev*. 1969;835(16):693-795. doi:10.1021/cr60261a006.

105. J. J. Zuckerman APH. *Inorganic Reactions and Methods*. New York: VCH; 1988. https://books.google.dk/books?id=KNQOZBreJhgC&pg=PA8&lpg=PA8&dq=Reduction+of+carbon+x+bond+with+lithium&source=bl&ots=bpdEClGavj&sig=ExtiixgEl3JaSGRAYAxtYPEHf6I&hl=da&sa=X&ved=0ahUKEwjD_I7Bkq3PAhUGliwKHdXrAGkQ6AEIZDAJ#v=onepage&q=Reduction of carbon x bond with lithium&f=false.

106. RAPPOPORT Z. *The Chemistry of Organolithium Compounds*. Jerusalem: John Wiley & Sons; 2004.

107. Bauer W, Winchester WR, Schleyer PVR. Monomeric Organolithium Compounds in Tetrahydrofuran: fert-Butyllithium, sec-Butyllithium, “Supermesityllithium”, Mesityllithium, and Phenyllithium. Carbon-Lithium Coupling Constants and the Nature of Carbon-Lithium Bonding. 1987;(7):2371-2379.

108. Raposo ML, Fernández-Nieto F, Garcia-Rio L, Rodríguez-Dafonte P, Paleo MR, Sardina FJ. Mechanism of the deprotonation reaction of alkyl benzyl ethers with n-butyllithium. *Chem - A Eur J*. 2013;19(29):9677-9685. doi:10.1002/chem.201204467.

109. Organolithium-verbindungen MN Von, Giinther VH, Moskau D, Bast P. Moderne NMR-Spektroskopie von Organolithium-Verbindungen.

110. Kaufmann E, Houk KN, Wu Y. + Q. 1985;(7):5560-5562.

111. Siegel D, Brubaker J, Liu F. Organolithium Reagents. *Chem 115 Handouts*. 2016:4.

112. Ajani OO, Shomade MO, Edobor-osoh A, Ajanaku CO, Ajani AO. Complex-Induced Proximity Effect in Lithiation : Unveiling Recent Potentials in Organic Synthesis of Biologically Relevant Heterocyclic Compounds. 2015:16-34. doi:10.2174/1874095201509010016.

113. Krouse IH, Wenthold PG. Fluorotrimethylsilane affinities of anionic nucleophiles: A study of fluoride-induced desilylation. *J Am Soc Mass Spectrom*. 2005;16(5):697-707. doi:10.1016/j.jasms.2005.01.014.

114. Simas ABC, Pereira VLP, Barreto CB, De Sales DL, De Carvalho LL. An expeditious and consistent procedure for tetrahydrofuran (THF) drying and deoxygenation by the still apparatus. *Quim Nova*. 2009;32(9):2473-2475. doi:10.1590/S0100-40422009000900042.

115. Wills B, Finch J. Particle size analysis. *Wills’ Miner Process Technol 8th Ed*. 2002;211:91-107. doi:10.1016/S1369-7021(02)00647-8.

116. Graham MD. The Coulter Principle: Foundation of an industry. *JALA - J Assoc Lab Autom*. 2003;8(6):72-81. doi:10.1016/S1535-5535(03)00023-6.

117. Mosmann T. Rapid colorimetric assay for cellular growth and survival: Application to proliferation and cytotoxicity assays. *J Immunol Methods*. 1983;65(1-2):55-63. doi:10.1016/0022-1759(83)90303-4.

118. Al-araji YH, Shneine JK, Ahmed AA. Chemistry of formazan. 2015;5(1):41-76.

119. Berridge M V., Herst PM, Tan AS. Tetrazolium dyes as tools in cell biology: New insights into their cellular reduction. *Biotechnol Annu Rev*. 2005;11(SUPPL.):127-152. doi:10.1016/S1387-2656(05)11004-7.

120. Berridge MV, Tan AS. Characterization of the Cellular Reduction of 3-(4,5-dimethylthiazol-2-yl)-2,5-diphenyltetrazolium bromide (MTT): Subcellular Localization, Substrate Dependence, and Involvement of Mitochondrial Electron Transport in MTT Reduction. *Arch Biochem Biophys*. 1993;303(2):474-482. doi:10.1006/abbi.1993.1311.

121. Bounous DI, Campagnoli RP, Brown J, Bounous DI, Campagnoli ARP, Brownb J. Comparison of MTT Colorimetric Assay and Tritiated Thymidine Uptake for Lymphocyte Proliferation Assays Using Chicken Splenocytes Published by : American Association of Avian Pathologists Stable URL : http://www.jstor.org/stable/1591566 REFERENCES Linked . 2016;36(4):1022-1027.

122. O'Neill K, Aghaeepour N, Špidlen J, Brinkman R. Flow Cytometry Bioinformatics. *PLoS Comput Biol*. 2013;9(12). doi:10.1371/journal.pcbi.1003365.

123. Wilson GD. Probing the Cell Cycle with Flow Cytometry. *J Biomed Sci Eng*. 2014;7(9):698-711. http://www.scirp.org/journal/PaperDownload.aspx?DOI=10.4236/jbise.2014.79069\npapers3://publication/doi/10.4236/jbise.2014.79069.

124. Quiroz-Florentino H, Hernández-Benitez R, Aviña J, Burgueño-Tapia E,

Tamariz J. Total Synthesis of Naturally Occurring Furan Compounds 5-{[(4-Hydroxybenzyl)oxy]methyl}-2-furaldehyde and Pichiafuran C. *Synthesis (Stuttg)*. 2011;2011(7):1106-1112. doi:10.1055/s-0030-1258455.

125. Publication A. Direct Conversion of Benzylic and Allylic Alcohols to Diethyl Phosphonates. *Org Synth*. 2013;90(September):145. doi:10.15227/orgsyn.090.0145.

126. Mahyar-Roemer M, Katsen A, Mestres P, Roemer K. Resveratrol induces colon tumor cell apoptosis independently of p53 and preceded by epithelial differentiation, mitochondrial proliferation and membrane potential collapse. *Int J Cancer*. 2001;94(5):615-622. doi:10.1002/ijc.1516.

127. Bruder JL, Hsieh T, Lerea KM, Olson SC, Wu JM. Induced cytoskeletal changes in bovine pulmonary artery endothelial cells by resveratrol and the accompanying modified responses to arterial shear stress. *BMC Cell Biol*. 2001;2:1. doi:10.1186/1471-2121-2-1.

128. Mech LD. A Gray Wolf (Canis lupus) Delivers Live Prey to a Pup. *Can Field-Naturalist*. 2014;128(2):189-190. doi:10.1016/j.

129. Russell RC, Fang C, Guan K-L. An emerging role for TOR signaling in mammalian tissue and stem cell physiology. *Development*. 2011;138(16):3343-3356. doi:10.1242/dev.058230.

130. Fingar DC, Richardson CJ, Tee AR, Cheatham L, Tsou C, Blenis J. mTOR controls cell cycle progression through its cell growth effectors S6K1 and 4E-BP1/eukaryotic translation initiation factor 4E. *Mol Cell Biol*. 2004;24(1):200-216. doi:10.1128/MCB.24.1.200.

131. Fingar DC, Salama S, Tsou C, Harlow E, Blenis J. Mammalian cell size is controlled by mTOR and its downstream targets S6K1 and 4EBP1/eIF4E. *Genes Dev*. 2002;16(12):1472-1487. doi:10.1101/gad.995802.

132. Rosner M, Fuchs C, Siegel N, Valli A, Hengstschläger M. Functional interaction of mammalian target of rapamycin complexes in regulating mammalian cell size and cell cycle. *Hum Mol Genet*. 2009;18(17):3298-

3310. doi:10.1093/hmg/ddp271.

133. Jacinto E, Loewith R, Schmidt A, et al. Mammalian TOR complex 2 controls the actin cytoskeleton and is rapamycin insensitive. *Nat Cell Biol*. 2004;6(11):1122-1128. doi:10.1038/ncb1183.

134. Turner JJ, Ewald JC, Skotheim JM. Cell size control in yeast. *Curr Biol*. 2012;22(9):R350-R359. doi:10.1016/j.cub.2012.02.041.

135. Bernhard D, Schwaiger W, Crazzolara R, Tinhofer I, Kofler R, Csordas A. Enhanced MTT-reducing activity under growth inhibition by resveratrol in CEM-C7H2 lymphocytic leukemia cells. *Cancer Lett*. 2003;195(2):193-199. doi:10.1016/S0304-3835(03)00157-5.

136. Duranton Ã, Badolo L, Schneider Y, et al. Anti-proliferative effect of resveratrol , a natural component of grapes and wine , on human colonic cancer cells. 2000;158.

137. Delmas D, Passilly-Degrace P, Jannin B, Malki MC, Latruffe N. Resveratrol, a chemopreventive agent, disrupts the cell cycle control of human SW480 colorectal tumor cells. *Int J Mol Med*. 2002;10(2):193-199.

138. Kim K-J, Chei S, Choi S-Y, Lee O-H, Lee B-Y. Pterostilbene activates the GRP78–elF2α–ATF3 cascade of ER stress and subsequently induces apoptosis in human colon cancer cells. *J Funct Foods*. 2016;26:539-547. doi:10.1016/j.jff.2016.08.027.

139. Mannal PW, Alosi JA, Schneider JG, McDonald DE, McFadden DW. Pterostilbene inhibits pancreatic Cancer in Vitro. *J Gastrointest Surg*. 2010;14(5):873-879. doi:10.1007/s11605-010-1164-4.

140. Fong Y, Yang W, Hsu S, et al. 2-Methoxyestradiol Induces Apoptosis and Cell Cycle Arrest in Human Chondrosarcoma Cells. 2007;(August):1106-1114. doi:10.1002/jor.

Appendix A

HNMR spectrum of compound 5 in $CDCl_3$

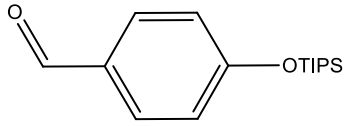

5

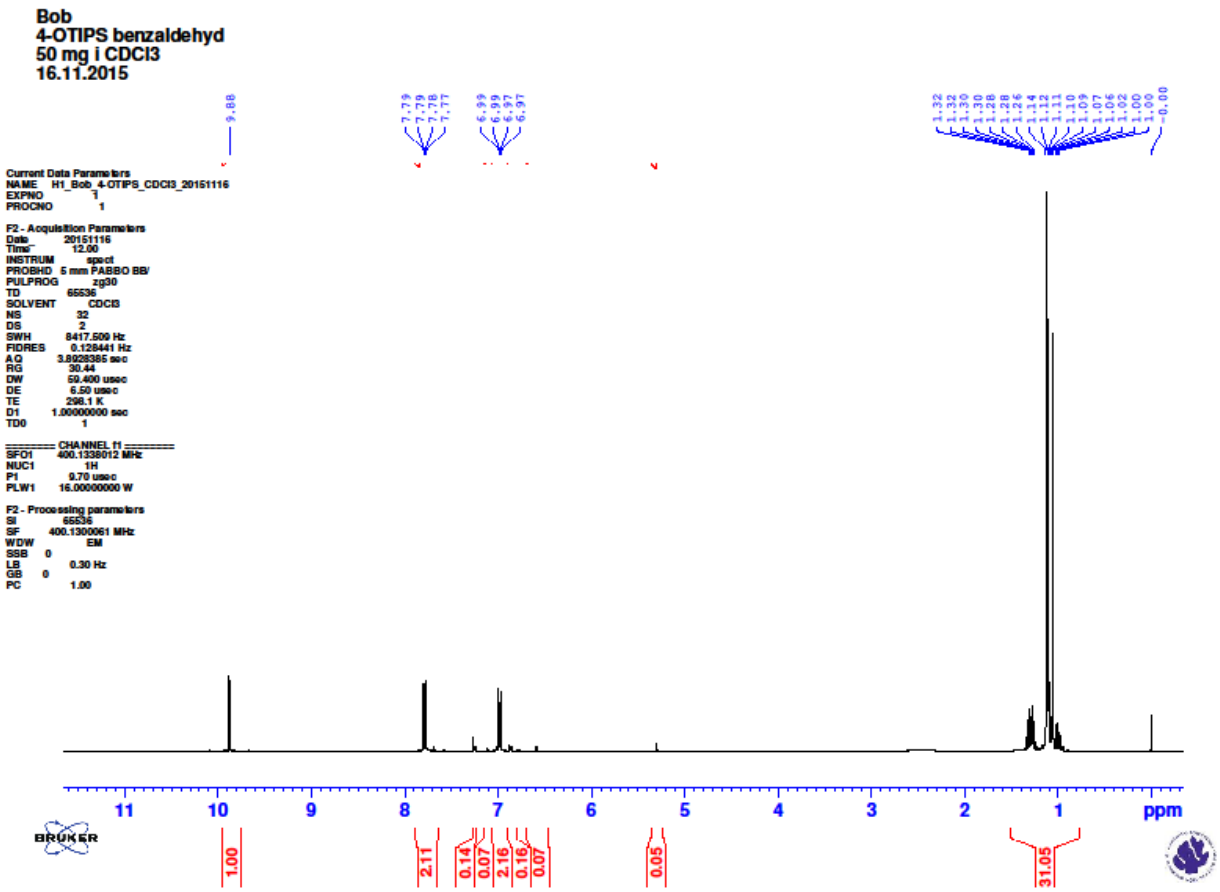

HNMR spectrum of compound 6

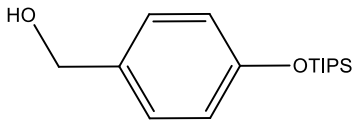

6

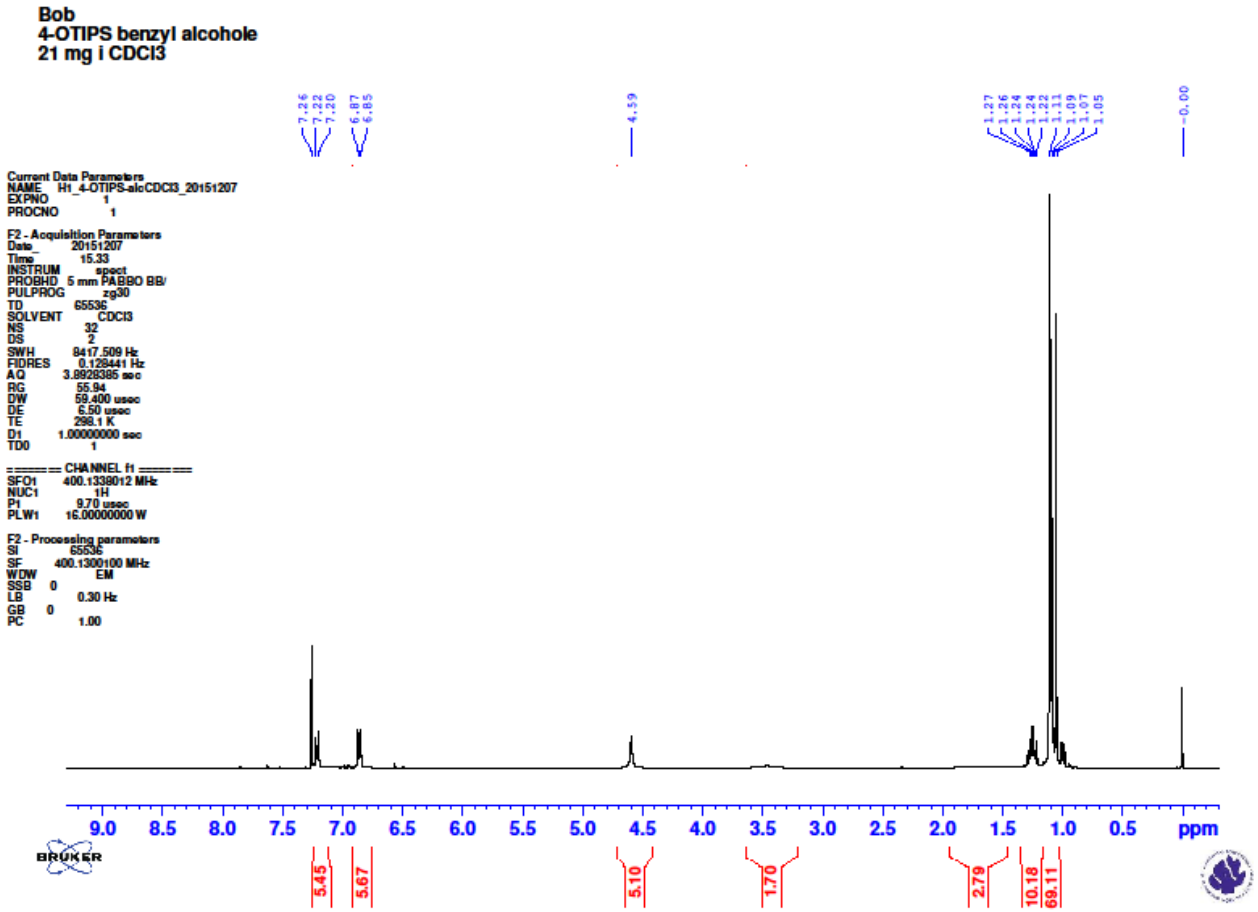

HNMR spectrum of compound 7

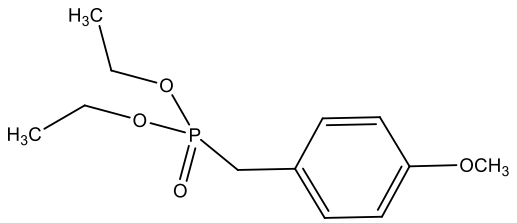

7

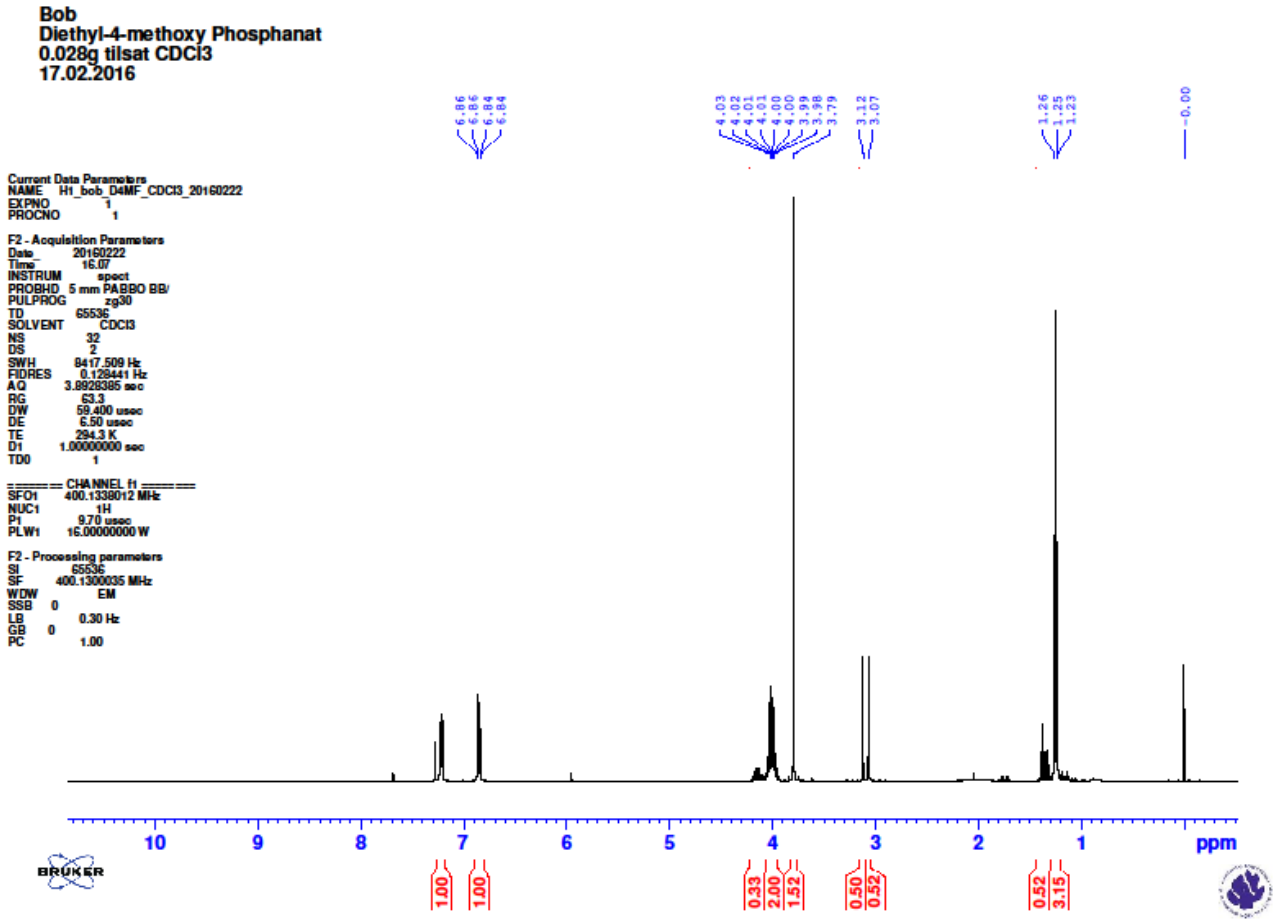

HNMR spectrum of compound 8

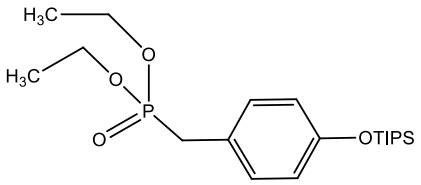

8

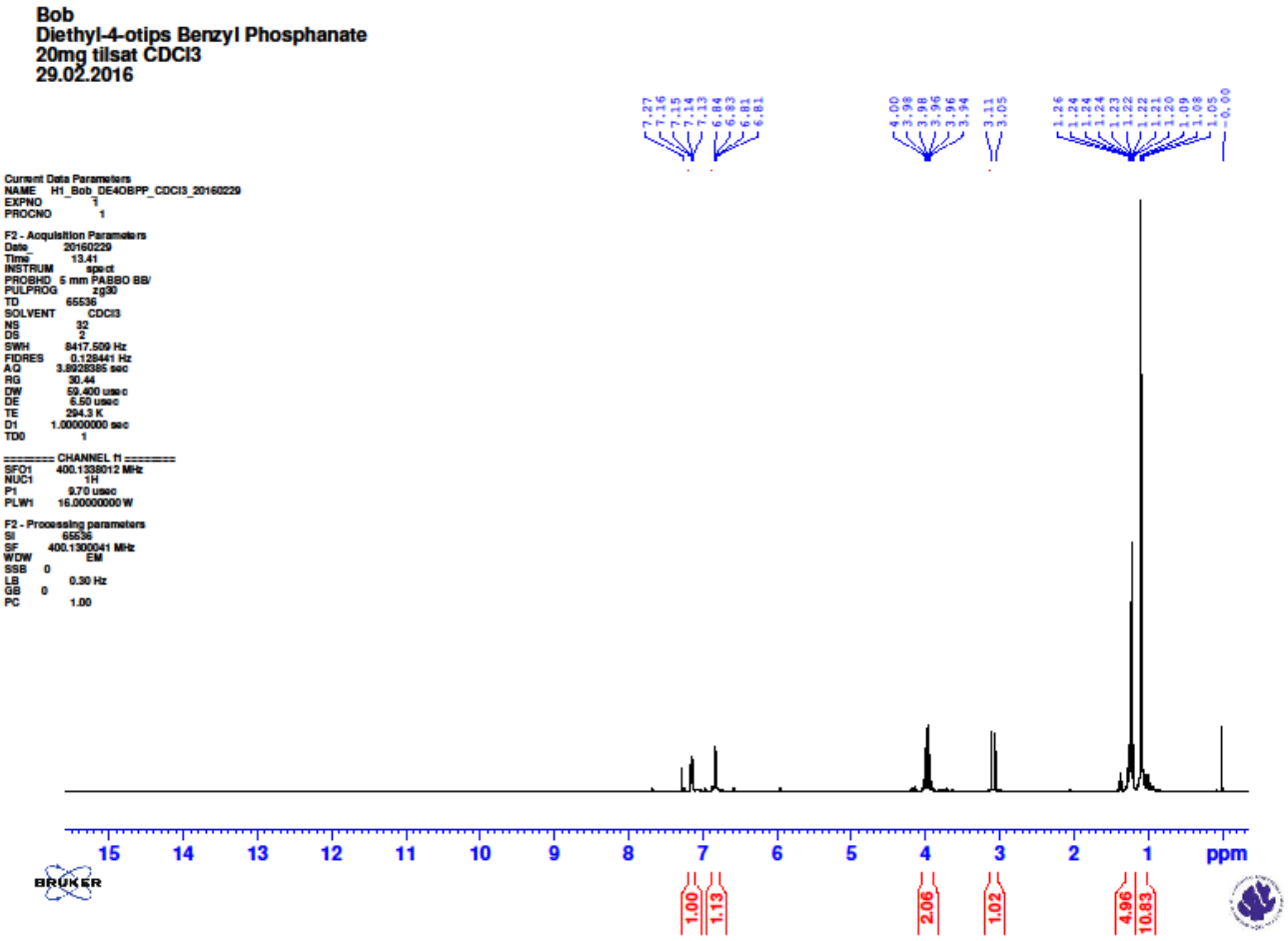

HNMR spectrum of compound 10

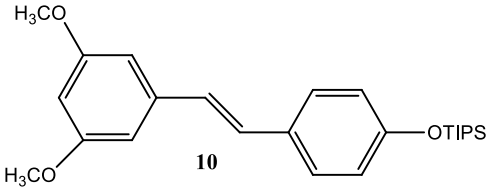

10

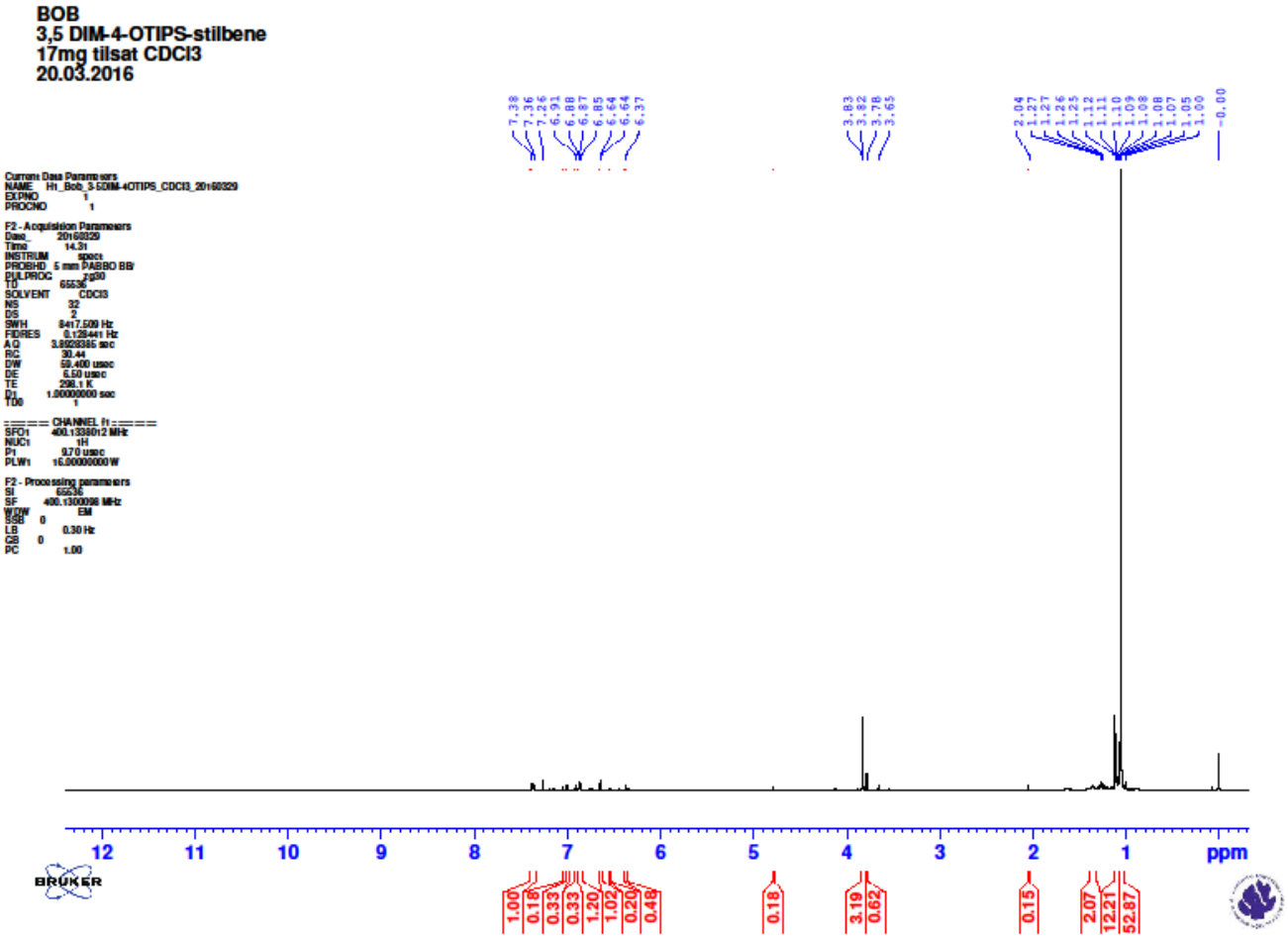

HNMR spectrum of compound 11

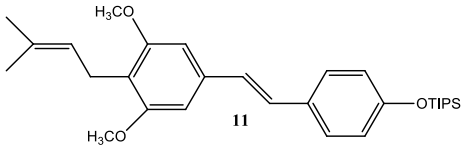

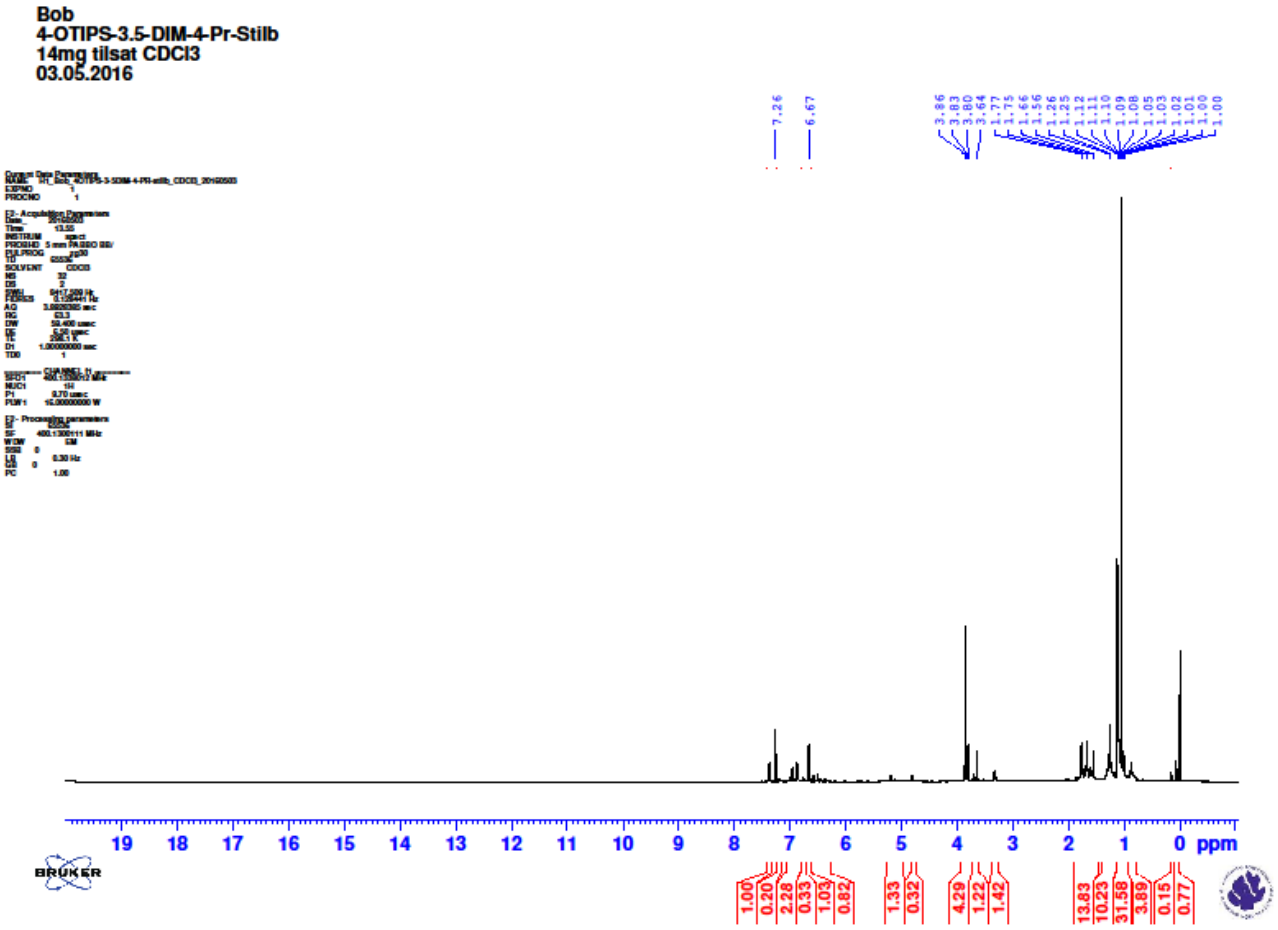

HNMR spectrum of compound 12

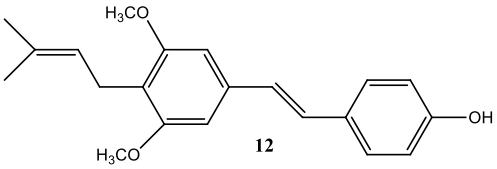

12

BOB final B

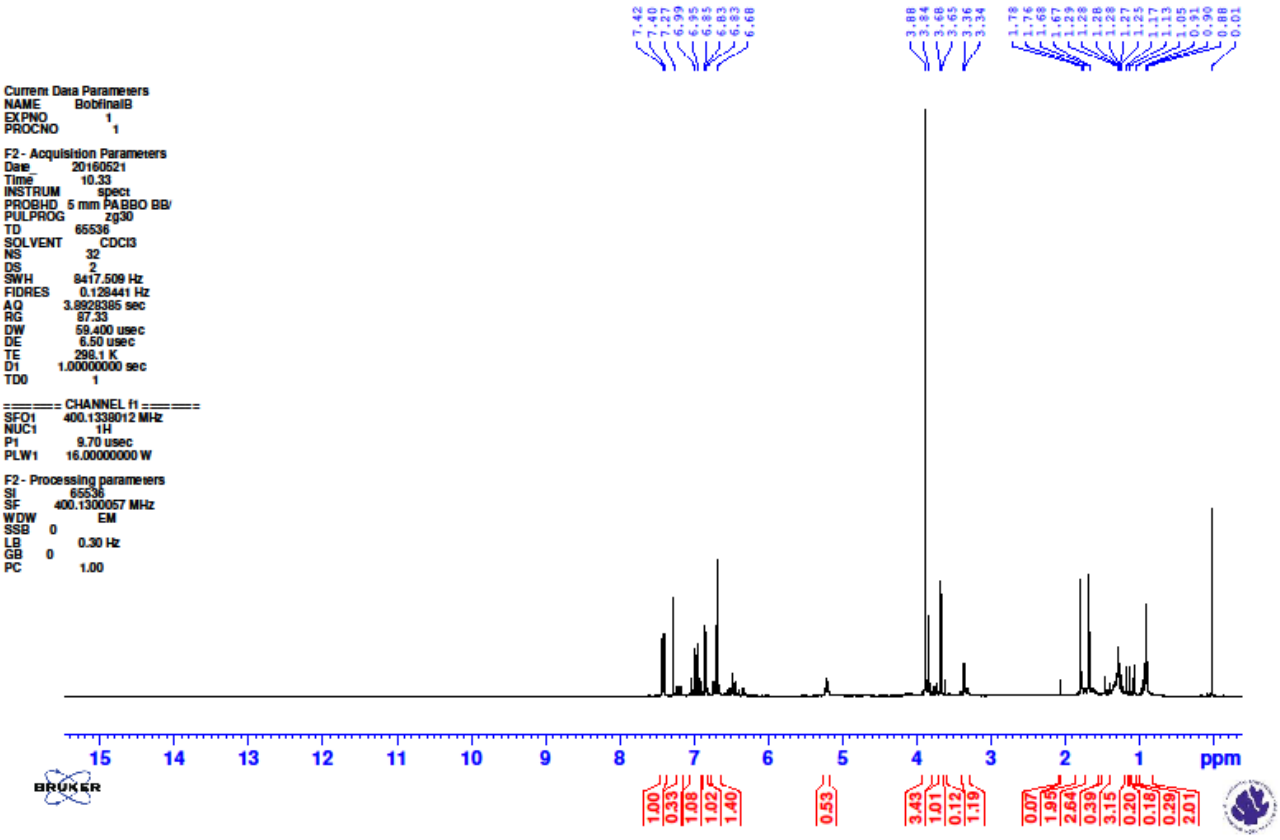

Appendix B

MS spectrum of compound 12

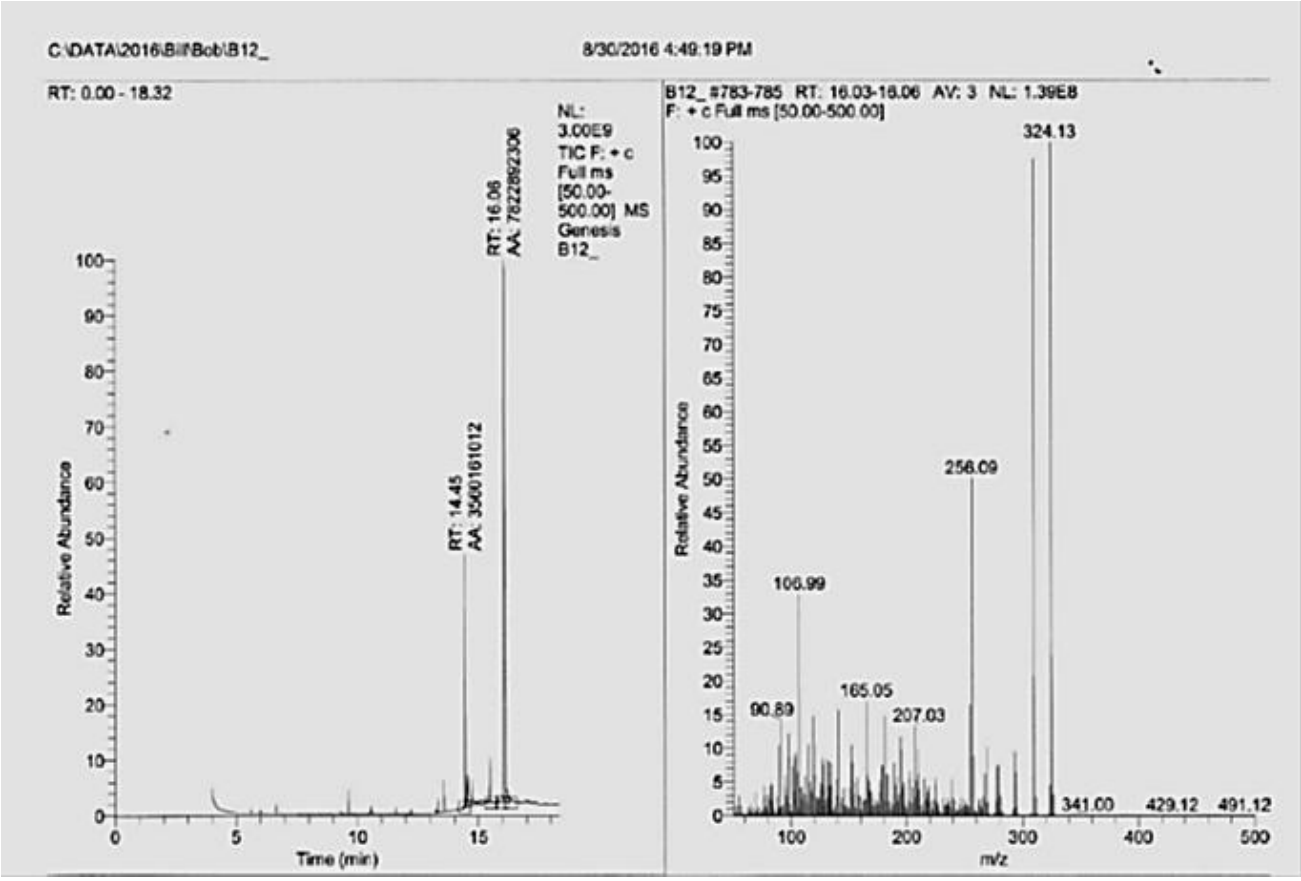

Abbreviations

ANOVA	Analysis of Variance
APC	Adenomatous Polyposis coli
Bax	Bcl-2- associated X protein
Bcl-2	B- cell leukemia/lymphoma 2
Bid	BH3 interacting domain death agonist
CDK	Cyclin Dependent Kinase
COX-2	Cyclooxygenase-2
CRC	Colon Rectal Cancer
DCM	Dichloromethane
DIABLO	Direct Inhibitor of Apoptosis Binding protein with Low pI
DISC	Death-inducing signaling complex
DMF	Dimethyl formamide
DMG	Directed Metalation Group
DMSO	Dimethyl Sulfoxide
DMSO	Dimethyl Sulphoxide
DoM	Directed *Ortho*-Metalation
E2F	Transcription factors
FACS	Fluoresces-activated cell sorting
FADD	Fas associated protein with death-domain
FSC	Forward Scatter of Cells
$G_0/G_1/G_2$	Gap phase 0 /Gap phase 1/Gap phase 2
GC-MS	Gas Chromatography-Mass spectroscopy
GLOBOCAN	Global Burden of Cancer study
HBSS	Hank`s Balance Salt Solution
HWE	Horner- Wadsworth-Emmons
IAP	Inhibitors of Apoptosis Proteins
IC_{50}	50% inhibitory concentration
iNOS	inducible Nitic Oxide Synthase
KRAS	Kirsten rat sarcoma oncogene
LOH	Loos of Heterozygosity

m- TOR	Mammalian target of rapamycin
m/z	Mass/Charge
MeOH	Methanol
Mmol	Millimole
MOM	Methoxymethyl
N_2	Nitrogen
NADH	Nicotineamide Adenine Dinucleotide
n-BuLi	n-Butyllithium
NMR	Nuclear Magnetic Resonance
PBS	Phosphate Buffer Saline
PI	Propidium iodide
PI3K	Phosphatidyl inositol 3-kinase
Pr. Pter	Prenylated Pterostilbene
Pter	Pterostilbene
Rb	Retinoblastoma protein
RV	Resveratrol
S/M	Synthesis phase/ Mitosis phase
S6K	S6 kinase
SMAC	Second mitochondria derived activator of caspases
Smad	Second mitochondria derived activator
SSC	Side Scatter of Cells
TBAF	Tetra-n-buty ammonium fluoride
TCT	2,4,6-tri chloro-1,3,5-triazine
TES	Triethylsilane
THF	Tetrahydrofuran
TIPS-CL	Tri-isopropylchlorosilane
TLC	Thin Layer Chromatography
TMS	Trimethylsilyl
TNF	Tumor Necrosis Factor
TNM	Tumour Node Metastasis
TSG	Tumor Suppressor Genes
VEGF	Vascular endothelial growth factor